

150 Years Periodic Table of the Chemical Elements

Mendeleev + Meyer

125 Years Georges Lemaitre

and the Expanding Universe

62 years after the first general reviews on nuclear astrophysics by

B²FH and Cameron in 1957

Making the Elements in the Universe: From the Big Bang to Stars and Stellar Explosions

Friedrich-Karl Thielemann

Departement Physik and Helmholtz-Zentrum für Schwerionenforschung

Universität Basel

Schweiz

GSI Darmstadt

Deutschland

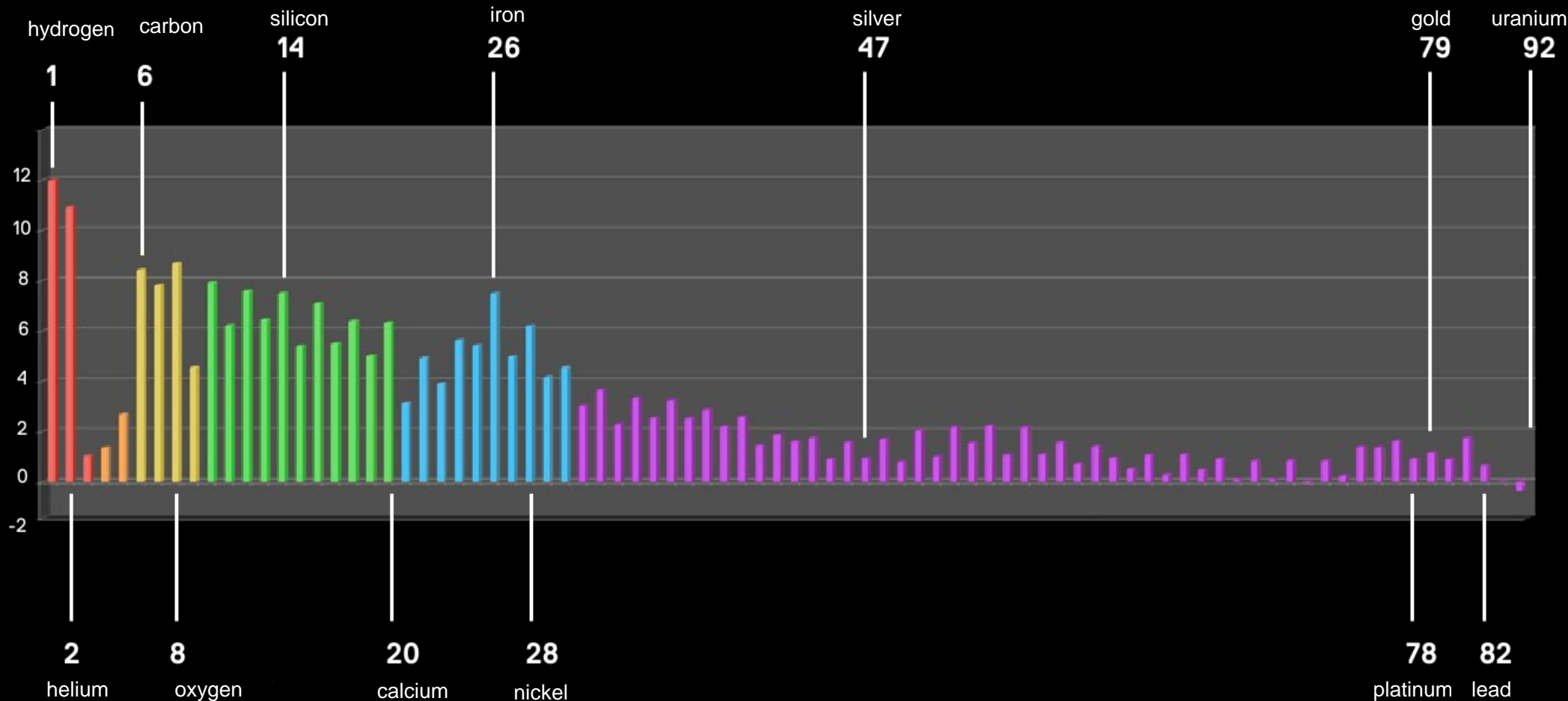
Chemical Elements known today

Up to Oganesson (Z=118), Elements with Z>94 (Plutonium) are unstable, short-lived and only created in nuclear accelerator labs

([wikimedia](#))

1																		2																		13																		14																		15																		16																		17																		18																	
1																		2																		13																		14																		15																		16																		17																		18																	
1																		2																		13																		14																		15																		16																		17																		18																	
1																		2																		13																		14																		15																		16																		17																		18																	
1																		2																		13																		14																		15																		16																		17																		18																	
1																		2																		13																		14																		15																		16																		17																		18																	
1																		2																		13																		14																		15																		16																		17																		18																	
1																		2																		13																		14																		15																		16																		17																		18																	
1																		2																		13																		14																		15																		16																		17																		18																	
1																		2																		13																		14																		15																		16																		17																		18																	
1																		2																		13																		14																		15																		16																		17																		18																	
1																		2																		13																		14																		15																		16																		17																		18																	
1																		2																		13																		14																		15																		16																		17																		18																	
1																		2																		13																		14																		15																		16																		17																		18																	
1																		2																		13																		14																		15																		16																		17																		18																	
1																		2																		13																		14																		15																		16																		17																		18																	
1																		2																		13																		14																		15																		16																		17																		18																	
1																		2																		13																		14																		15																		16																		17																		18																	
1																		2																		13																		14																		15																		16																		17																		18																	
1																		2																		13																		14																		15																		16																		17																		18																	
1																		2																		13																		14																		15																		16																		17																		18																	
1																		2																		13																		14																		15																		16																		17																		18																	
1																		2																		13																		14																		15																		16																		17																		18																	
1																		2																		13																		14																		15																		16																		17																		18																	
1																		2																		13																		14																		15																		16																		17																		18																	
1																		2																		13																		14																		15																		16																		17																		18																	
1																		2																		13																		14																		15																		16																		17																		18																	
1																		2																		13																		14																		15																		16																		17																		18																	
1																		2																		13																		14																		15																		16																		17																		18																	
1																		2																		13																		14																		15																		16																		17																		18																	
1																		2																		13																		14																		15																		16																		17																		18																	
1																		2																		13																		14																		15																		16																		17																		18																	
1																		2																		13																		14																		15																		16																		17																		18																	
1																		2																		13																		14																		15																		16																		17																		18																	
1																		2																		13																		14																		15																		16																		17																		18																	
1																		2																		13																		14																		15																		16																		17																		18																	
1																		2																		13																		14																		15																		16																		17																		18																	
1																		2																		13																		14																		15																		16																		17																		18																	
1																		2																		13																		14																		15																		16																		17																		18																	
1																		2																		13																		14																		15																		16																		17																		18																	
1																		2																		13																		14																		15																		16																		17																		18																	
1																		2																		13																		14																		15																		16																		17																		18																	
1																		2																		13																		14																		15																		16																		17																		18																	
1																		2																		13																		14																		15																		16																		17																		18																	
1																		2																		13																		14																		15																		16																		17																		18																	
1																		2																		13																		14																		15																		16																		17																		18																	
1																		2																		13																		14																		15																		16																		17																		18																	
1																		2																		13																		14																		15																		16																		17																		18																	
1																		2																		13																		14																		15																		16																		17																		18																	
1																		2																		13																		14																		15																		16																		17																		18																	
1																		2																		13																		14																		15																		16																		17																		18																	
1																		2																		13																		14																		15																		16																		17																		18																	
1																		2																		13																		14																		15																		16																		17																		18																	
1																		2																		13																		14																		15																		16																		17																		18																	
1																		2																		13																		14																		15																		16																		17																		18																	
1																		2																		13																		14																		15																		16																		17																		18																	
1																		2																		13																		14																		15																		16																		17																		18																	
1																		2																		13																		14																		15																		16																		17																		18																	
1																		2																		13																		14																		15																		16																		17																		18																	
1																		2																		13																		14																		15																		16																		17																		18																	
1																		2																		13																		14																		15																		16																		17																		18																	
1																		2																		13																		14																		15																		16																																																					

Abundances in the Solar System (from carbonaceous chondrites and solar absorption spectra)



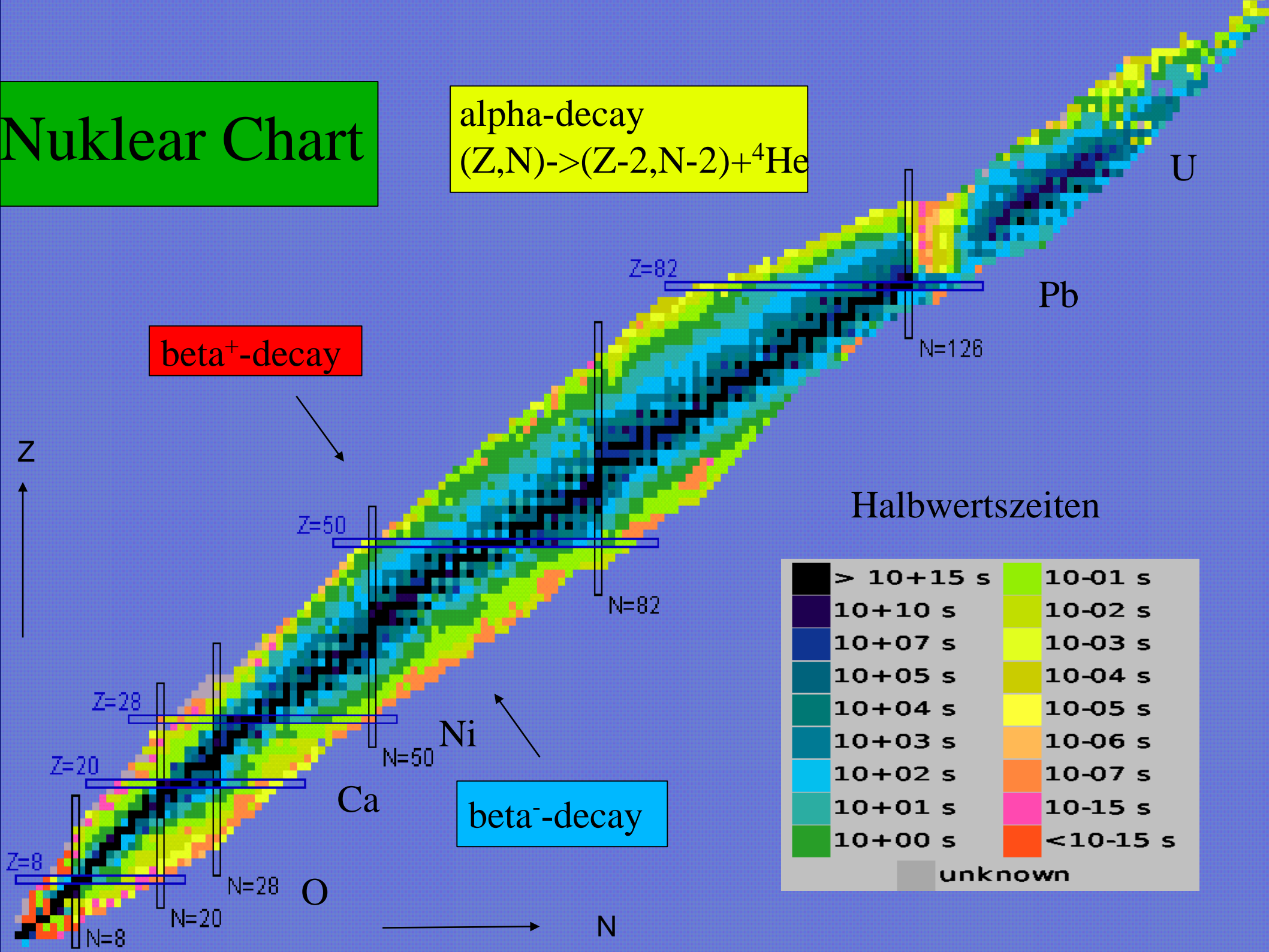
One unit on the y-axis corresponds to a factor of 10, i.e. hydrogen is about 10^{12} more abundant than uranium

Nuklear Chart

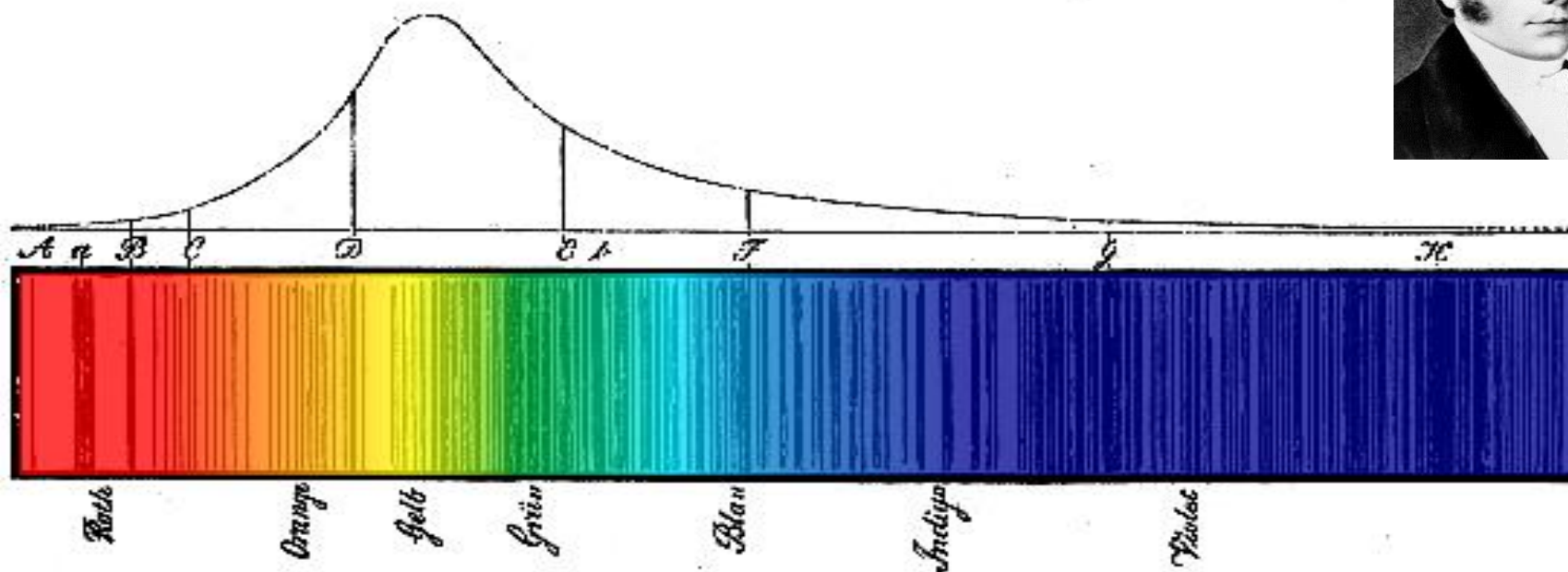
alpha-decay
 $(Z,N) \rightarrow (Z-2, N-2) + {}^4\text{He}$

beta⁺-decay

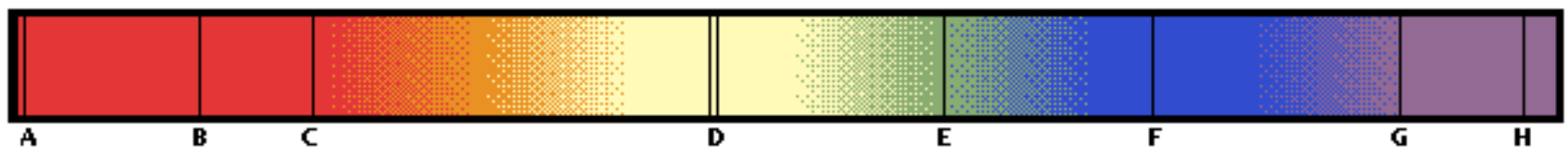
Halbwertszeiten



Fraunhofer's absorption lines in the Solar Spectrum

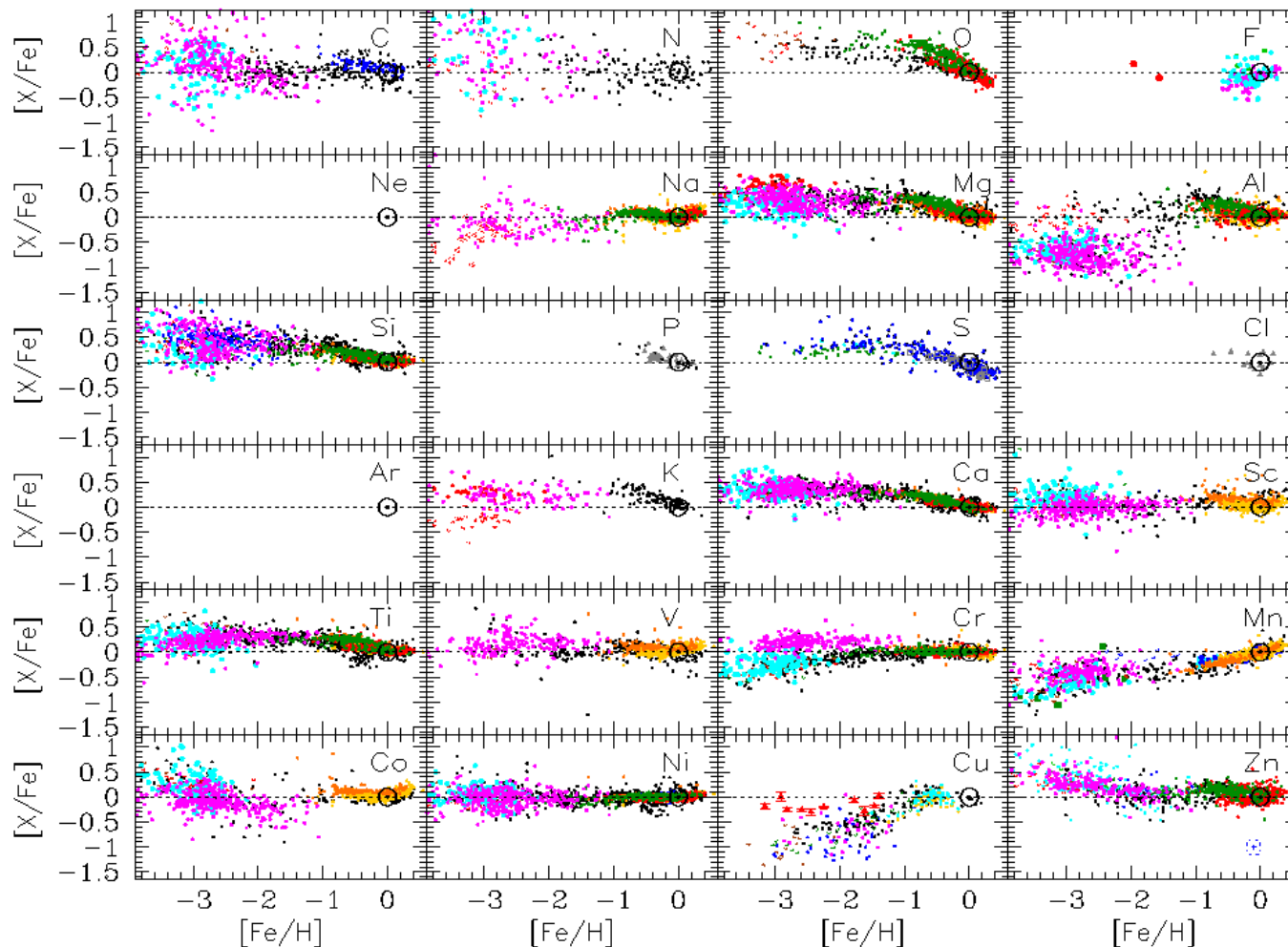


Zu Fraunhofer's Abh. Denkschr. 1814-15.



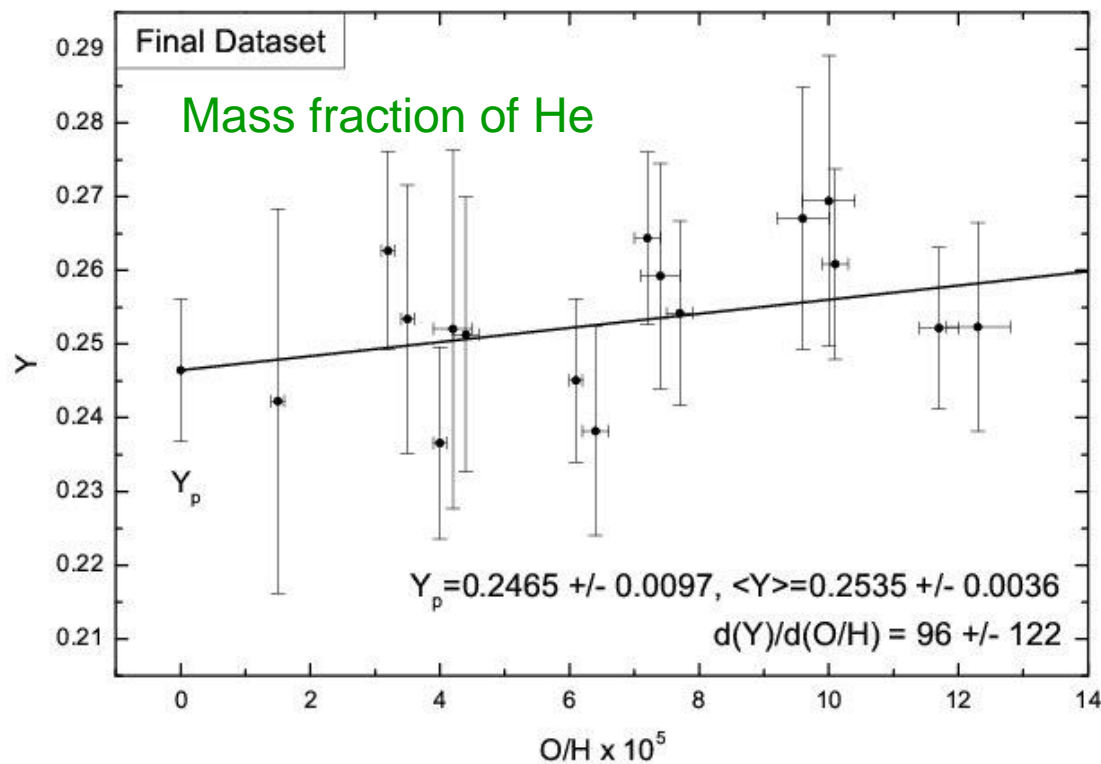
A	(äußerstes Rot)	Terrestrischer Sauerstoff
B	(Rot)	Terrestrischer Sauerstoff
C	(Rot)	Solarer Wasserstoff
D ₁	(Gelb)	Solares Natrium
D ₂	(Gelb)	Solares Natrium
E	(Grün)	Solares Eisen
F	(Blau)	Solarer Wasserstoff
G	(Violett)	Solares Eisen und solares Calcium
H	(äußerstes Violett)	Solares Calcium

Spektra of old stars witness the evolution of the elements in our Galaxy (the Milky Way)



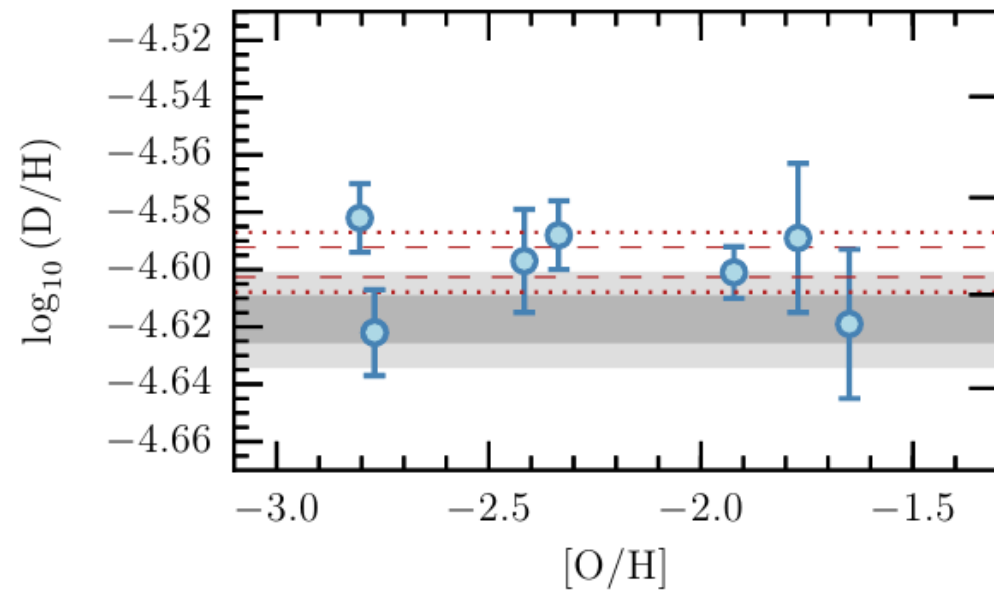
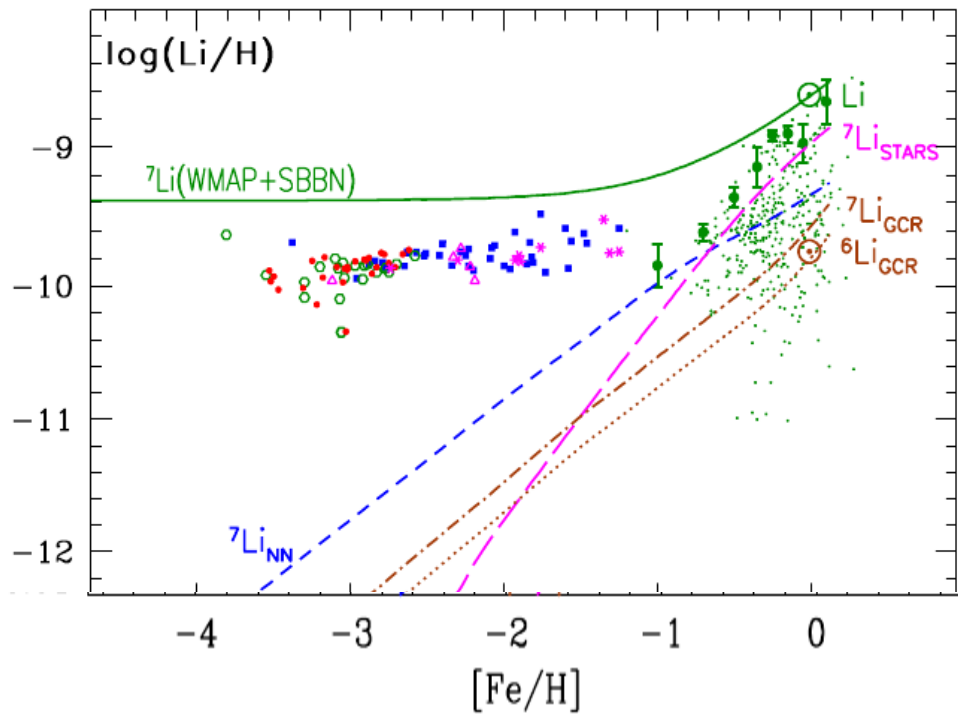
N. Prantzos

stars burn via fusion reactions in their interior, but the surface composition is inherited from the gaseous cloud out of which they formed, i.e. we can view the past of the galaxy via observing stars of different age. The abundance ratios are given as logarithm (0=solar, -1=1/10 solar, -3=1/1000 solar). The ratios of elements like $X=C, N, O, Mg, Si, S, Ca, Ti$ to Fe vary with its increase, i.e. with time, but if Fe goes to 0 all these other elements shown here, go to 0 as well.



Exceptions: When following **Helium**, **Lithium** and **Deuterium** down to the smallest Fe or O-values, they do not vanish but become constant, i.e. they must have formed before the formation of the Milky Way
➡ Big Bang.

While normally spectra of isotopes are not easily to disentangle (isotope shift), this is not the case between ^1H (1 Proton) and ^2H with a nucleus of twice the mass



The Expanding Universe

The Universe is homogeneous und isotropic and its expansion can be described via the Friedmann-Lemaitre equations

$$\begin{aligned} \left(\frac{\ddot{R}}{R}\right) &= -\frac{4\pi}{3c^2}(\rho_\epsilon + 3P)G + \frac{1}{3}\Lambda c^2 \\ \left(\frac{\dot{R}}{R}\right)^2 &= H(t)^2 = \frac{8\pi G}{3c^2}\rho_\epsilon - \frac{kc^2}{R^2(t)} + \frac{1}{3}\Lambda c^2 \\ 0 &= \frac{d(\rho_\epsilon R^3)}{dt} + P\frac{dR^3}{dt} \end{aligned}$$

cosmological constant

Hubble-"constant"

where P , ρ_ϵ and Λ denote pressure, total relativistic energy density and the cosmological constant

k describes the curvature (-1 open; 0 flat, +1 closed)

$v=cz=Hr$, velocity v , velocity of light c , redshift z , distance r

Introduction to nuclear reaction rates

$$\sigma = \frac{\text{number of reactions target}^{-1}\text{sec}^{-1}}{\text{flux of incoming projectiles}} = \frac{r/n_i}{n_j v} \quad r = \sigma v n_i n_j$$

reaction rate r (per volume and sec) for a fixed bombarding velocity/energy (like in an accelerator)

$$r_{i;j} = \int \sigma \cdot |\vec{v}_i - \vec{v}_j| dn_i dn_j \quad \text{for thermal distributions in a hot plasma}$$

e.g. Maxwell-Boltzmann (nuclei/nucleons) or Planck (photons)

$$dn_j = n_j \frac{4\pi p_j^2}{(2\pi m_j kT)^{3/2}} \exp\left(-\frac{p_j^2}{2m_j kT}\right) dp_j \quad dn_\gamma = \frac{8\pi}{c^3} \frac{\nu^2 d\nu}{\exp(h\nu/kT) - 1} = \frac{1}{\pi^2 (c\hbar)^3} \frac{E_\gamma^2 dE_\gamma}{\exp(E_\gamma/kT) - 1}$$

for two MB-distributions for i and j one obtains after variable transformations

$$r_{i;j} = n_i n_j \langle \sigma v \rangle_{i;j} \quad \langle \sigma v \rangle (T) = \left(\frac{8}{\mu\pi} \right)^{1/2} \frac{1}{(kT)^{3/2}} \int_0^\infty E \sigma(E) \exp(-E/kT) dE$$

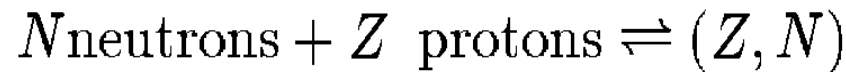
Highly (exponentially) dependent on T for charged-particle reactions due to Coulomb repulsion, close to constant (slightly decreasing with T) for neutron induced reactions. Also highly temperature-dependent for photo-disintegrations (inverse to capture reactions), they win typically when $30kT > Q$ (energy gain for capture reaction), but high densities (entering only linearly) can enhance capture.

Global Chemical (=Nuclear Statistical) Equilibrium (NSE)

$$\begin{aligned}\bar{\mu}(Z, N) + \bar{\mu}_n &= \bar{\mu}(Z, N + 1) \\ \bar{\mu}(Z, N) + \bar{\mu}_p &= \bar{\mu}(Z + 1, N)\end{aligned}\quad \bar{\mu}_i = kT \ln \left(\frac{\rho N_A Y_i}{G_i} \left(\frac{2\pi\hbar^2}{m_i kT} \right)^{3/2} \right) + m_i c^2$$

Neutron and proton captures as well as their inverse photo-disintegrations are in equilibrium

Chemical potential (including rest mass) for particles following Maxwell-Boltzmann statistics



$$N \bar{\mu}_n + Z \bar{\mu}_p = \bar{\mu}_{Z,N}.$$

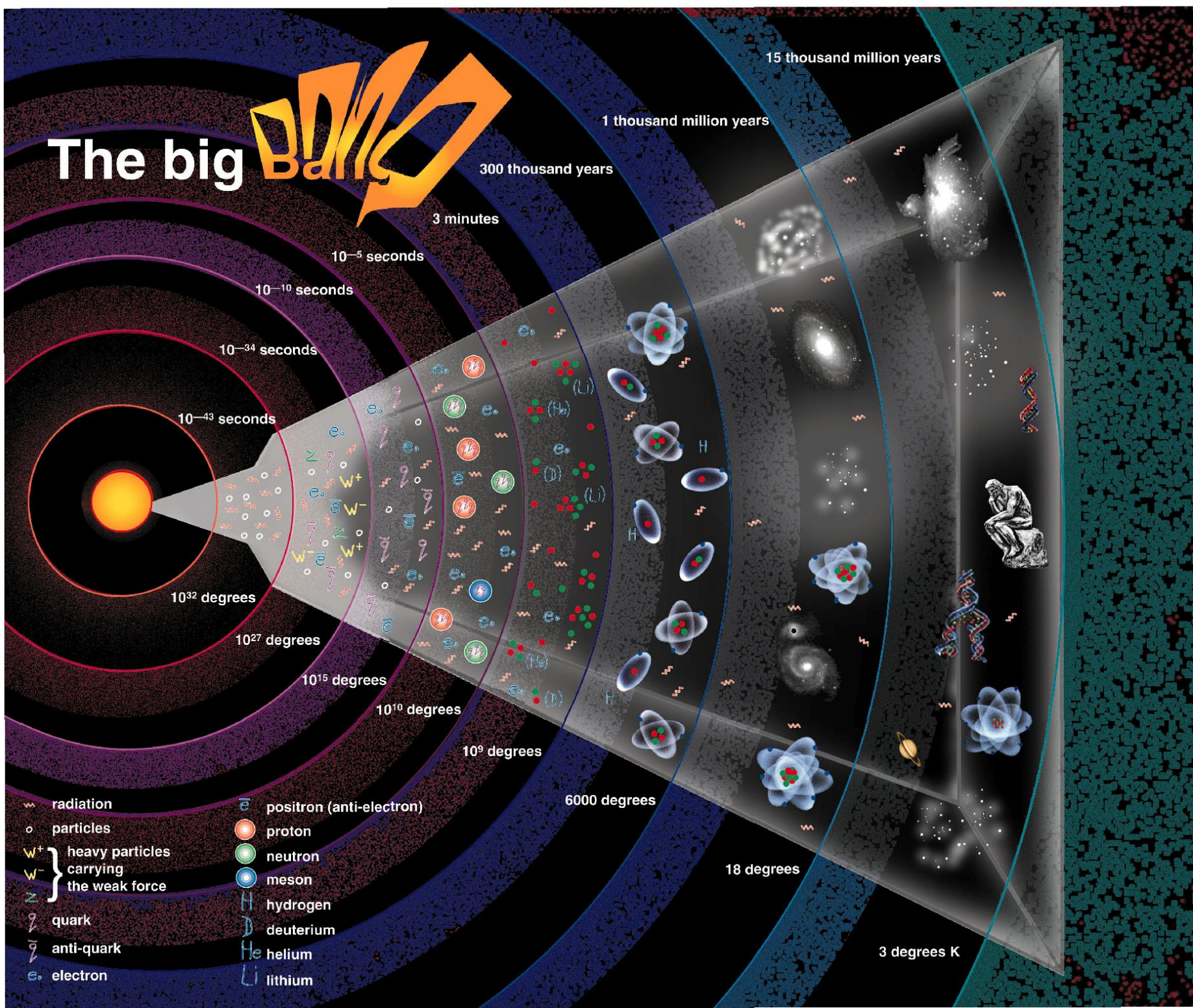
$$Y(Z, N) = G_{Z,N} (\rho N_A)^{A-1} \frac{A^{3/2}}{2^A} \left(\frac{2\pi\hbar^2}{m_u kT} \right)^{\frac{3}{2}(A-1)} \exp(B_{Z,N}/kT) Y_n^N Y_p^Z$$

$$\sum_i A_i Y_i = 1$$

$$\sum_i Z_i Y_i = Y_e$$

For temperatures T being sufficiently high to enable all capture as well as photo-disintegration reactions an equilibrium sets in, favoring for moderate densities and temperatures nuclei with the highest binding energies (around Fe and Ni). For extremely high temperatures ($>5-6 \cdot 10^9$ K) everything is disintegrated into neutrons and protons. Extremely high densities (still below nuclear matter density) can lead to nuclei as heavy as $A=500$.

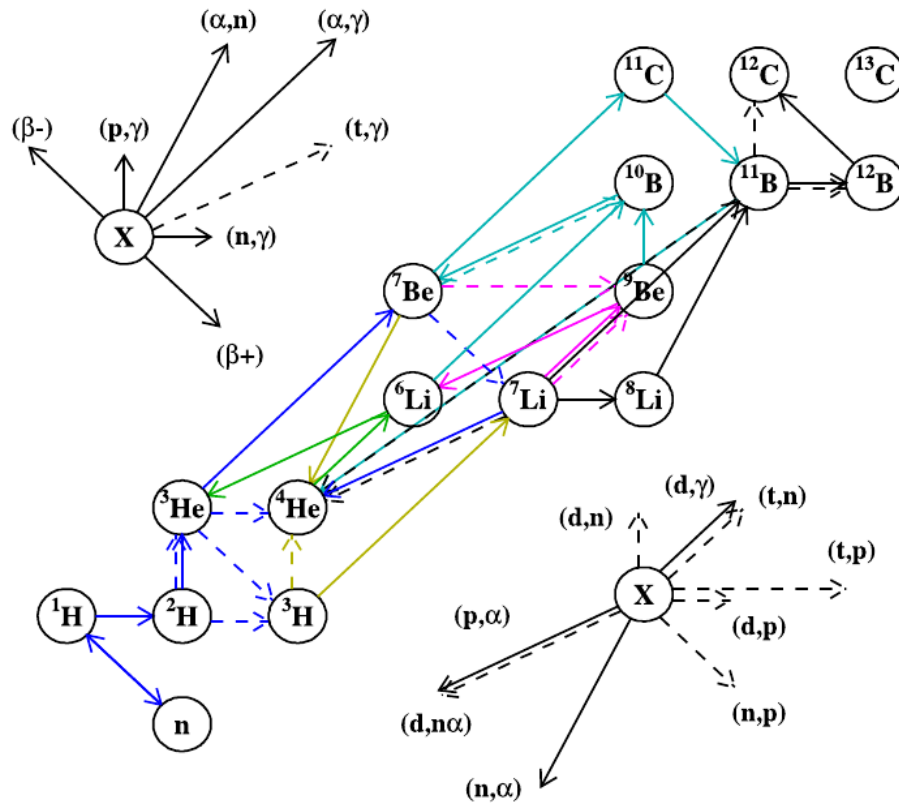
The big Bang



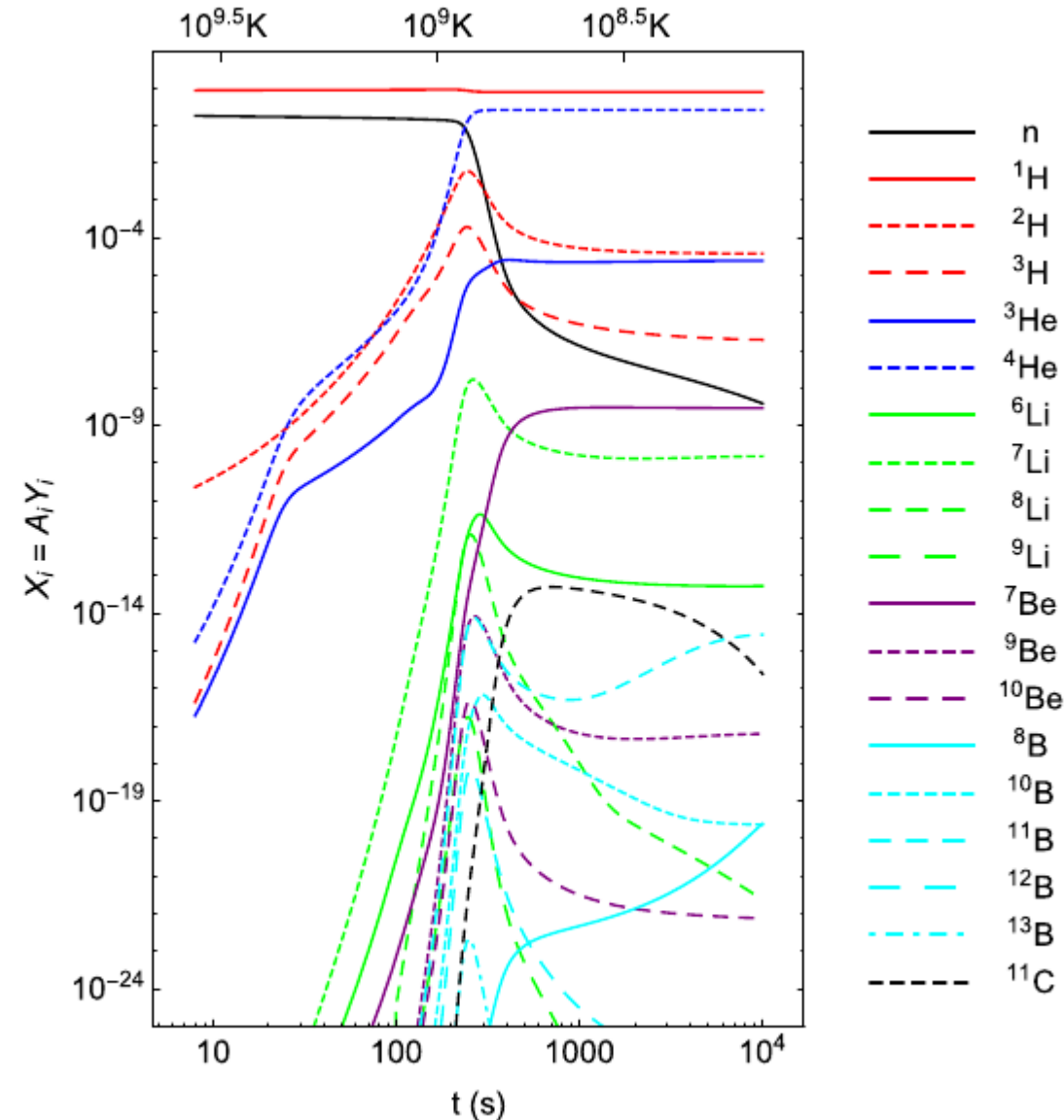
Reactions during big bang nucleosynthesis

Pitrou et al. (2018)

and resulting “primordial abundances”



possible reactions (in the Nuclear chart)



Mass fractions of individual isotopes during the expansion as a function of time

Primordial Abundances

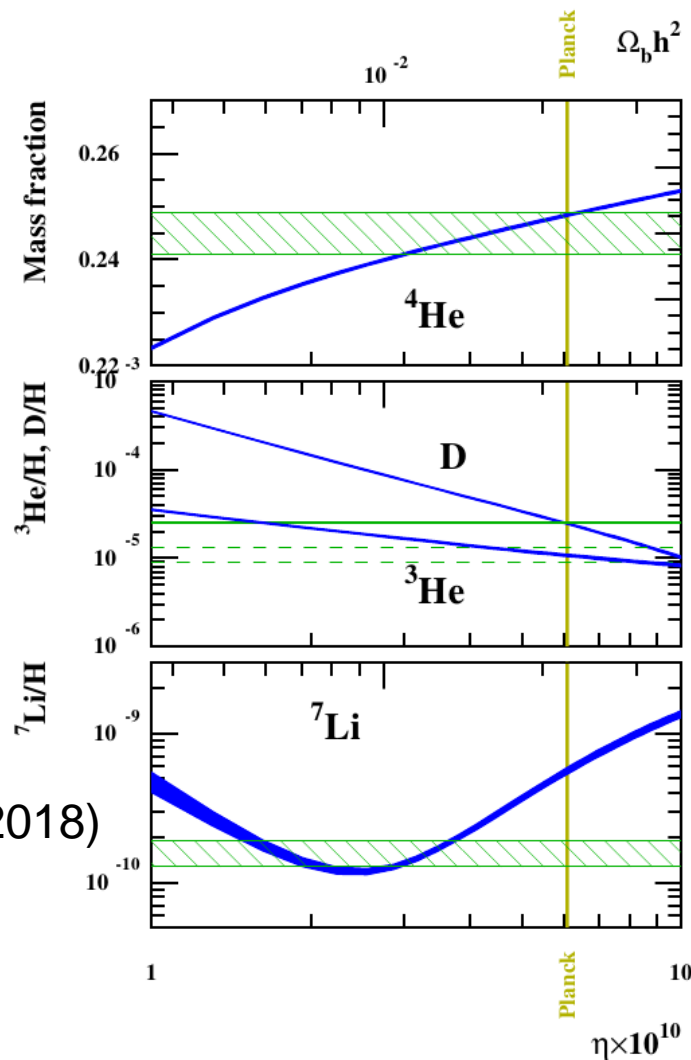
Abundances as found at the onset of galaxies (our galaxy) for ^1H , ^2H , ^3He , ^4He und ^7Li (horizontal lines)

compared to predictions as a function of the parameter $\eta = n_B/n_\gamma$, inversely proportional to the original entropy ($n_\gamma \approx T^3$, $n_B \approx \rho$, entropy of a radiation dominated gas $S \approx T^3 / \rho$)

the value $\eta = 6 \times 10^{-10}$ corresponds to the Planck results of the Cosmic Microwave Background CMB

(the observed Li abundance in old star has uncertainties due to possible destruction or gravitational settling in the stellar surface layers)

with these abundances only about 4.8% of the total energy density of the Universe is found in baryonic matter known to us



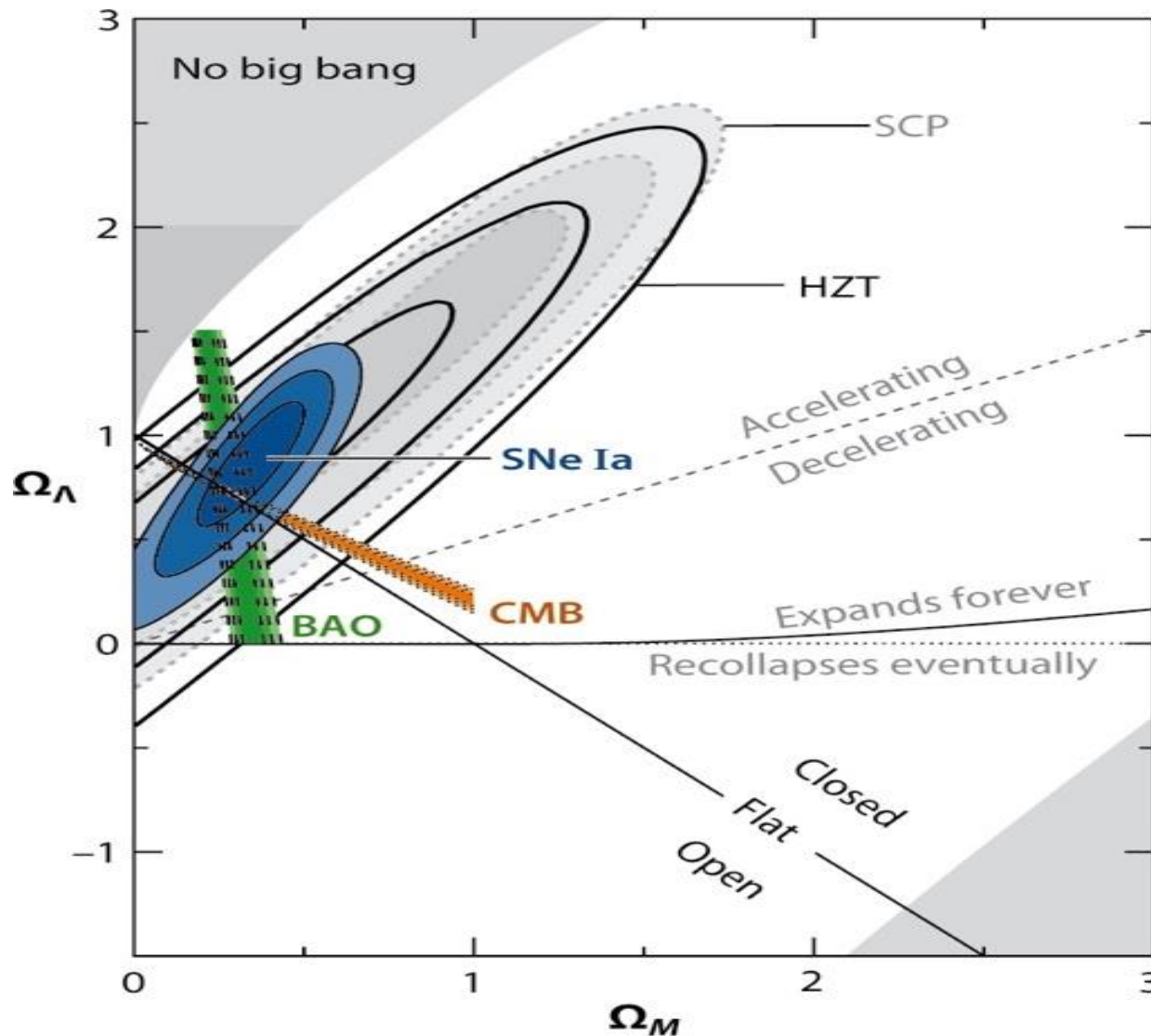
Coc et al. (2018)

“free“ Parameter $\eta = n_B/n_\gamma$, a measure of the entropy of the Universe, is related to the relativistic energy density and the Hubble-Expansion)

Agreement of CMB, matter (Baryon Accoustic Oscillations), and (Type Ia) Supernovae on $\Omega=1$, $\Omega_m=0.31$, $\Omega_\Lambda=1-\Omega_m=0.69$, $\Omega_b=0.048$ (part of Ω_m), consistent with Big Bang Nucleosynthesis and $\eta=n_B/n_\gamma$.

still debate on Hubble constant : CMB with Planck satellite 67.3km/s/Mpc,

Type Ia supernovae calibrated by cepheids 74 (Riess et al.) or red giants 69.8 (Freedman et al.)

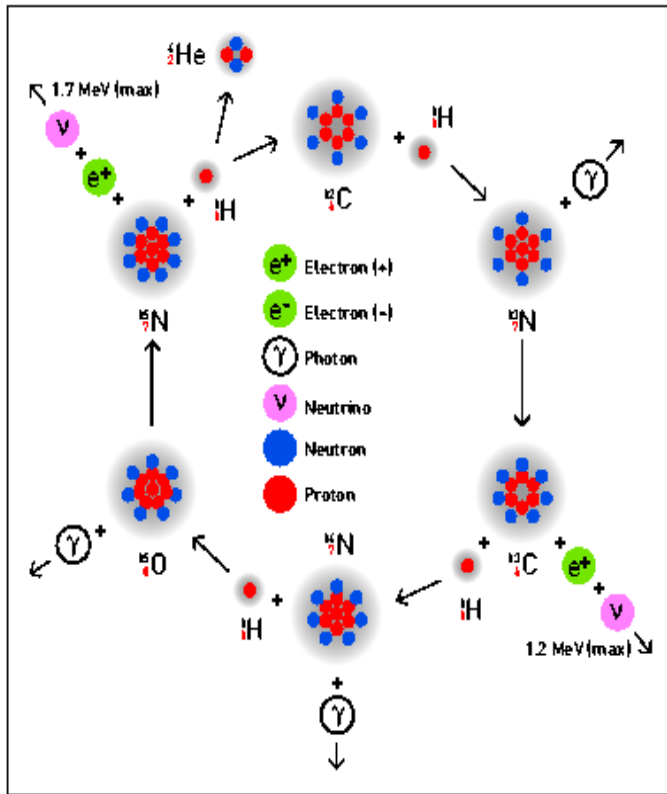


Goobar &
Leibundgut (2011)

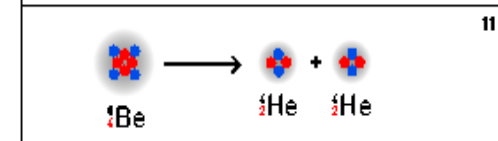
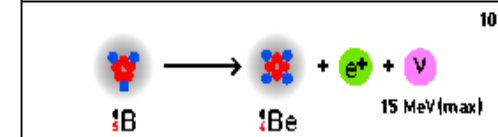
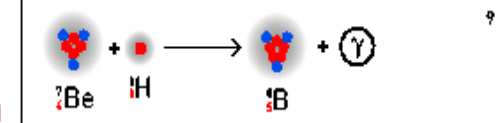
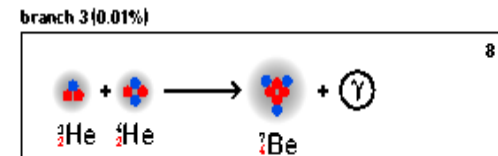
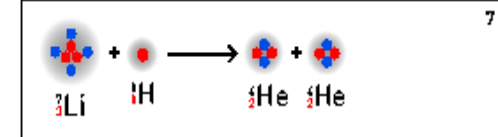
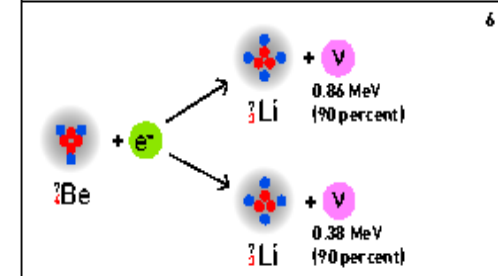
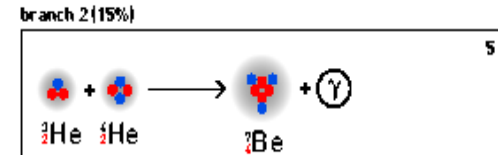
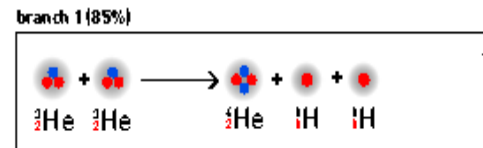
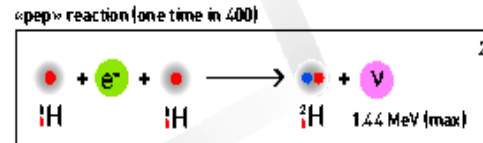
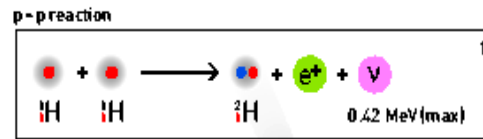
Stellar Burning Stages

Hydrogen Burning

The CNO Cycle



P-P Cycles



The first stars formed about 200 Million years after the Big Bang from cold interstellar gas clouds. Stars are those object that attain sufficiently high temperatures in their interior (due to the gain of gravitational binding energy during contraction) that the relative velocities of nuclei in the plasma are high enough to overcome their Coulomb repulsion and undergo nuclear fusion.

Stars are stable if the central energy gain is sufficient to balance the energy loss by radiation. The pressure, determined by temperature and density, balances the gravity of the stellar object.

Brief Summary of Stellar Burning Stages (Major Reactions)

1. Hydrogen Burning

$$T = (1-4) \times 10^7 \text{ K}$$

pp-cycles \rightarrow



CNO-cycle \rightarrow slowest reaction



2. Helium Burning

$$T = (1-2) \times 10^8 \text{ K}$$



3. Carbon Burning

$$T = (6-8) \times 10^8 \text{ K}$$



4. Neon Burning

$$T = (1.2-1.4) \times 10^9 \text{ K}$$



$$30kT = 4\text{MeV}$$

5. Oxygen Burning

$$T = (1.5-2.2) \times 10^9 \text{ K}$$



6. “Silicon” Burning

$$T = (3-4) \times 10^9 \text{ K}$$

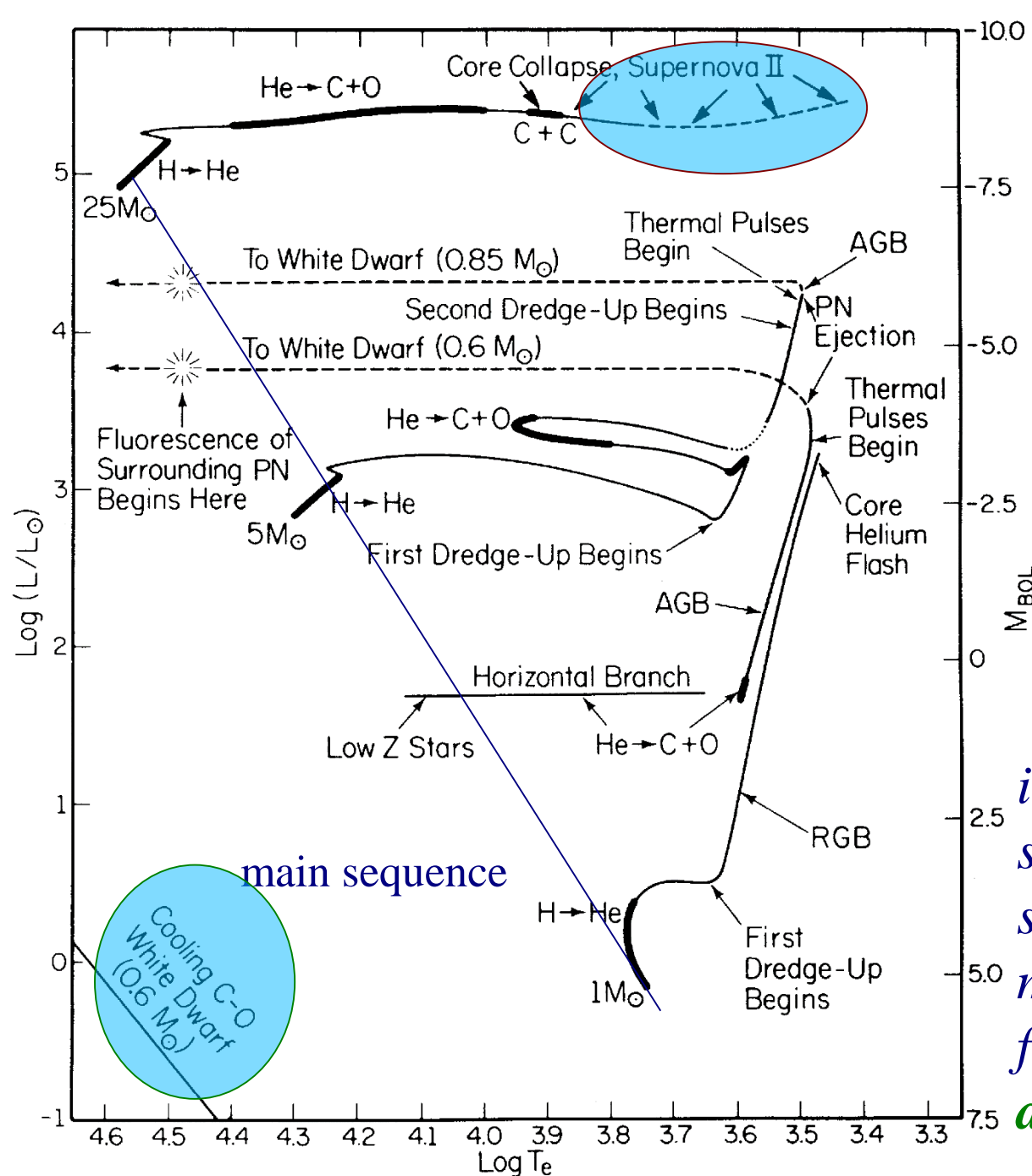
(all) photodisintegrations and capture reactions possible

\Rightarrow thermal (chemical) equilibrium

ongoing
measurements of
key fusion
reactions at low
energies

*proton/nucleon
ratio Y_e decreases
with enrichment of
“metals”!!*

Astrophysical Sites



Hertzsprung-Russell Diagram of Stellar Evolution from Iben, showing as end stages

white dwarfs and planetary nebulae

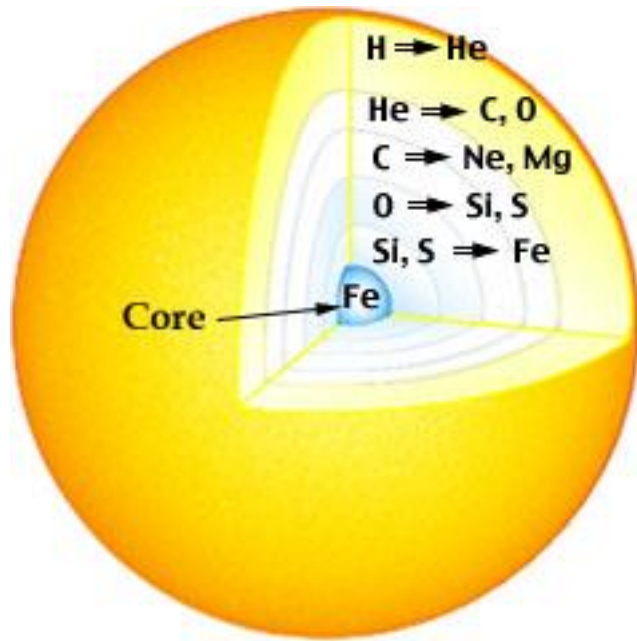
and

core collapse

(supernovae/neutron stars, black holes, hypernovae, GRBs), pair instability SNe?

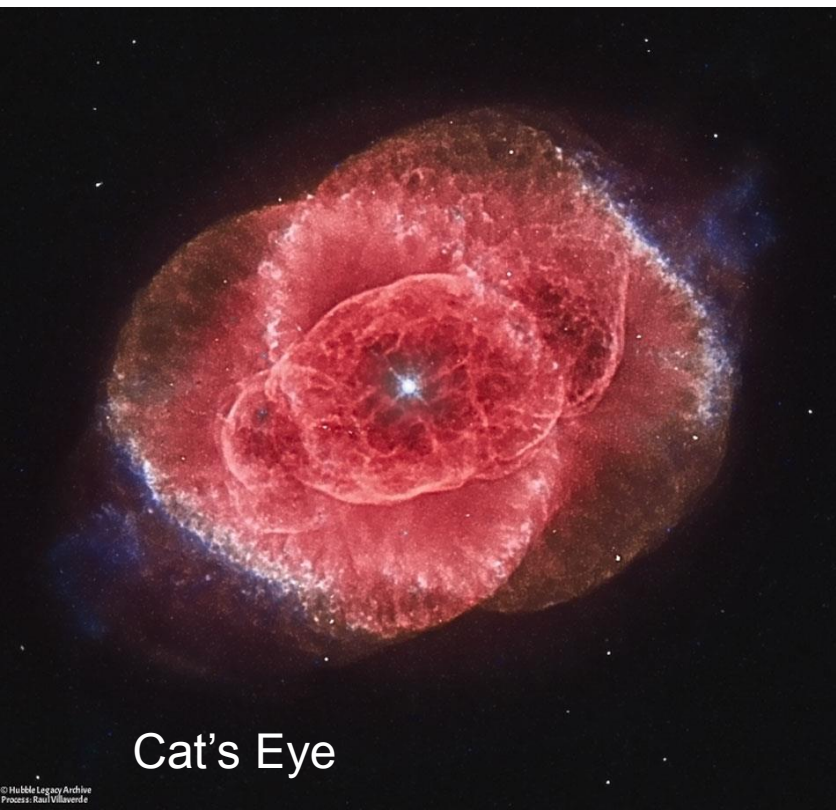
influence of reaction cross sections, e-capture in late burning stages, metallicity, rotation, magnetic fields, stellar winds on final outcome

and there are also binary systems

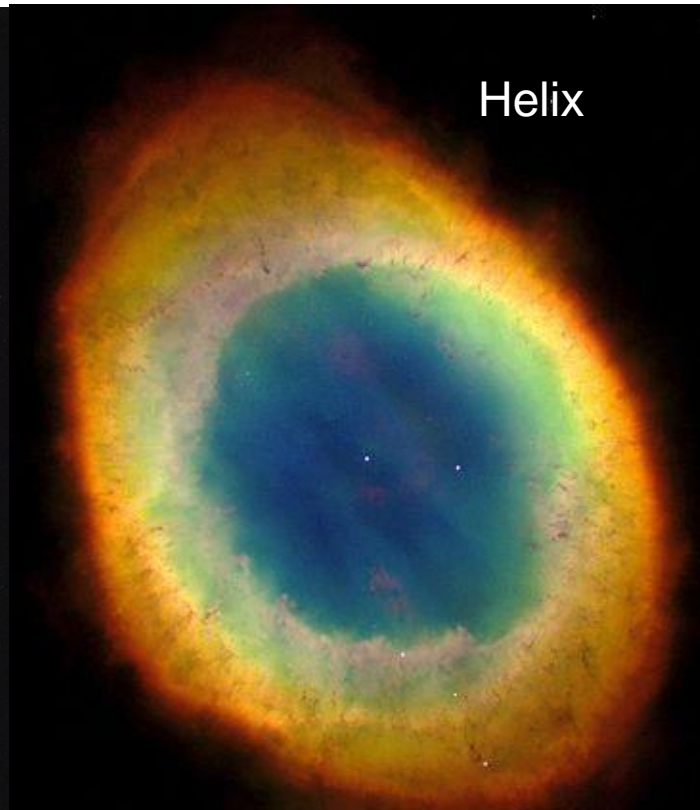


massive stars with $M > 8M_{\odot}$ pass through all burning stages up to **silicon burning**

low and intermediate mass stars experience only hydrogen and **helium burning** and end as **white dwarfs** after ejecting the outer layers in a strong wind as a planetary nebula



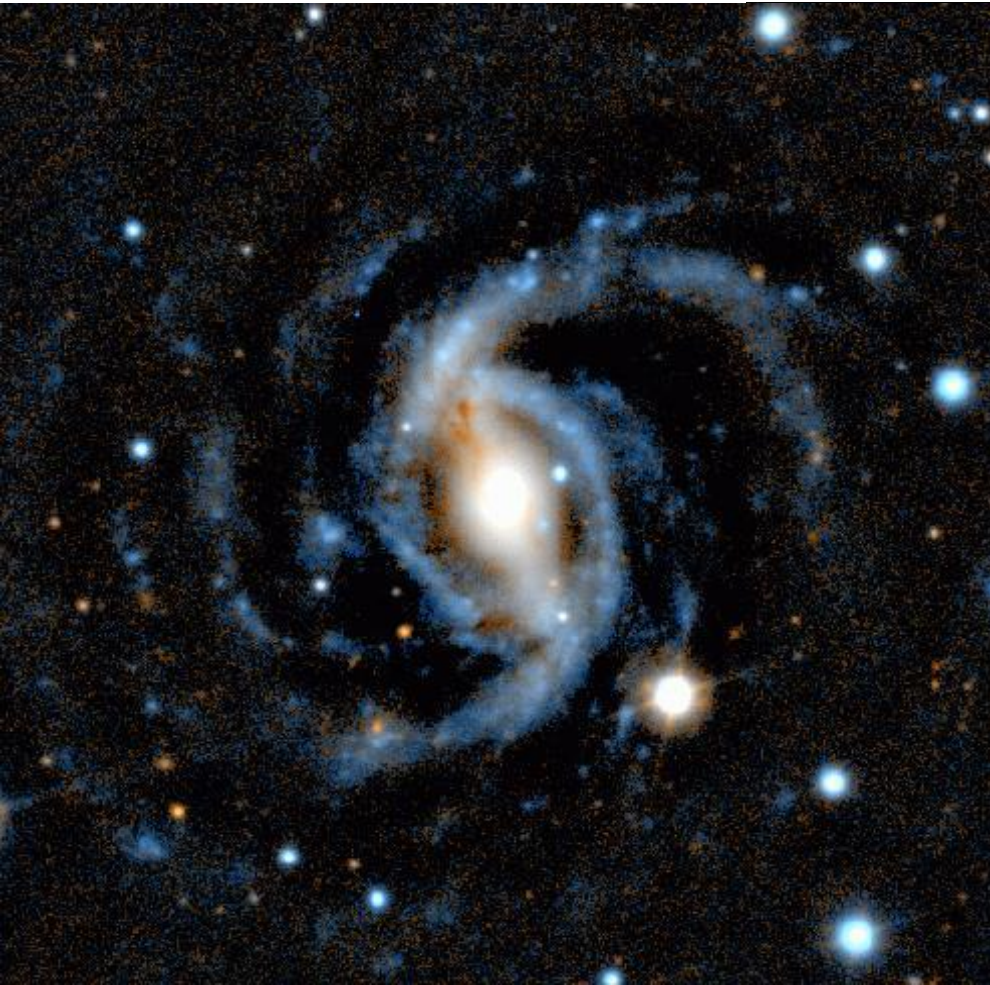
Cat's Eye



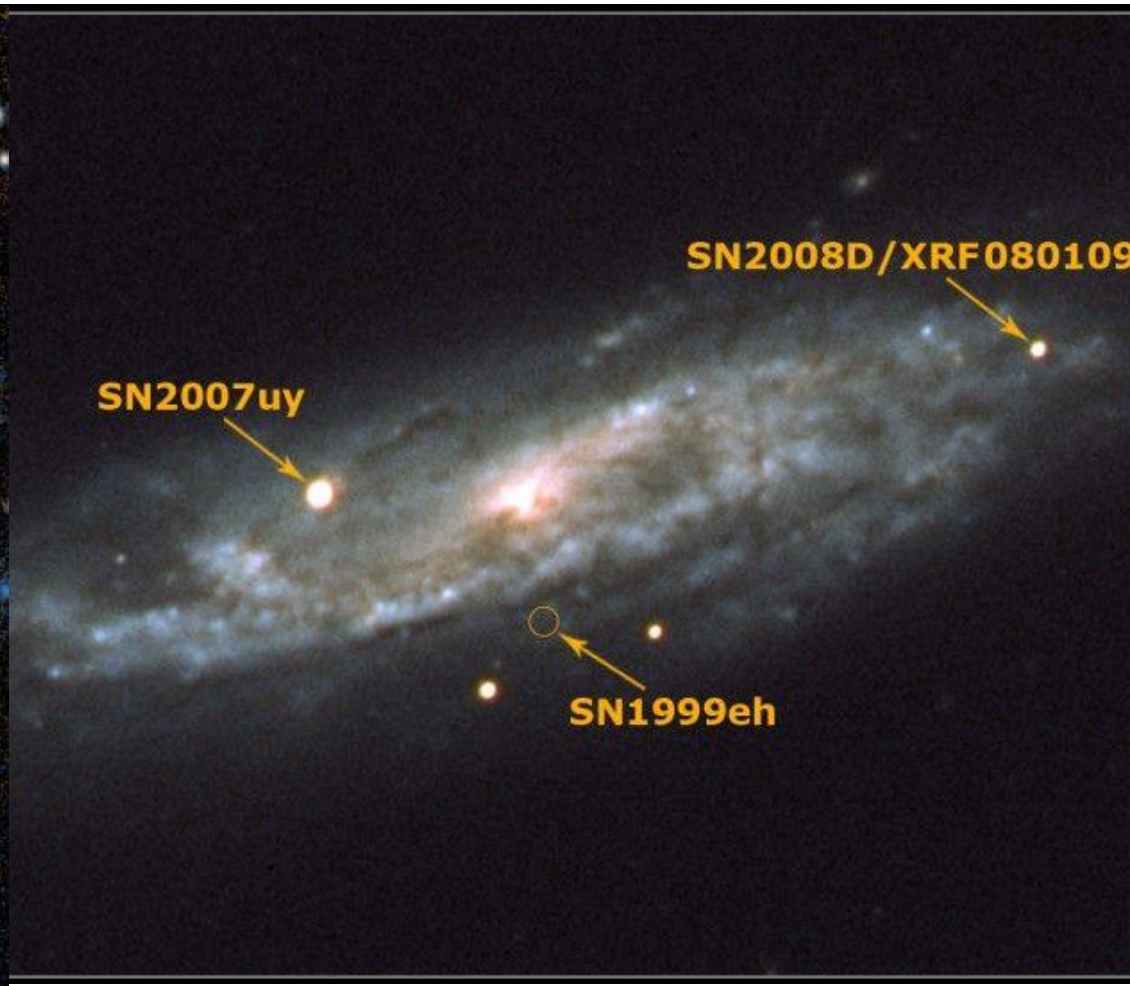
Helix

Planetary Nebulae
Cat's Eye and Helix.
Cat's Eye is on the way of forming a central white dwarf, the Helix Nebula contains already a central white dwarf.

Supernova explosions as bright as galaxies



Galaxies NGC5921



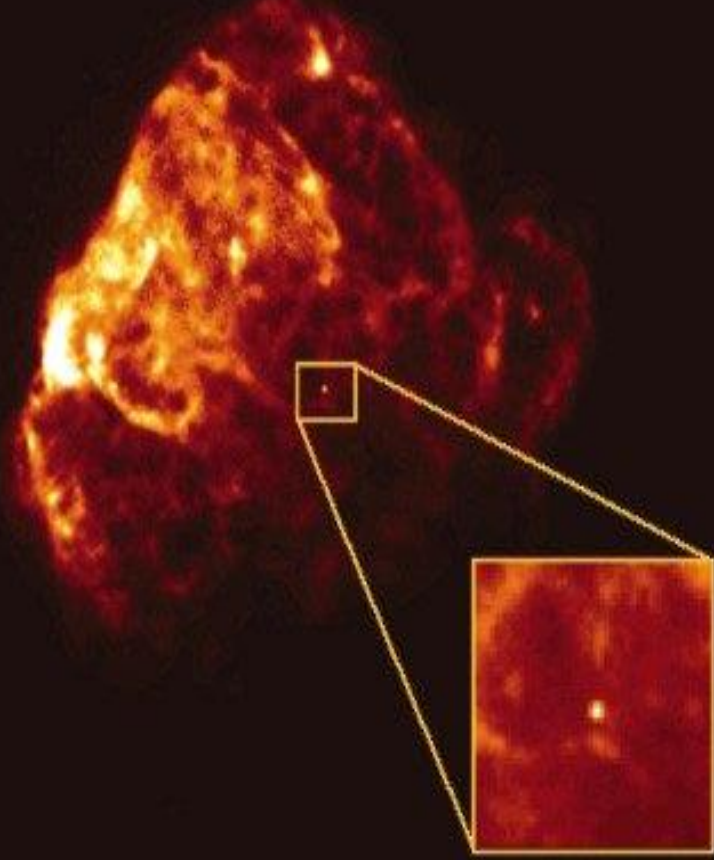
NGC2770 with supernovae (ESO)

Supernova 1987A (after and before explosion)

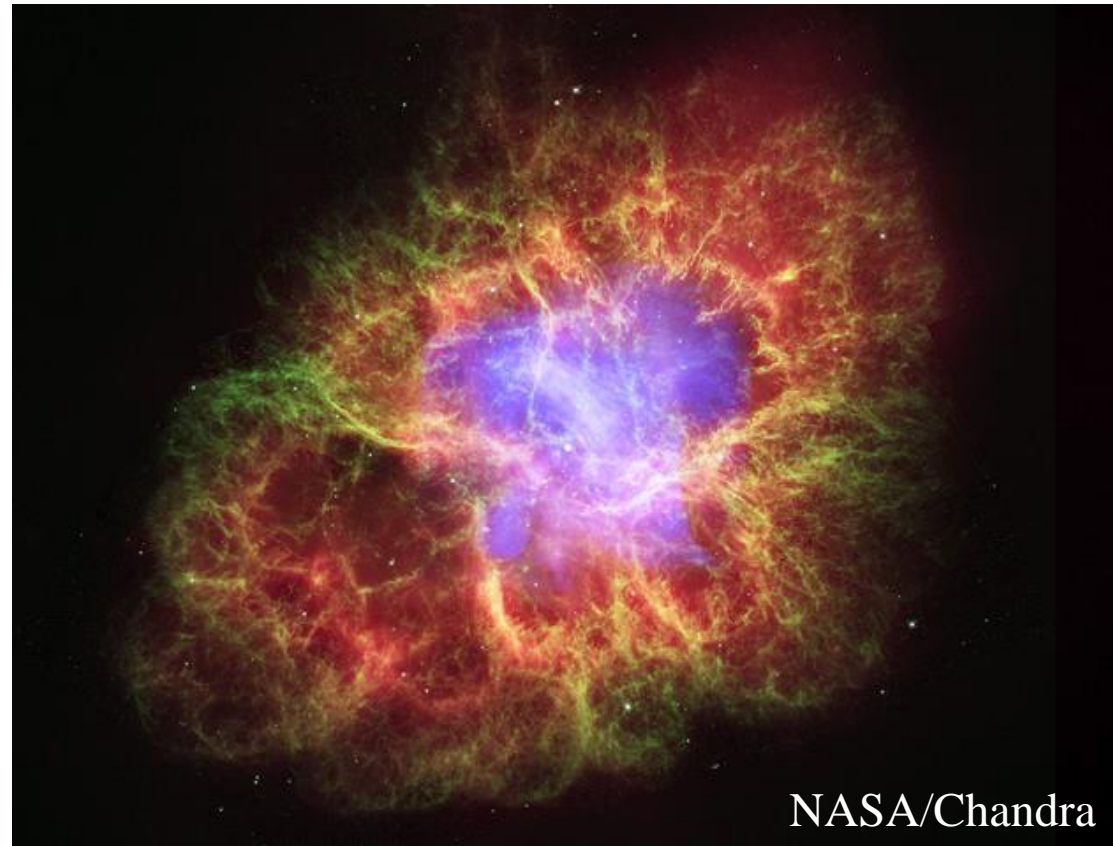


Neutron stars in supernova remnants

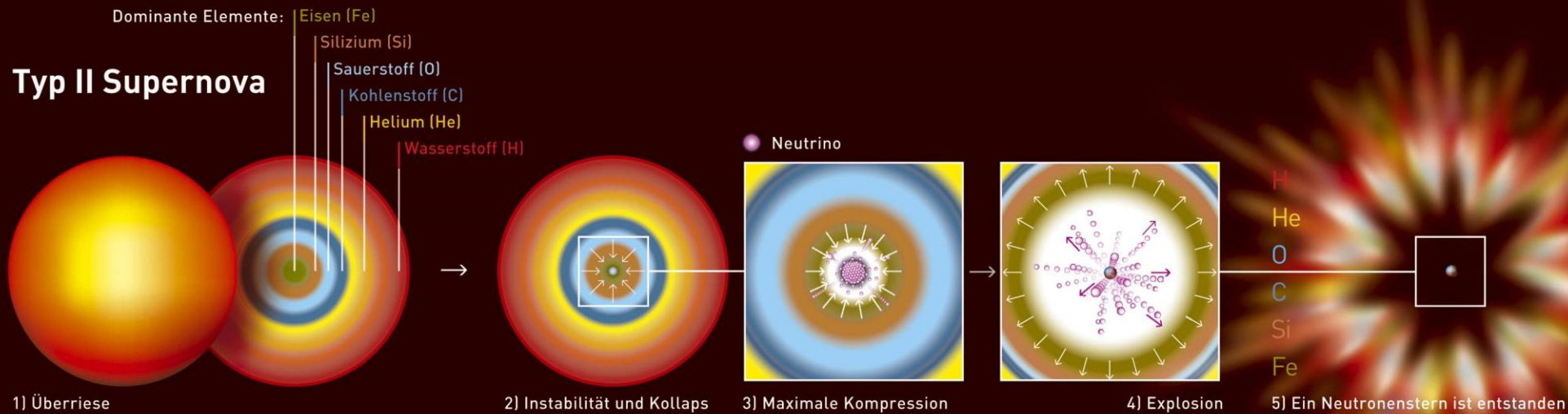
Puppis A in X-rays (ROSAT),
Supernova 3700 years ago



Crab Nebula, Explosion 1054 years ago

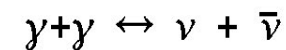
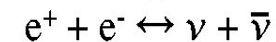
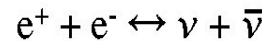
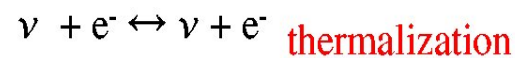
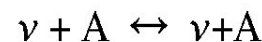
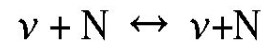
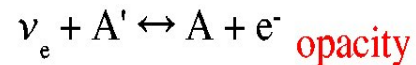
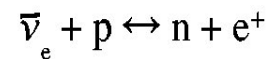
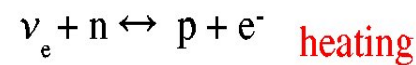
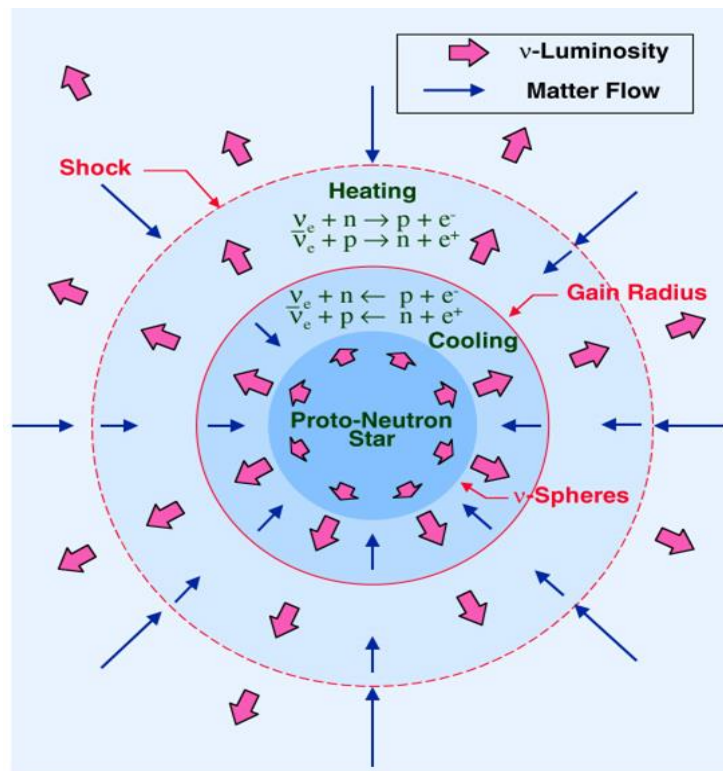


Core-collapse supernovae and neutron stars as end stages of massive stars

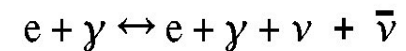


after passing through all burning stages the Fe-core collapses to a hot proto-neutron star, cooling via neutrino radiation, which heats up the surrounding layers and causes explosive ejection - for initial masses beyond $20\text{-}40M_{\odot}$ the central object exceeds the maximum stable neutron star mass and a black hole emerges

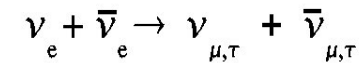
Neutrino-driven Core Collapse Supernovae



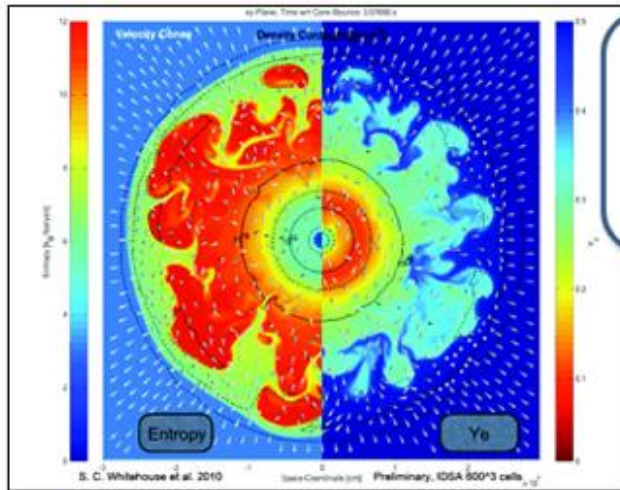
also



and



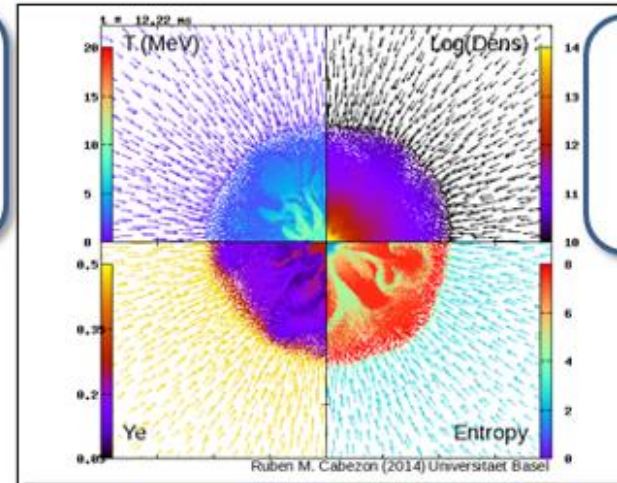
Basel activities with IDSA (Isotropic Diffusions Source Approximation) in Multi-D



Elephant

3D IDSA
Cartesian mesh
1D GR potential

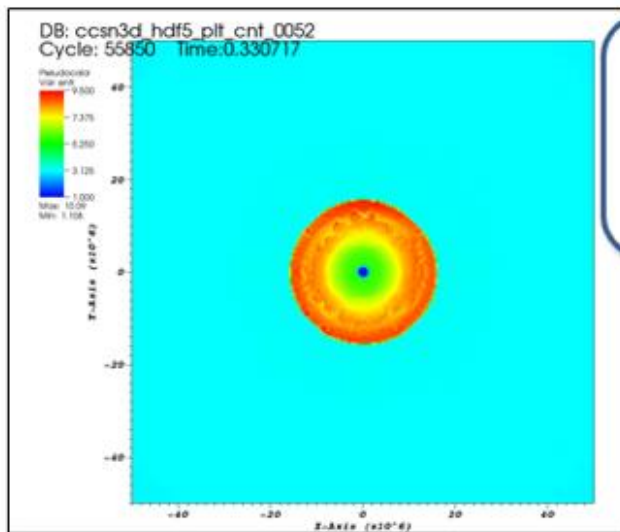
M. Liebendörfer
S. C. Whitehouse
R. Käppeli



SPHYNX

ASL
SPH
3D Newtonian

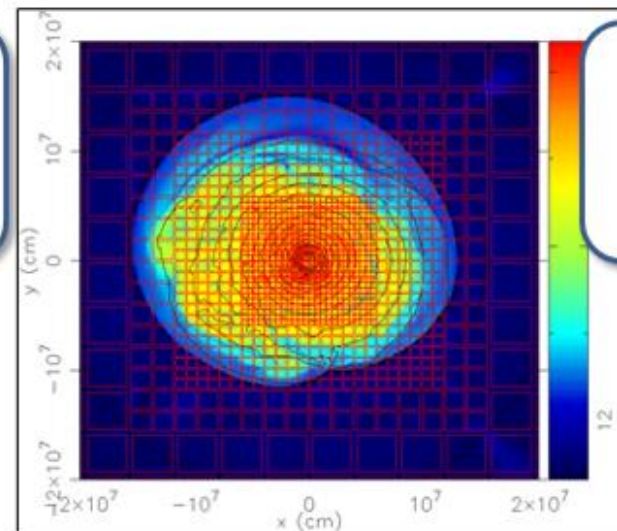
R. M. Cabezón



FLASH

3D IDSA
AMR
3D Newtonian

K.-C. Pan



fGR_M1

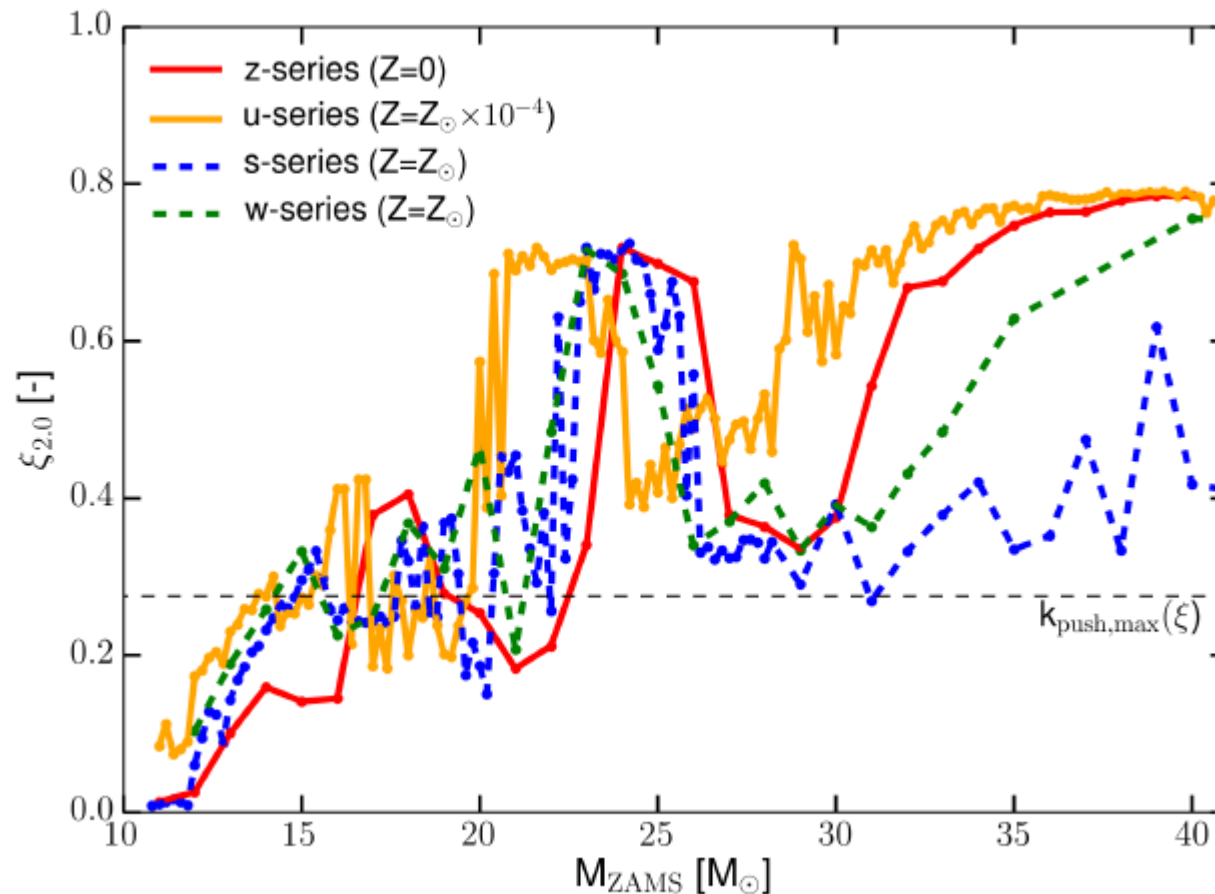
M1
Nested meshes
3D GR

T. Kuroda

Cabezón et al. (2018): a three-dimensional code-comparison project

For further comparison projects see also Just et al. (2018), 1D and 2D, O'Connor et al. (2018), 1D, but for more extended times after bounce! (also Burrows et al. 2019)

Properties of Progenitor Models for different «metallicities»



$$\xi_M = \frac{M/M_{\odot}}{R(M)/100\text{km}}$$

Compactness parameter measures in which radius a certain amount of mass is inclosed in the central region. Here $M=2M_{\odot}$ is utilized. **Provides a measure how easy it is for the neutrino heating explosion mechanism to result in a successful explosion.**

Ebinger et al. (2019)

Explosion energy (1Bethe= 10^{51} erg)

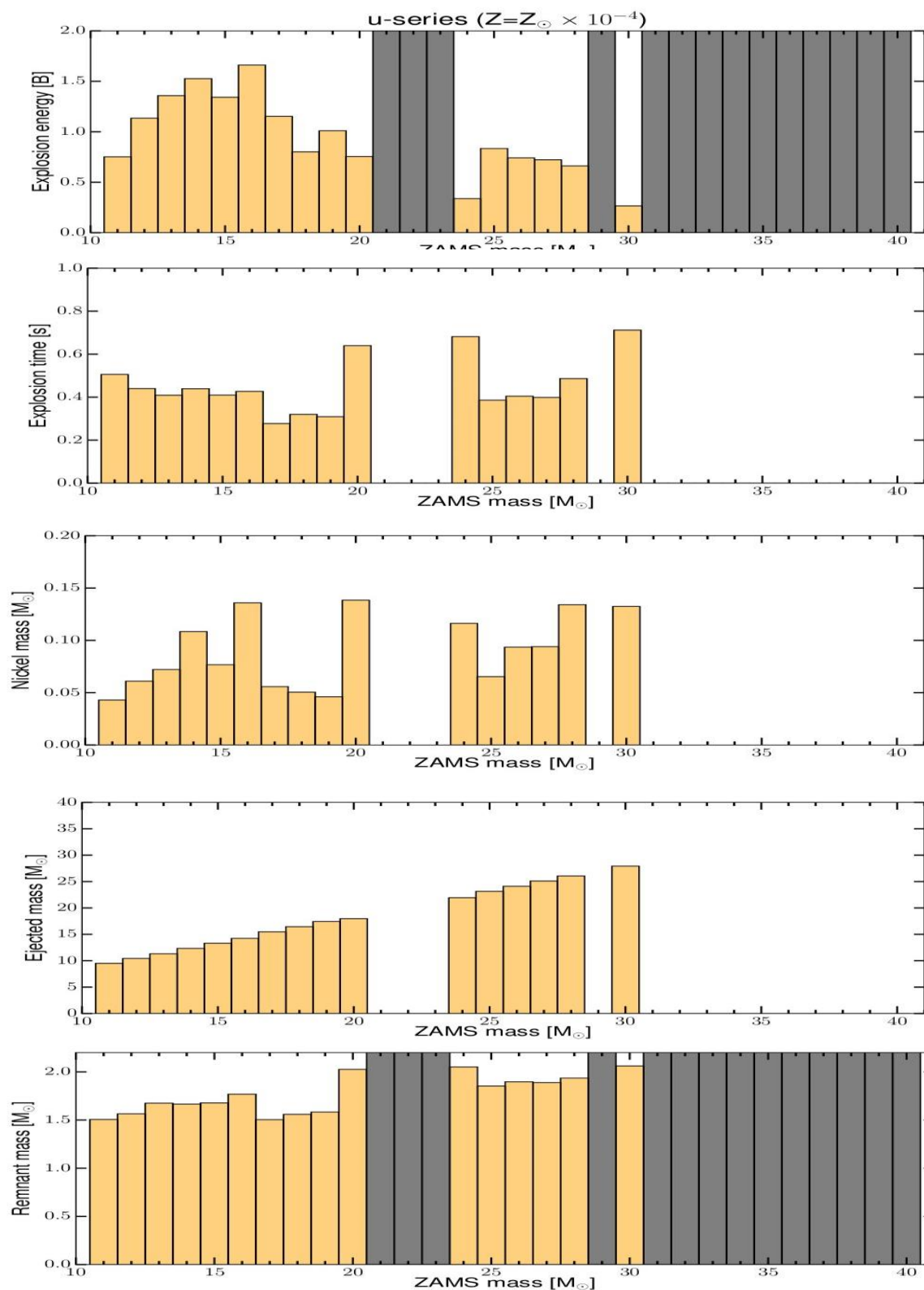
Results of supernova simulations

Explosion time after collapse

Ejected Ni (^{56}Ni) mass

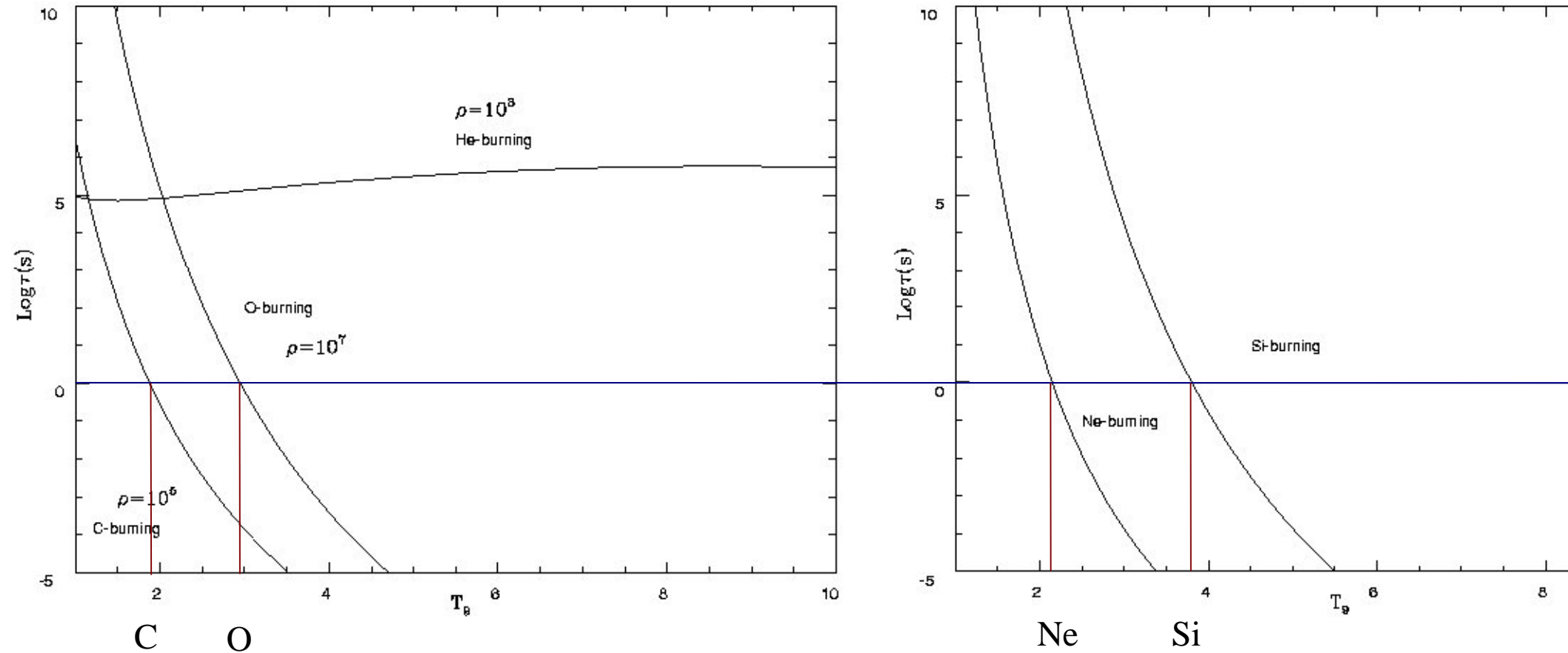
Ejected total mass

Remnant mass
neutron star



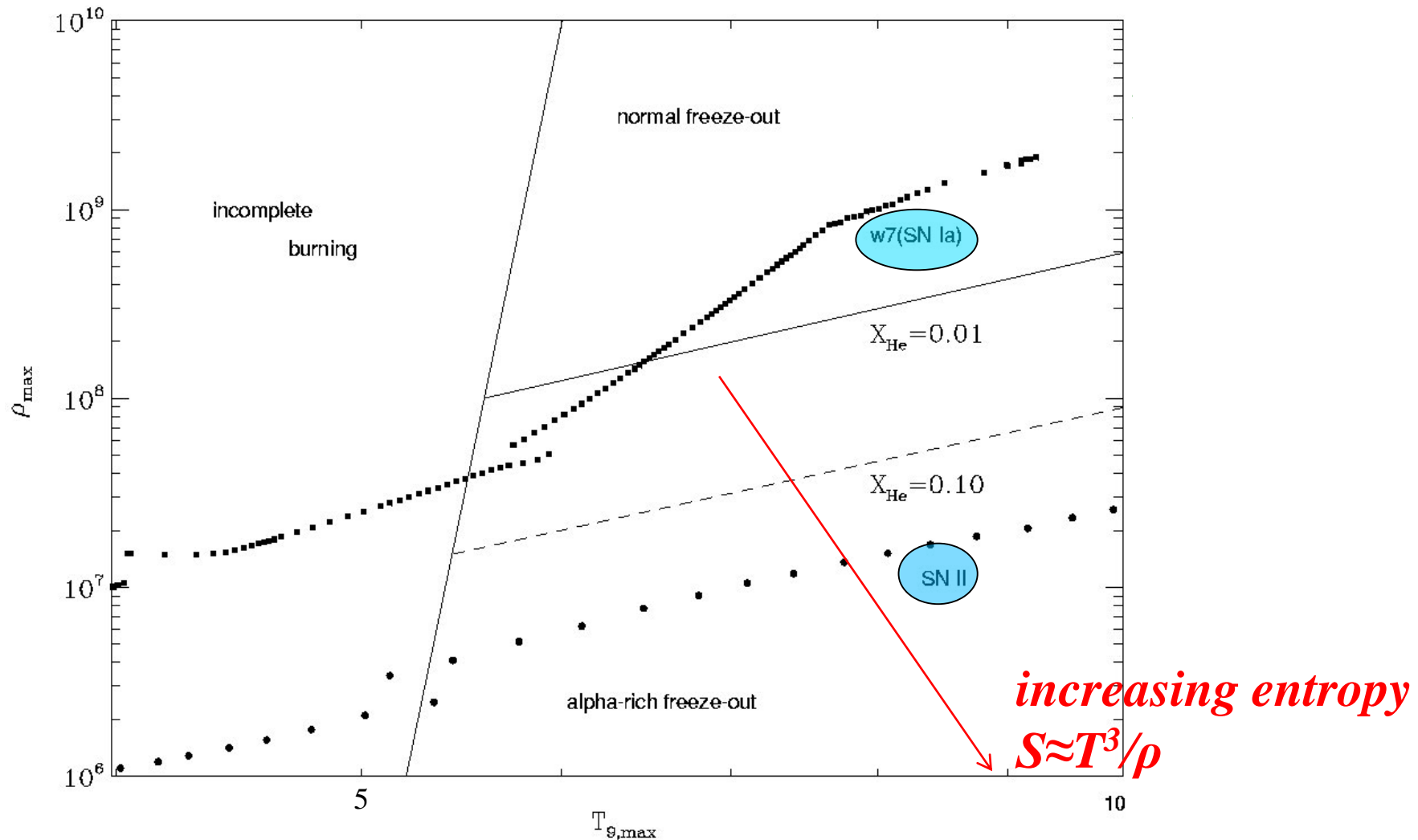
Explosive Burning

Time scales decrease exponentially with increasing temperature, in comparison with the long time scales at low temperatures in stellar evolution



typical explosive burning process timescale order of seconds: fusion reactions (He, C, O) density dependent (He quadratic, C,O linear)
photodisintegrations (Ne, Si) not density dependent

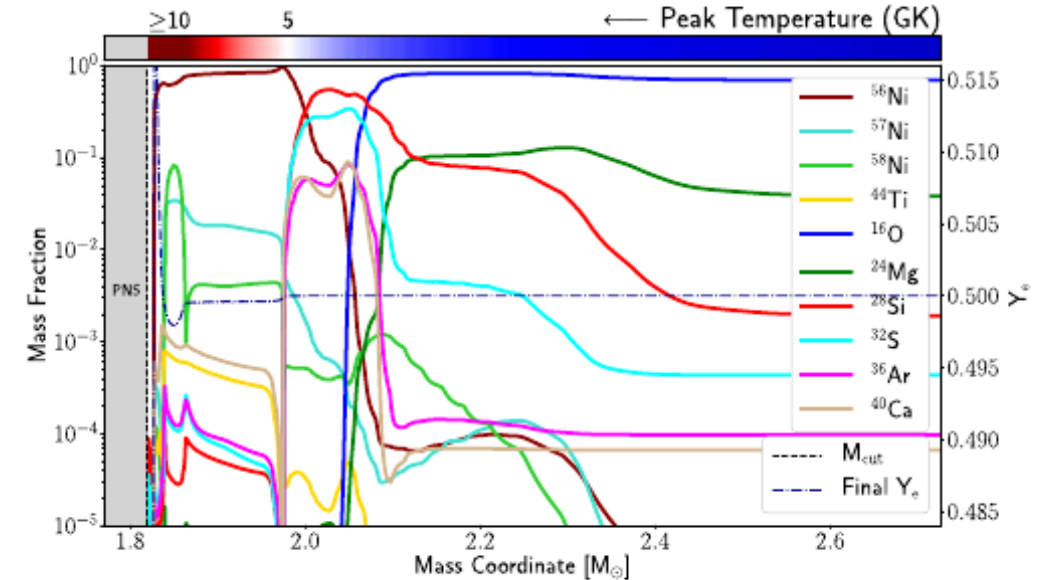
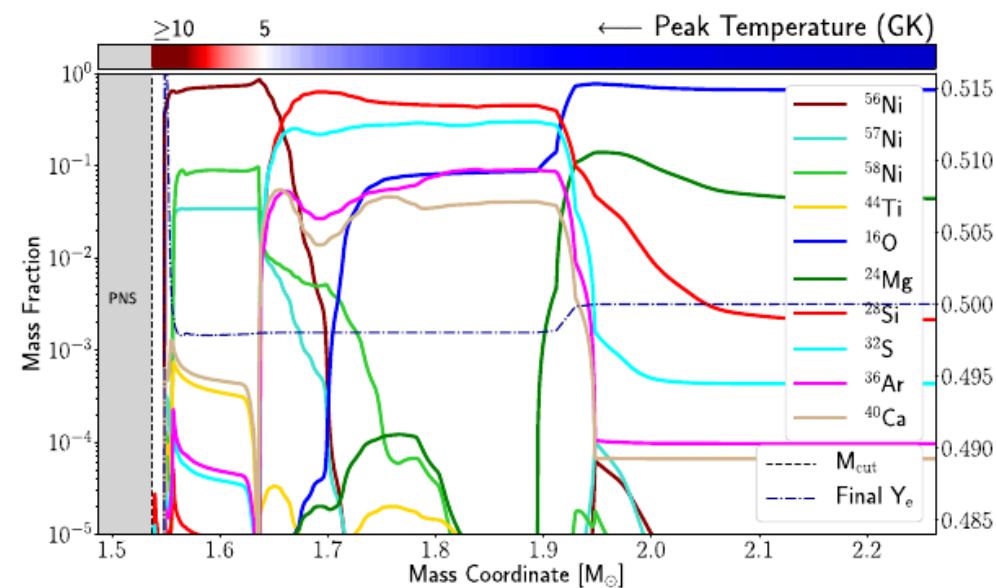
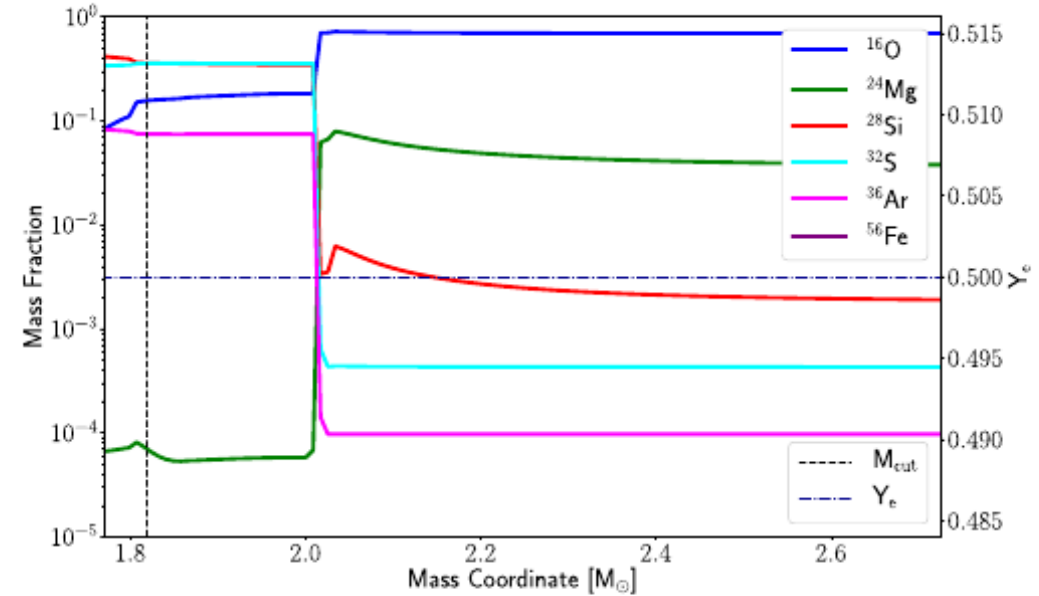
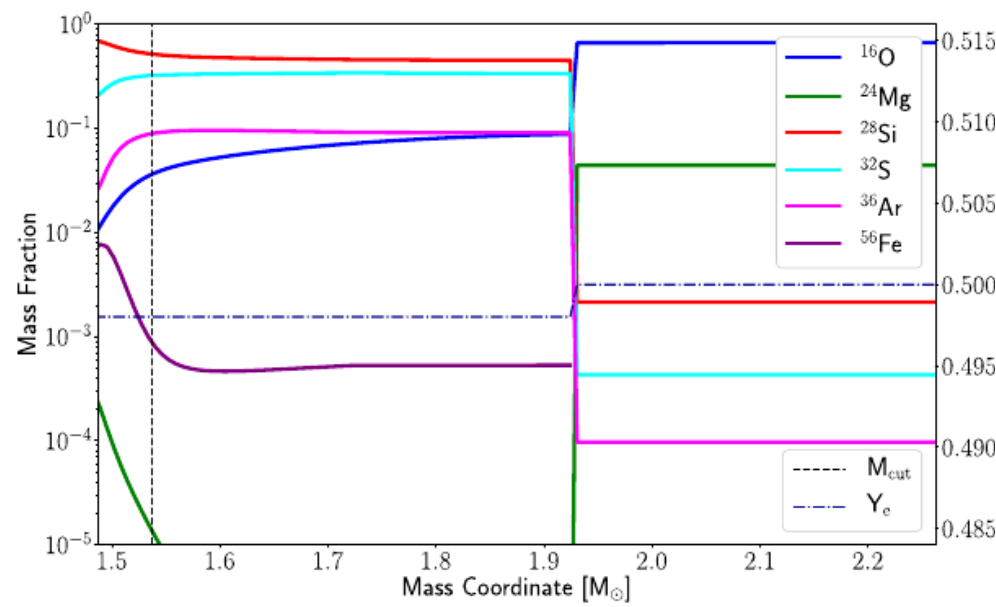
Explosive Si-Burning



Explosive Burning above a critical temperature destroys (photodisintegrates) all nuclei and (re-)builds them up during the expansion. Dependent on density, the full NSE is maintained and leads to only Fe-group nuclei (normal freeze-out) or the reactions linking ^4He to C and beyond freeze out earlier (alpha-rich freeze-out).

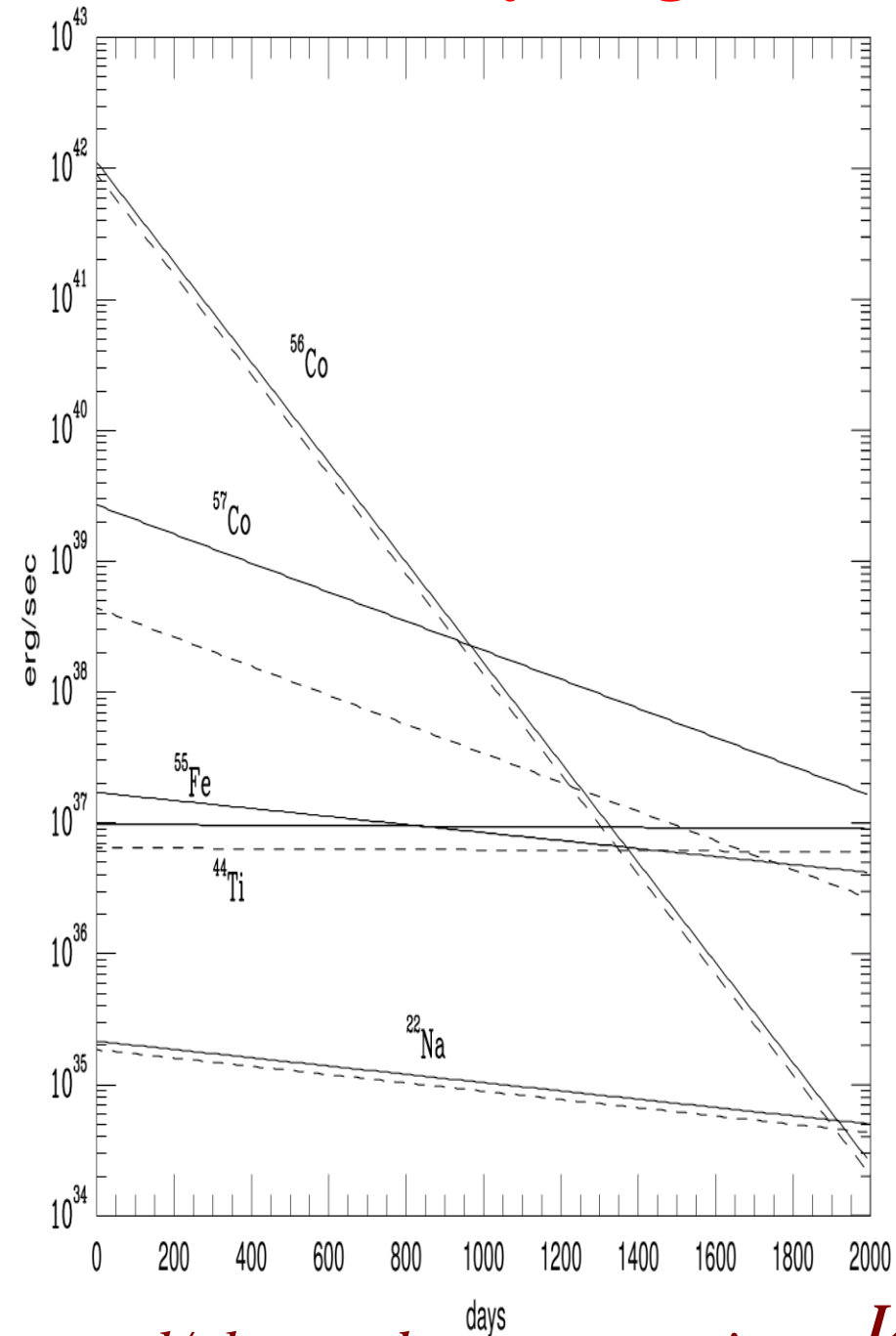
Composition in Pre-Explosion Model and Explosive Ejecta (Curtis et al. 2019)

for 16 and 21 Msol progenitors (based on PUSH approach)

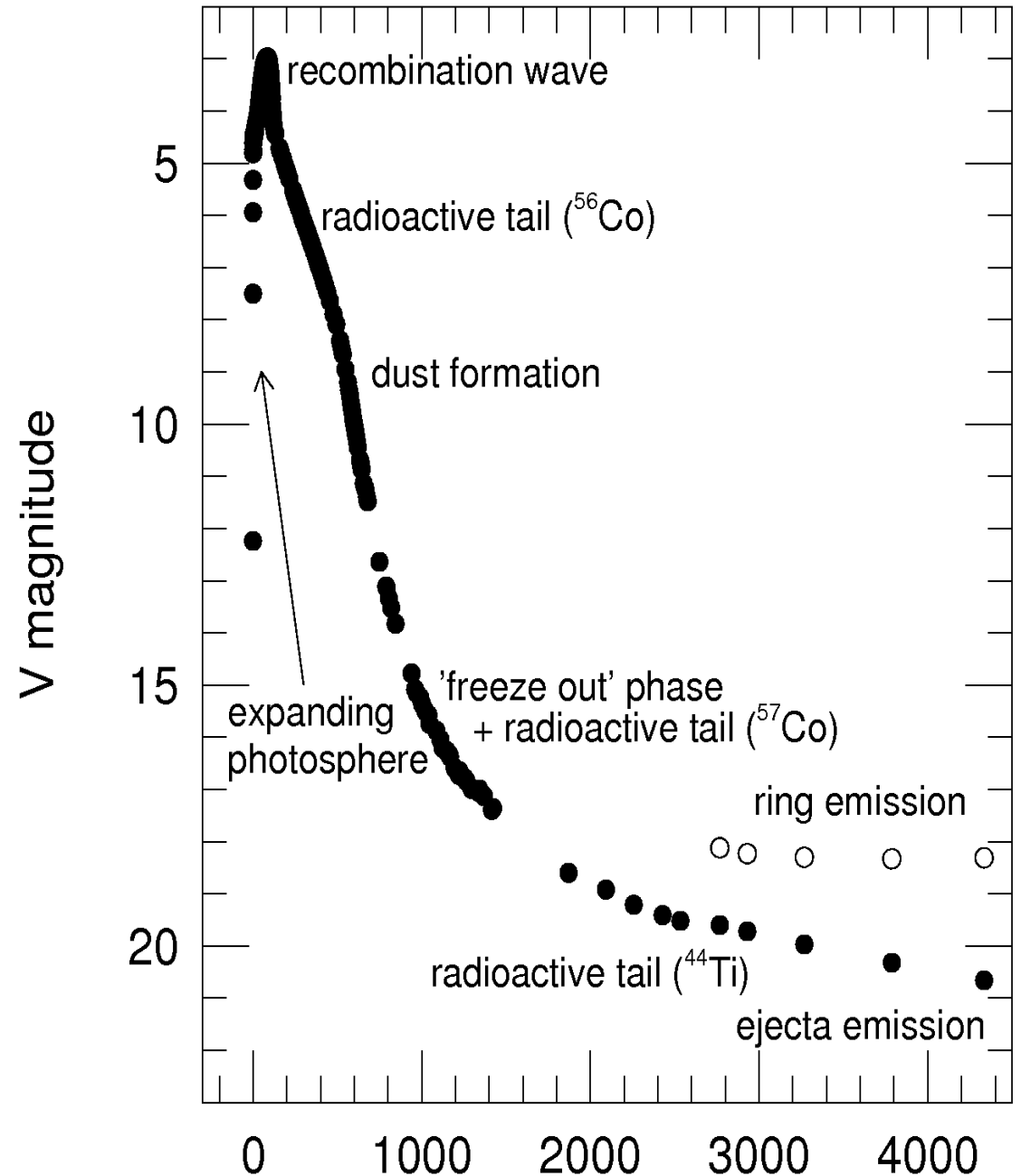


Y_e on right abscissa (dashed), being in the outer layers unchanged from the initial (hydrostatic) Y_e close to 0.5, decreased due to (beta⁺-decays and e-captures) in explosive Si-burning, and enhanced via neutrino interactions with matter in inner layers at small radii. Innermost layers not well visible here, see next transparency

Radioactivity Diagnostics of SN1987A: $^{56}\text{Ni}/\text{Co}$, $^{57}\text{Ni}/\text{Co}$, ^{44}Ti



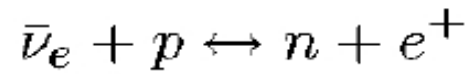
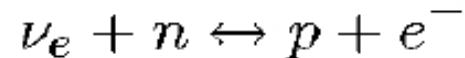
*total/photon decay energy input
from models*



Leibundgut (ESO) & Suntzeff 2003, other determinations (e.g. ^{44}Ti undertaken by Fransson+ Stockholm)

What determines the neutron/proton or proton/nucleon= Y_e ratio in ejecta?

Y_e dominantly determined by e^\pm and $\nu_e, \bar{\nu}_e$ captures on neutrons and protons



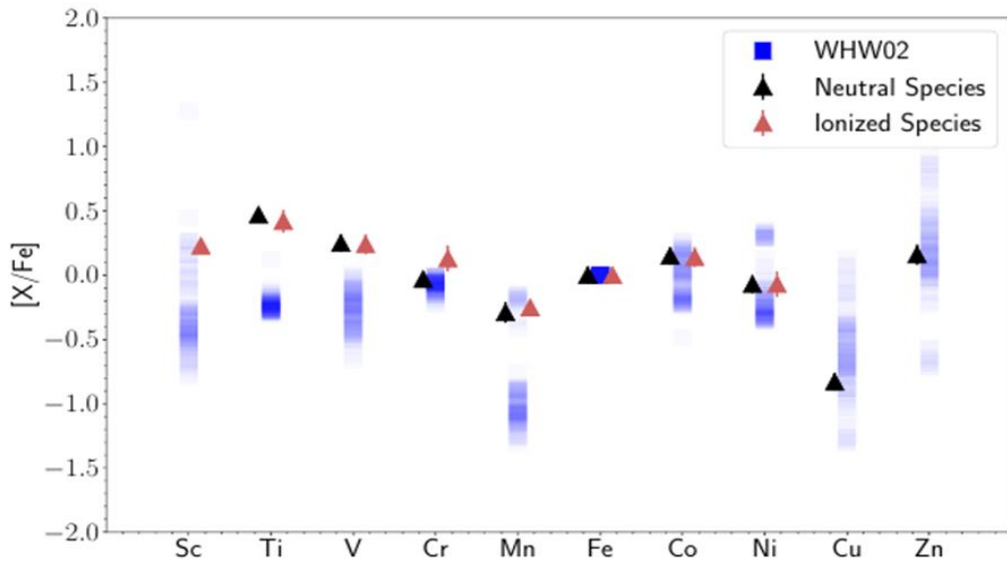
- high density / low temperature \rightarrow high E_F for electrons \rightarrow e-captures dominate \rightarrow n-rich composition
- if el.-degeneracy lifted for high $T \rightarrow \nu_e$ -capture dominates \rightarrow due to n-p mass difference, p-rich composition

If neutrino flux sufficient to have an effect (scales with $1/r^2$), and total luminosities are comparable for neutrinos and anti-neutrinos, only conditions with $E_{\bar{\nu}_e} - E_{\nu_e} > 4(m_n - m_p)c^2$ lead to $Y_e < 0.5$!

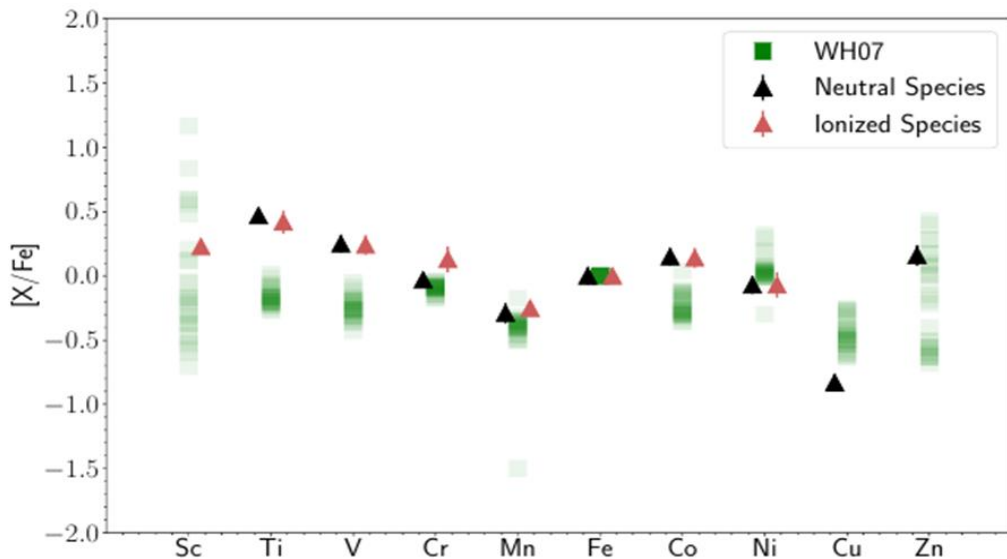
Otherwise the interaction with neutrinos leads to proton-rich conditions.

The latter favors improvements in the Fe-group composition Sc, Ti, Co, including the production of $^{64}\text{Ge} (\rightarrow ^{64}\text{Zn!})$, and the *vp-process*, which can produce nuclei up to Sr, Y, Zr and Mo. (Fröhlich, Martinez-Pinedo, Pruet, Wanajo .. Eichler)

Comparison of low metallicity star HD 84937 (Sneden et al. 2016) with predicted CCSN yields



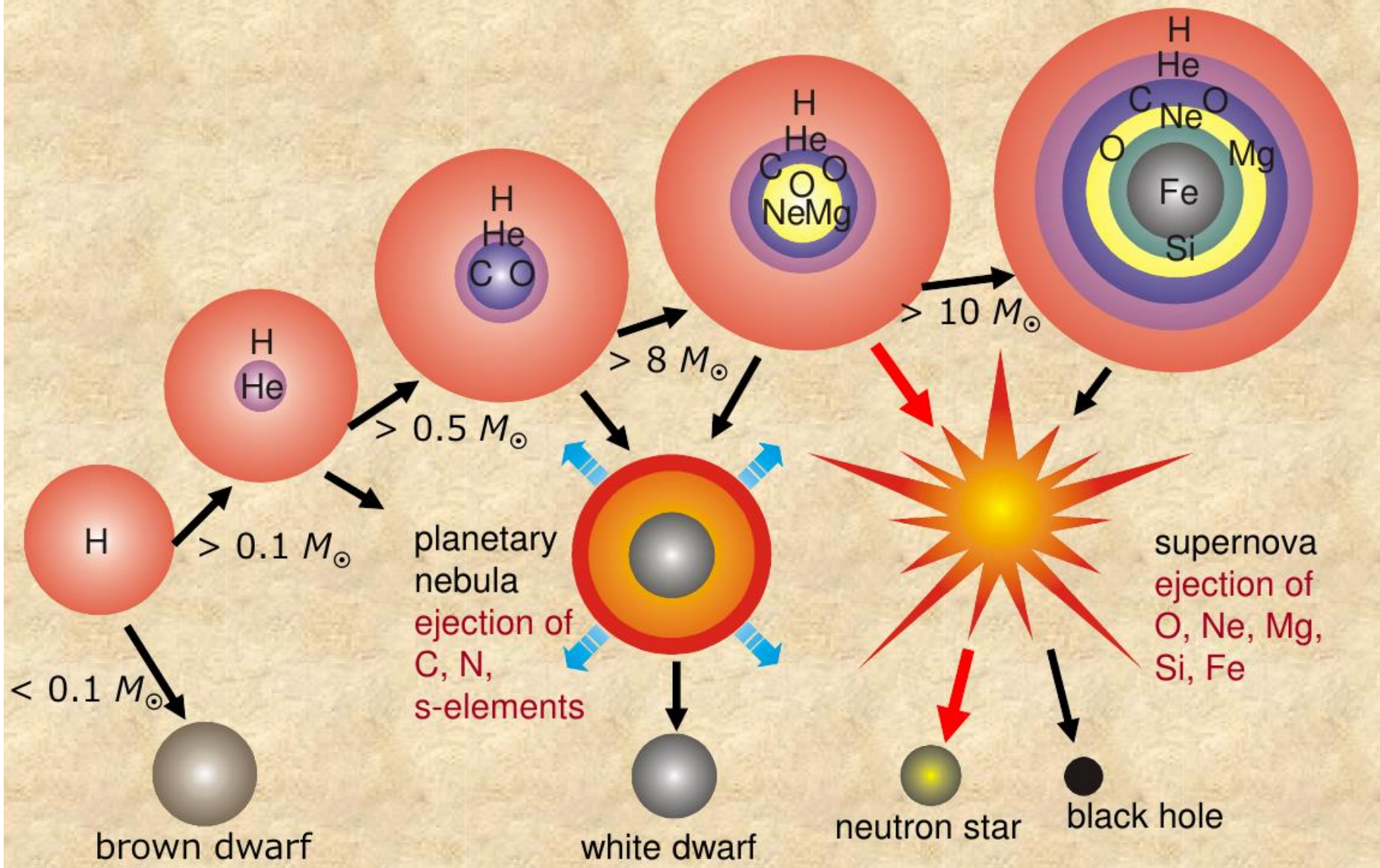
Good fit to Fe-group composition of low metallicity stars which is dominated by core-collapse supernovae and essentially due to introducing the Y_e -variations caused by neutrino interactions during core-collapse and explosion (first suggested by Fröhlich et al. 2006a).



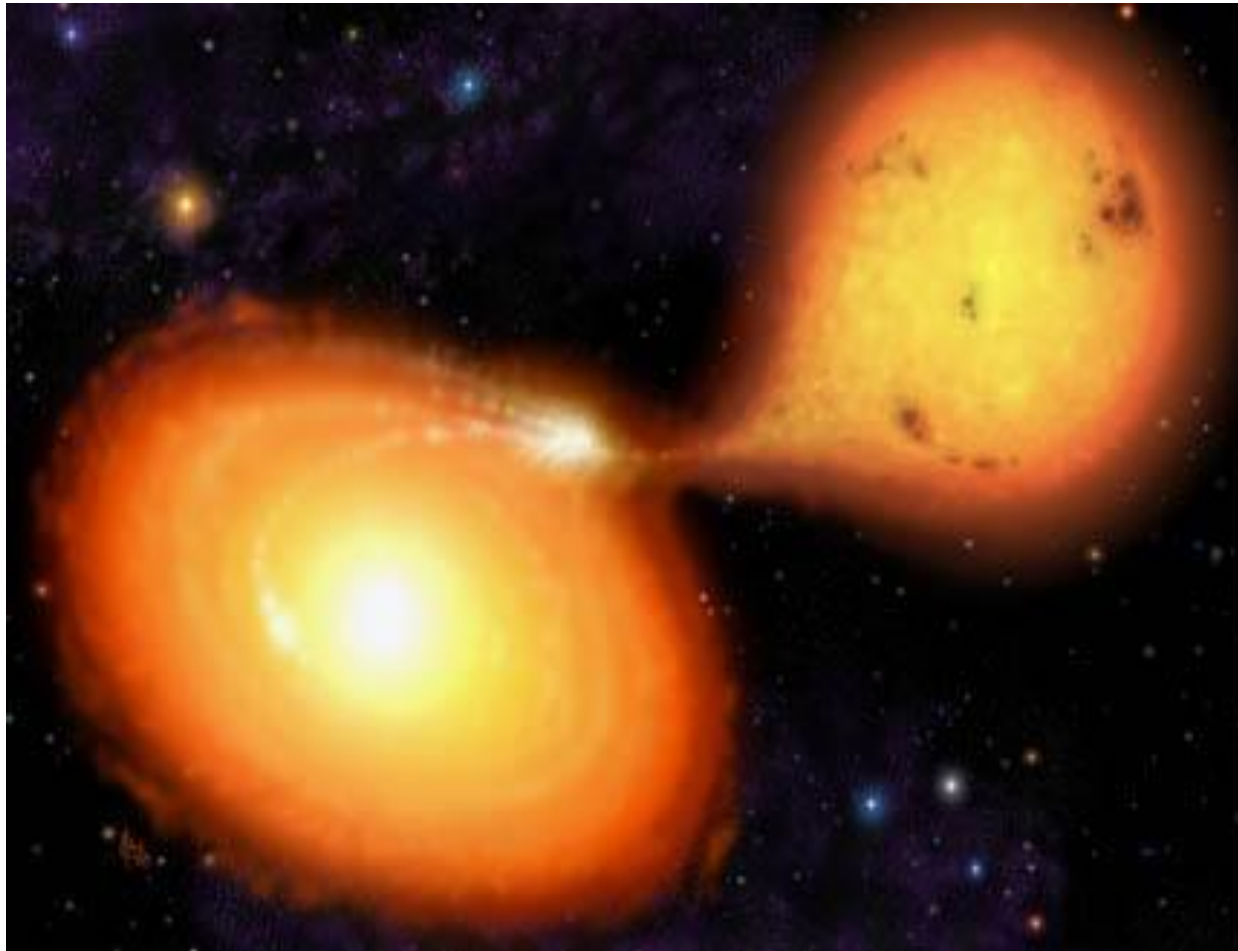
The shaded boxes pass through the whole mass sequence of the two progenitor sets.

Curtis et al. (2019)

fate of stars and nucleosynthesis



Mass transfer in binary stellar systems



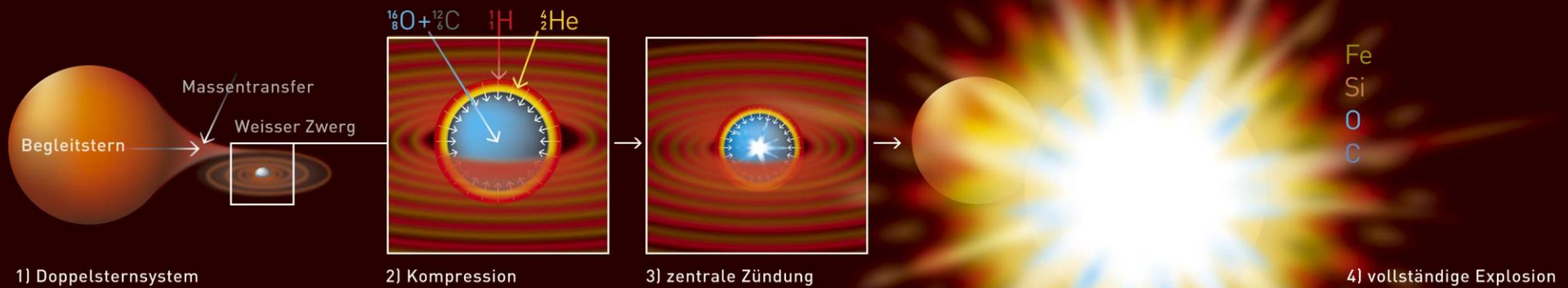
the growing radius of a star (when turning into a Giant) can lead to situations when the gravity towards the binary companion becomes larger than to its stellar center (mass transfer) - the star grows beyond the Roche Lobe

Unburnt hydrogen is accreted

When reaching a critical mass of the accreted layer explosive hydrogen burning is ignited (nova on a white dwarf, X-ray burst on a neutron star)

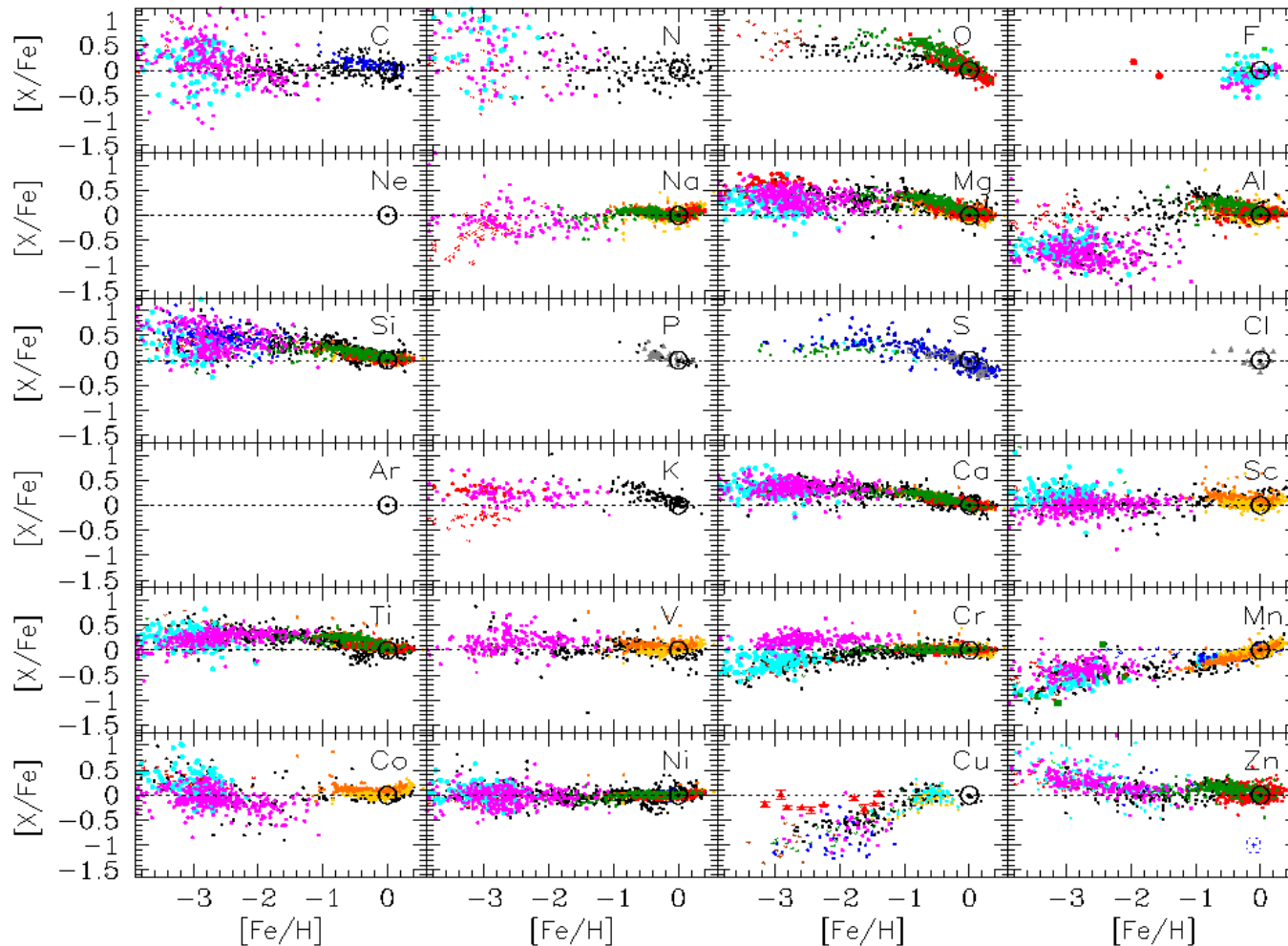
Typ Ia supernovae via massen transfer in binary systems containing a white dwarf

Typ I (a) Supernova



the “single degenerate” scenario, causing collapse and complete explosion when reaching the Chandrasekhar mass. In this case (dependening in initial WD mass and accretion rate) about $0.6 M_{\odot}$ of $^{56}\text{Ni} \rightarrow ^{56}\text{Fe}$ are produced. We know today that also “double-degenerate” (WD mergers) and sub-Chandrasekhar explosions contribute as well

Spektra of old stars witness the element evolution in the Galaxy



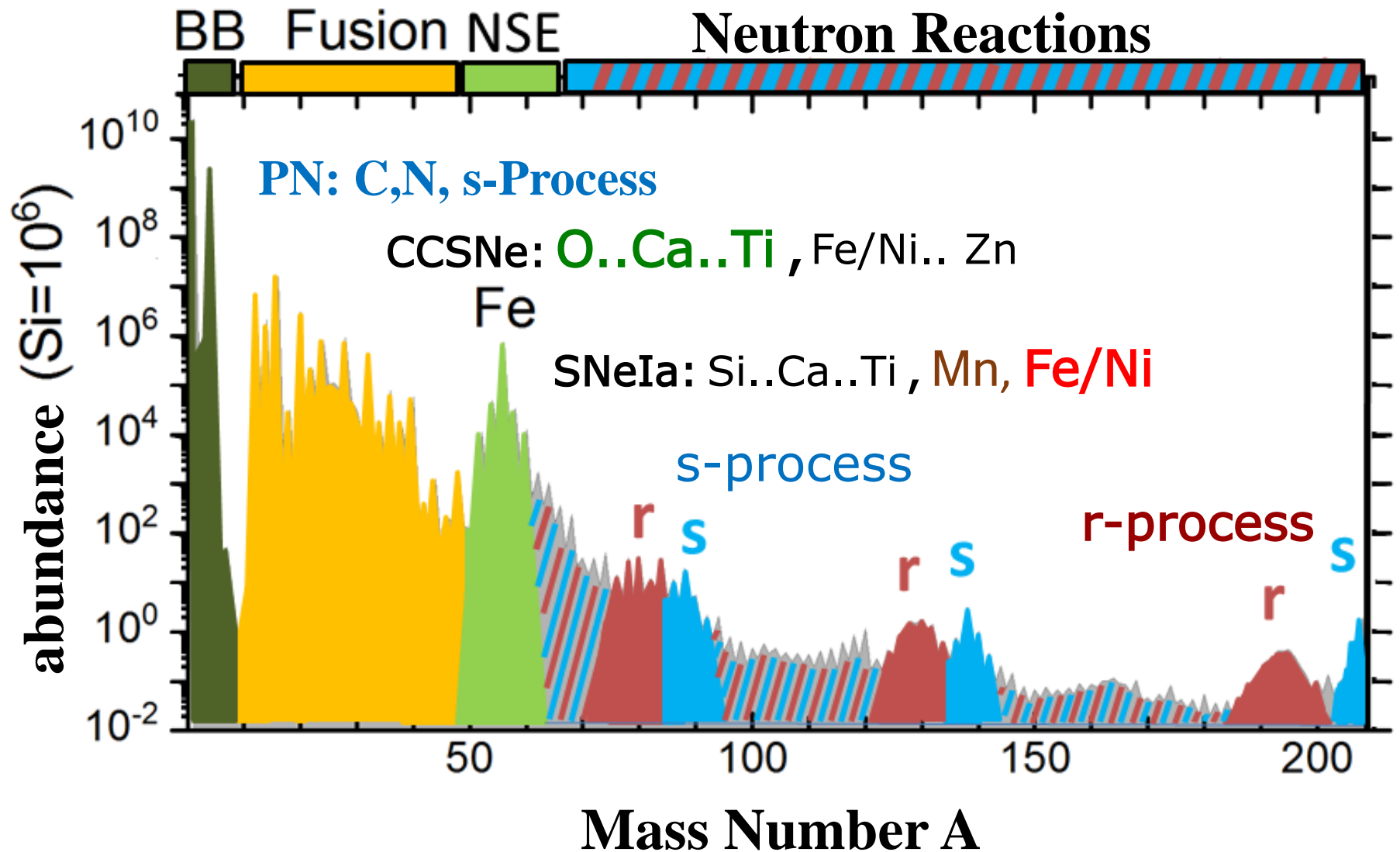
N. Prantzos

The ratio of the «alpha elements» ($X=O, Mg, Si, S, Ca, Ti$) vary with increasing Fe, i.e. time. Early on only fast evolving Core-collapse supernovae contribute with a higher ratio to Fe (e.g. O/Fe) than solar (logarithm = 0 solar, 0.5 faktor 3 larger than solar).

During galactic evolution Typ Ia supernovae set in delayed: (a) low mass stars take a long time to form White Dwarfs, (b) binary evolution with a White Dwarf up to the Typ Ia supernova explosion delayed further. Typ Ia supernovae produce large amounts of Fe and reduce the ratio of alpha elements to Fe.

BBN ${}_{1,2}\text{H}$, ${}_{3,4}\text{He}$, ${}_{7}\text{Li}$

How are elements heavier than Fe made?



slow neutron capture (s-process) and rapid neutron capture (r-process)

How can the heavy elements be made?

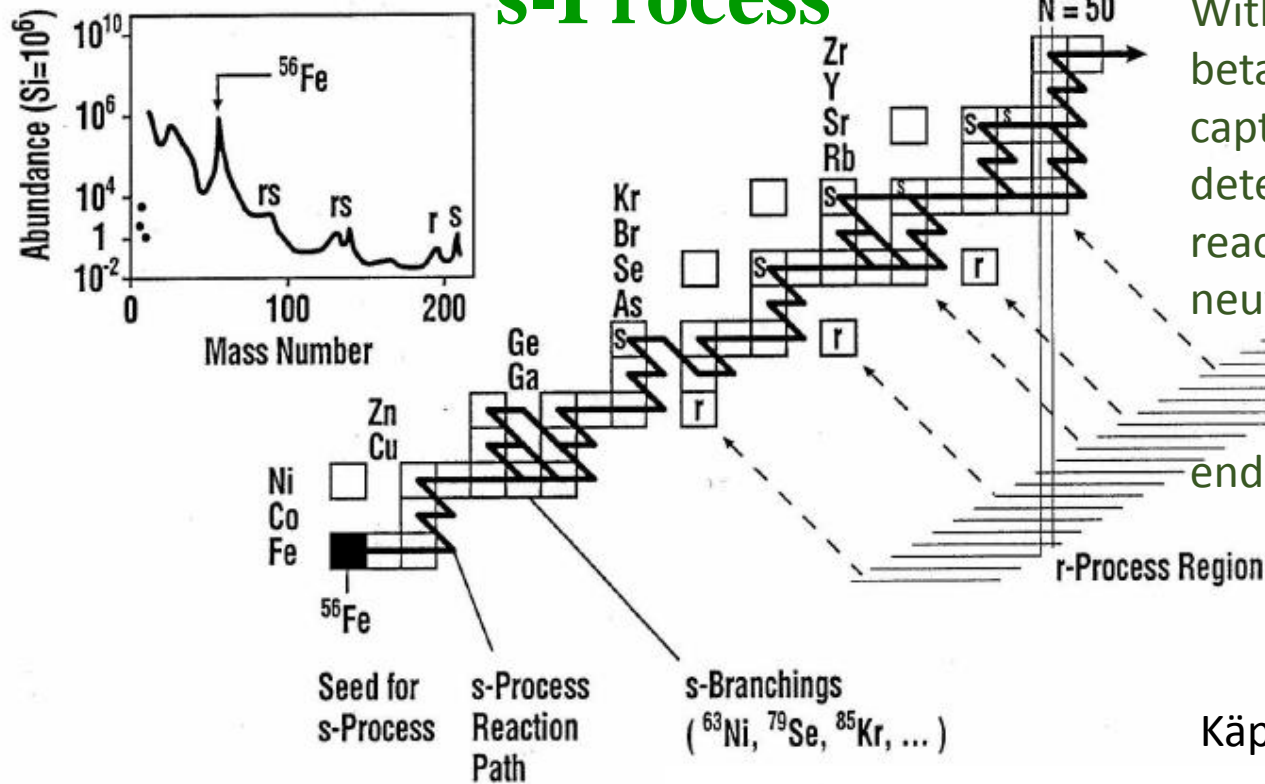
Fusion with charged particles (protons, alphas, nuclei) required increasing temperatures with the increasing charge of heavier nuclei. To enable such reactions above the Fe-group (which formed in a nuclear statistical (chemical) equilibrium) would need temperatures above $5 \cdot 10^9$ K, where the reverse photodisintegrations win and no built-up of heavier nuclei is possible with charged-particle reactions (minor exceptions are only possible for very high densities, which can be found on the surface of neutron stars).

The only way to produce heavier nuclei/elements is via the capture of neutrons which do not experience Coulomb repulsion and which is possible at low temperatures. The only caveat is that neutrons have a half-life of about 10min, i.e. they need to be produced locally via reactions.

In stellar evolution the neutron sources are $^{22}\text{Ne}(\alpha, n)^{25}\text{Mg}$ and $^{13}\text{C}(\alpha, n)^{16}\text{O}$ (the latter being much stronger). This leads to a low abundance of neutrons, i.e. in most cases the beta-decay of unstable nuclei is much faster than the next neutron capture and the reaction path of this slow process (*s-process*) passes close to stable nuclei.

If in an explosive environment huge amounts of neutrons are released, neutron captures can be much faster than beta-decays (i.e. this happens rapid), leading to an *r-process* up to 20 neutron numbers away from stable nuclei.

s-Process

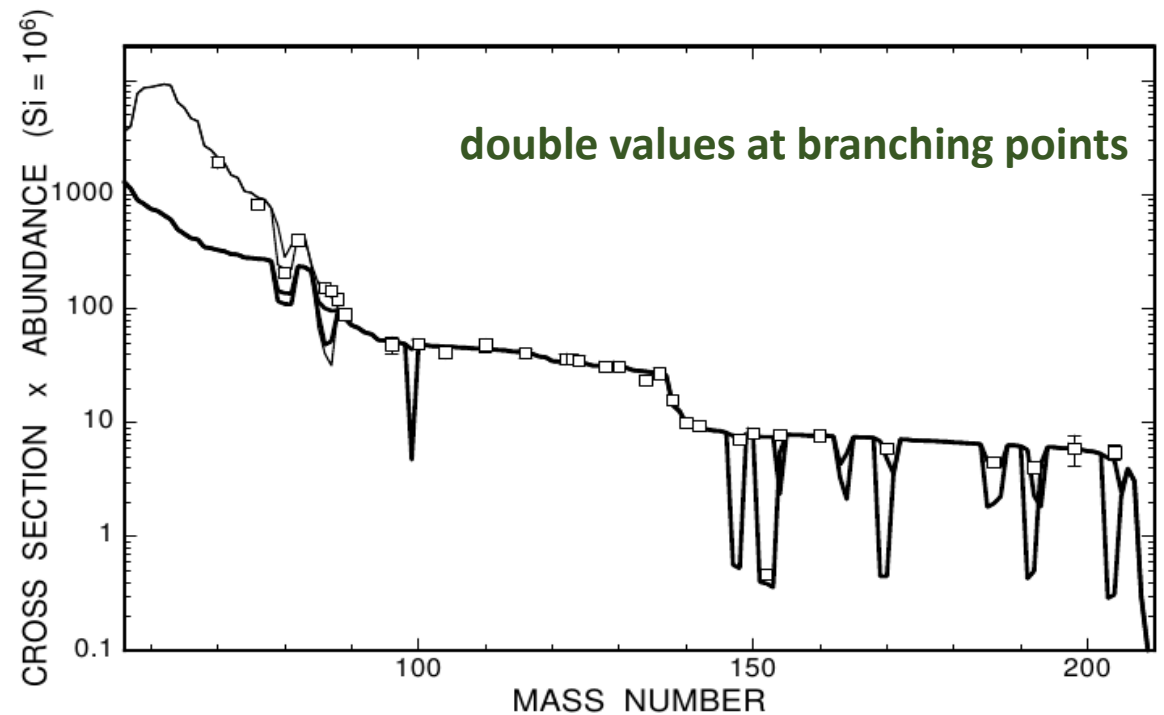


With few exceptions (so-called branchings) beta-decays are much faster than neutron captures and the speed of the process is determined by the neutron capture reaction cross sections. Above Pd and Bi neutron captures lead to alpha unstable nuclei, i.e. (n,α) reactions form nuclei with Z-2 and the process ends there to produce heavier nuclei.

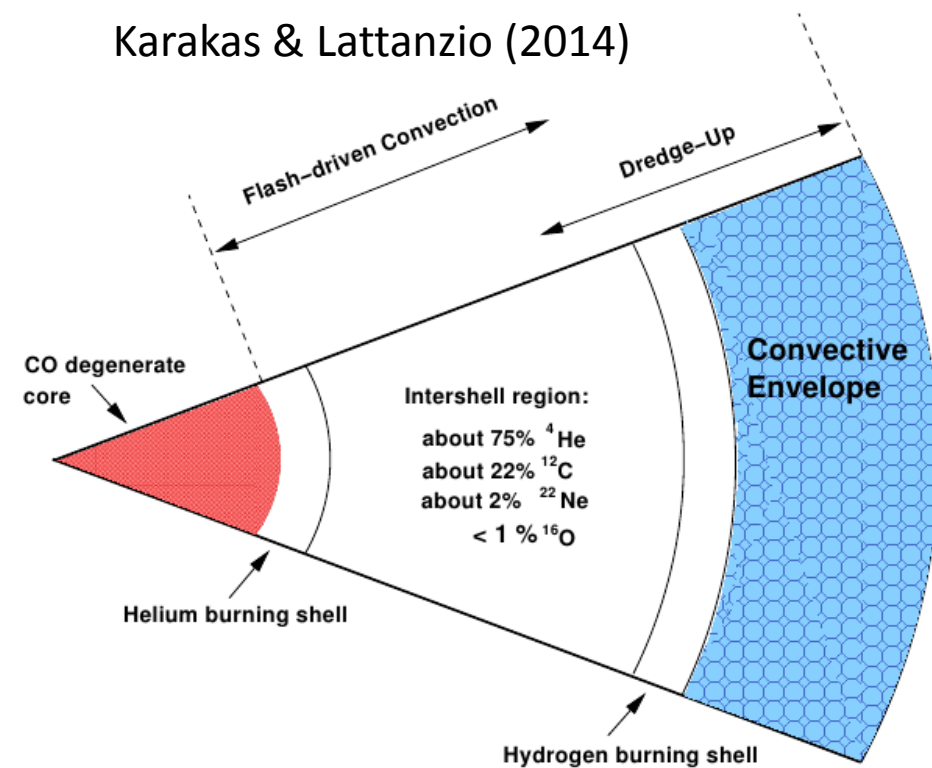
Käppeler et al. (2011)

In a steady-flow equilibrium the neutron capture on nucleus (Z,N) is as fast as its production via neutron capture on nucleus (Z,N-1).

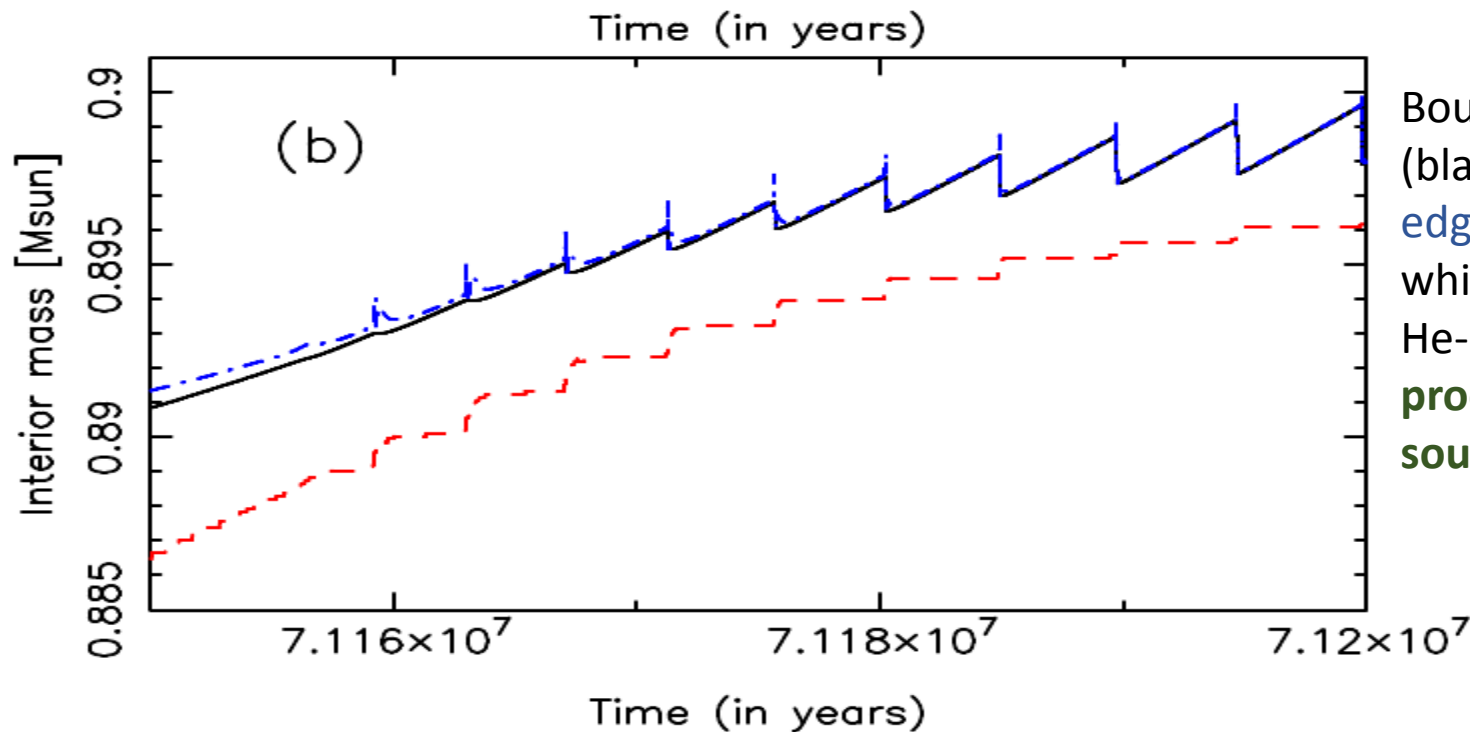
This leads to a steady-flow equilibrium, causing the product of the abundance of a nucleus and its neutron-capture cross section to be constant. The adjacent figure shows that this is the case with the exception of neutron shell closures, where reaction Q-values and reaction rates are small, i.e. they cause a barrier in the flow.



Karakas & Lattanzio (2014)

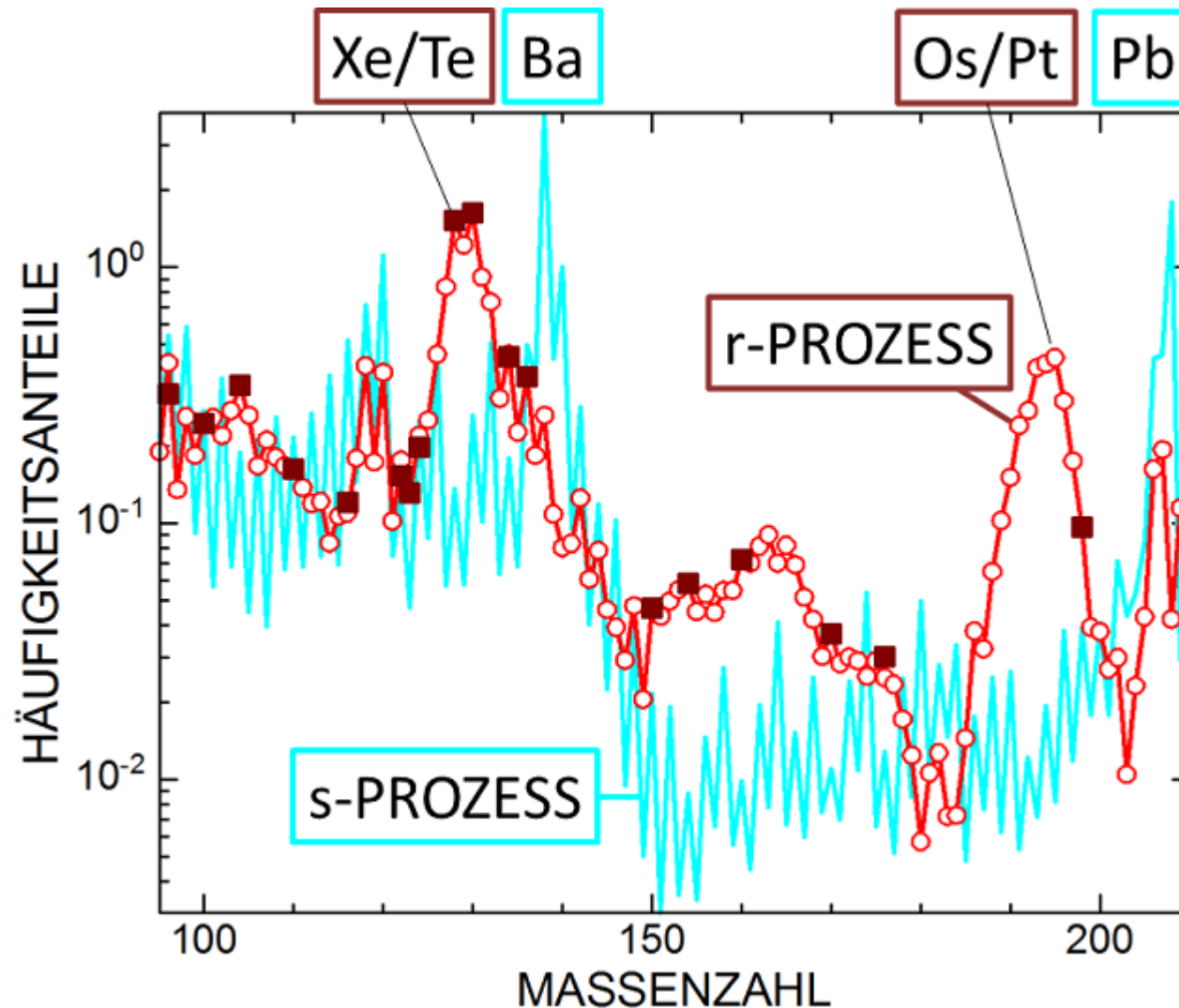


s-process in low and intermediate mass stars: the H- and He-shells are located at small distances. They do not burn in a constant fashion. If the H-burning zone is on, it creates He fuel. After sufficient He is produced, He is ignited in an unburned He-rich zone (at sufficient densities and temperatures). The burning is not stable, the amount of energy created in a shallow zone is not sufficient to lift the overlaying H-shell which would cause expansion + cooling, i.e. steady burning. Instead He-burning, being dependent on the density squared, burns almost explosively (flash), causing then a stronger expansion which even stops H-burning in the H-shell. This behavior repeats in recurrent flashes. **H is mixed into the unburned He fuel, causing $^{12}\text{C}(p,\gamma)^{13}\text{N}(\beta^+)^{13}\text{C}(\alpha,n)^{16}\text{O}$ and the production of neutrons.**



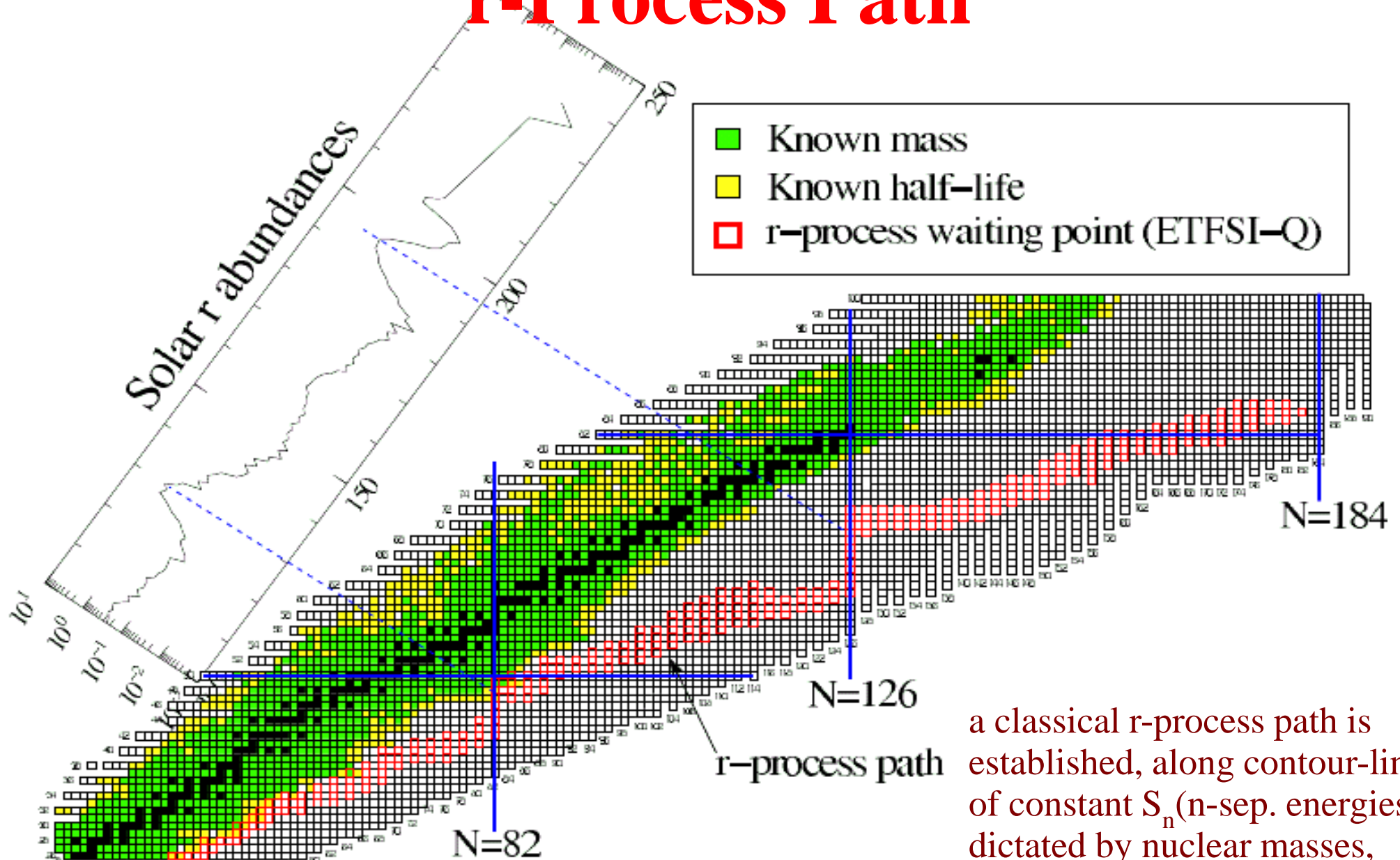
Boundary of H-free core (black), **He-free core (red)**, edge of convective zone (blue), which mixes H (protons) into He-burning, **leading to the production of the neutron source ^{13}C .**

Decomposition in s- and r-process



There exist pure s and r nuclei, others having s and r-process contributions. As the s-process is understood (known nuclear physics close to stability as well as stellar models), the r-process component is obtained via subtraction from solar abundances.

r-Process Path

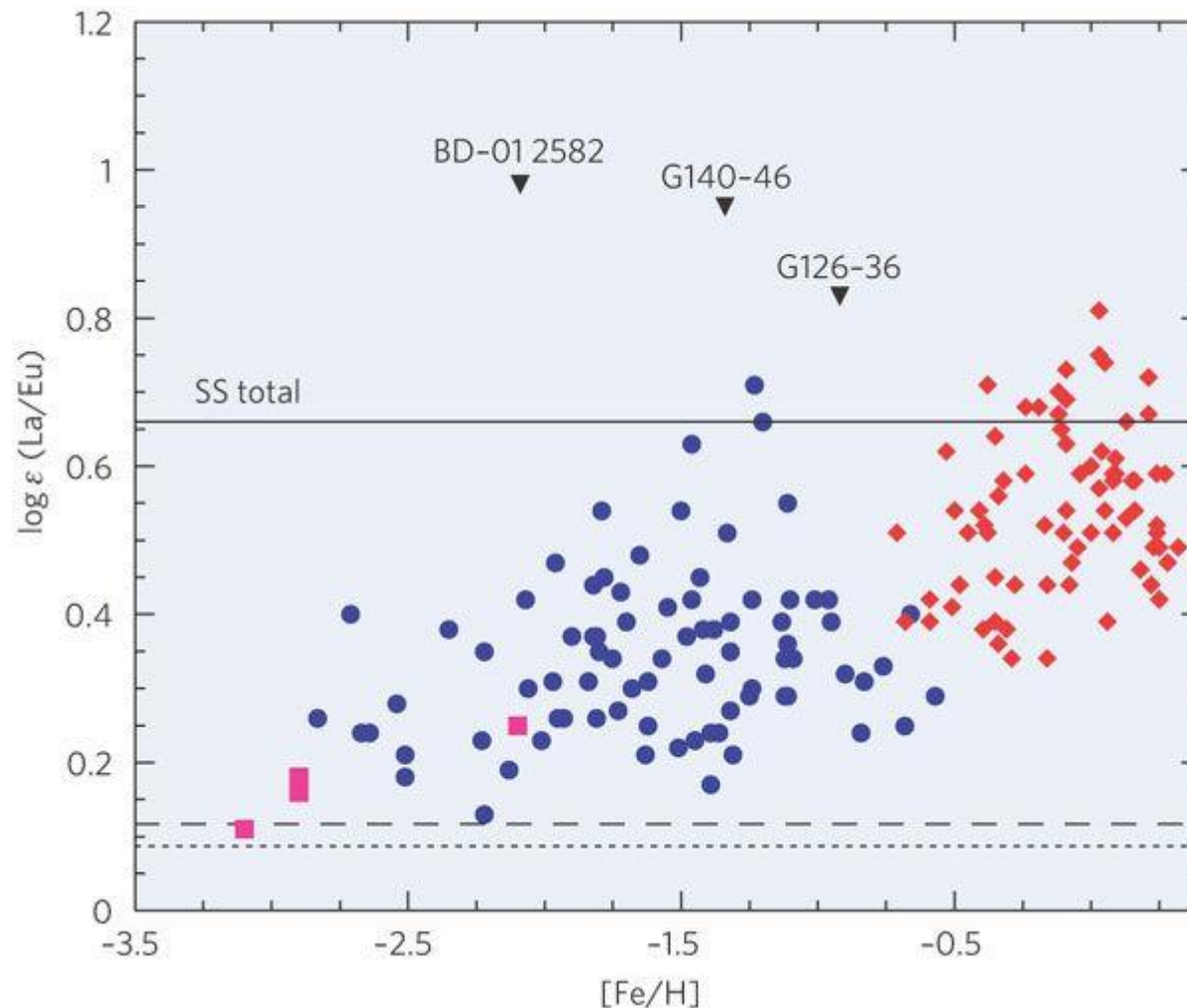


a classical r-process path is established, along contour-lines of constant S_n (n-sep. energies), dictated by nuclear masses, and due to (n,γ) - (γ,n) equilibrium, depending on the temperature and density. As in the r-process neutron captures and their reverse are fast, the process is controlled by beta-decay half-lives of “waiting points” in each isotopic chain, the longest encountered at closed shells close to stability.

Time Evolution of s- and r-Process

The isotopic decomposition in s- and r-nuclei can be utilized to come to an elemental decomposition of solar abundances into s- and/or r-process components.

As can be seen from the La/Eu ratio, the s-process sets in belated
for finally attaining the solar abundance ratio. **The early galaxy is dominated by the r-process.**
Low mass stars have a long evolution time before ending as planetary nebulae,
The r-process is correlated with fast evolving massive stars.

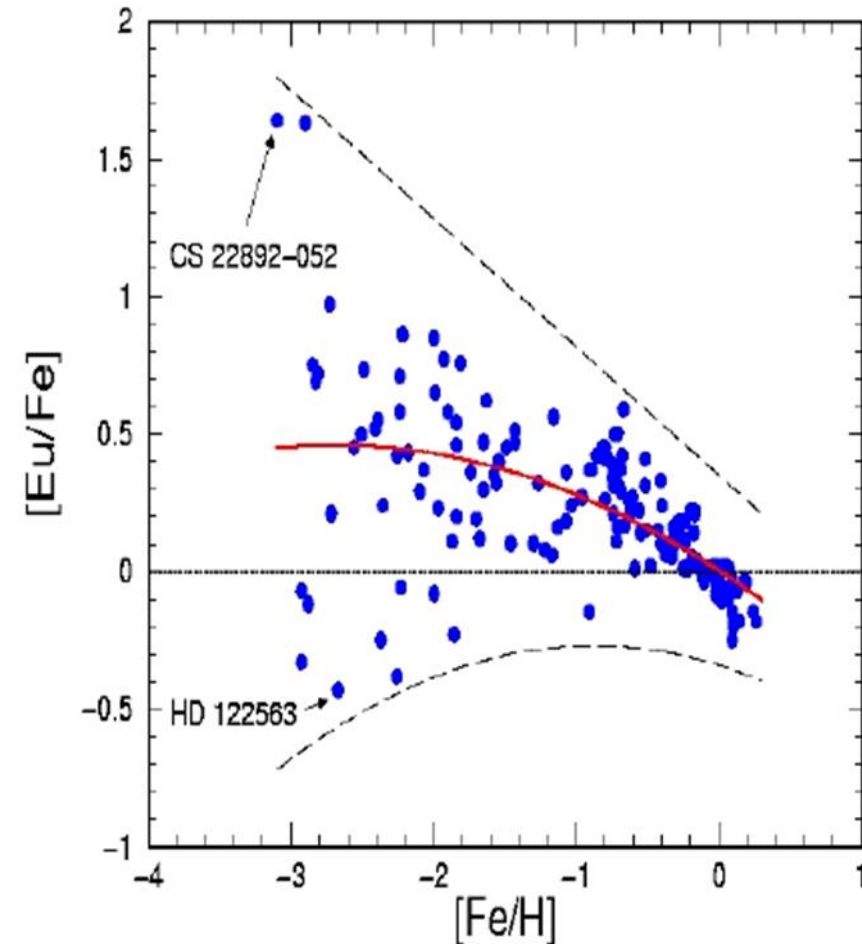


Solar

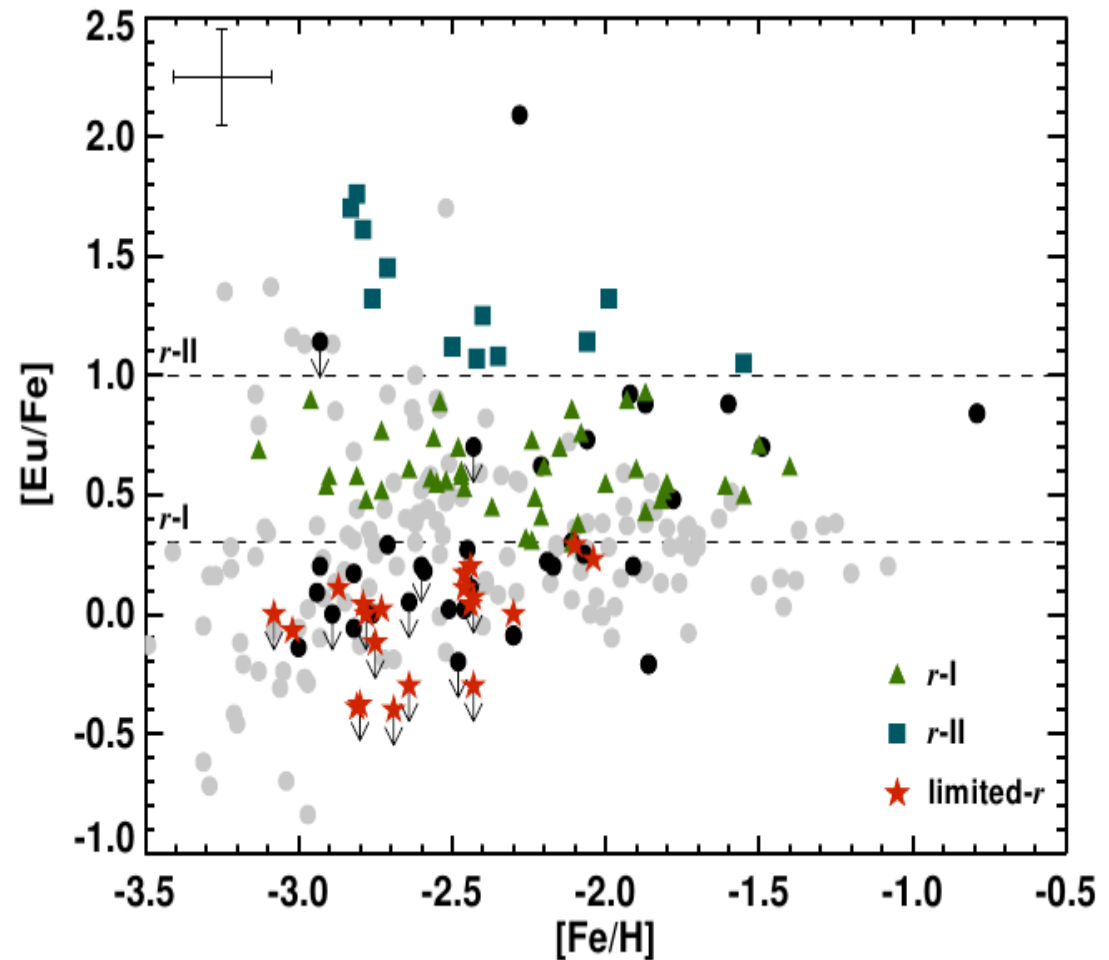
r-Process

The averaged Eu/Fe -ratio (r -process) evolves similar to the α/Fe ratio (O , Mg , Si , S , Ca , Ti) produced by CCSNe, but with a large scatter!

Can this scatter of $[\text{Eu}/\text{Fe}]$ at low metallicities be explained by rare events (NS-merger and/or MHD supernovae)?



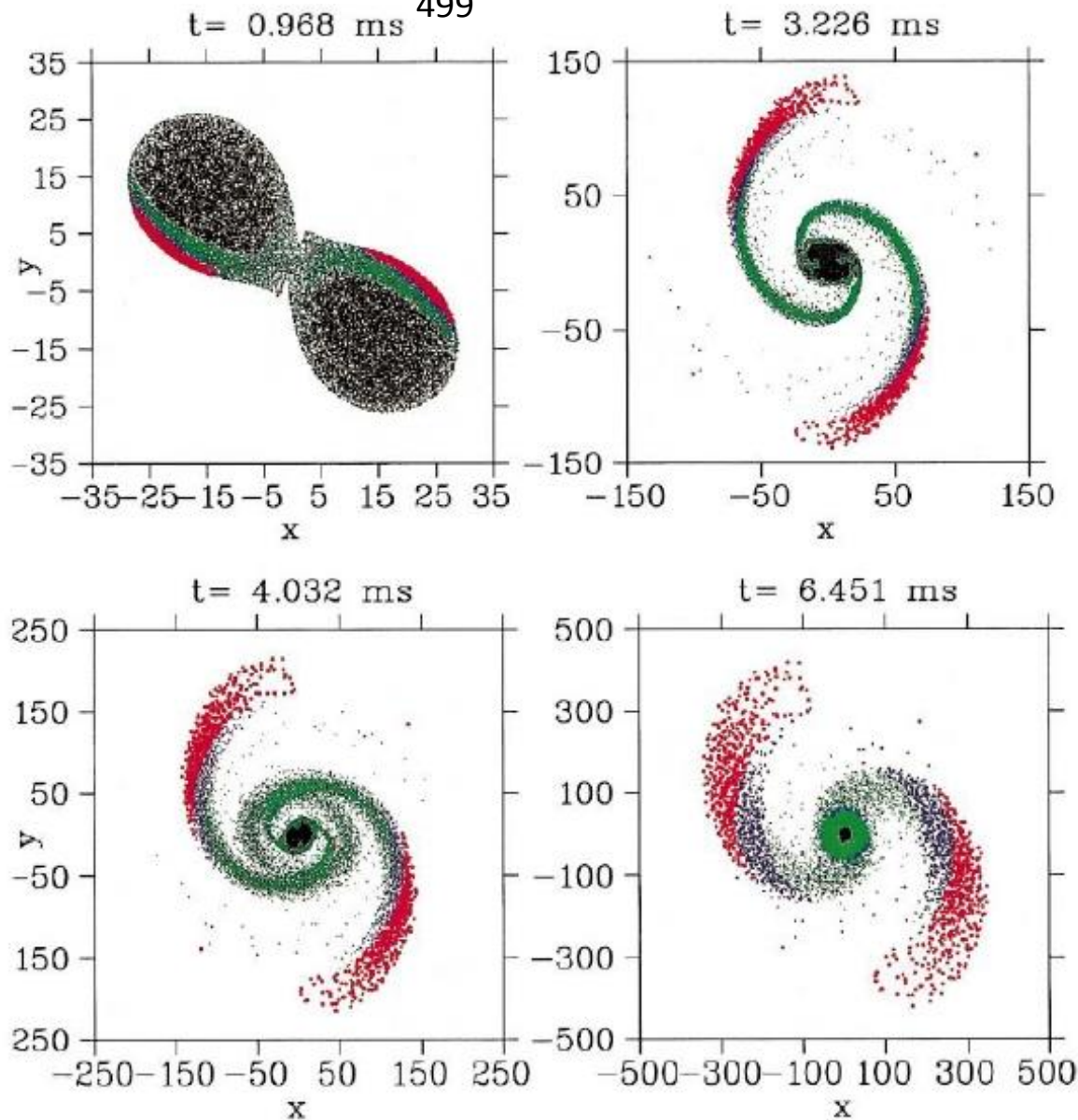
Cowan & Thielemann (2004)



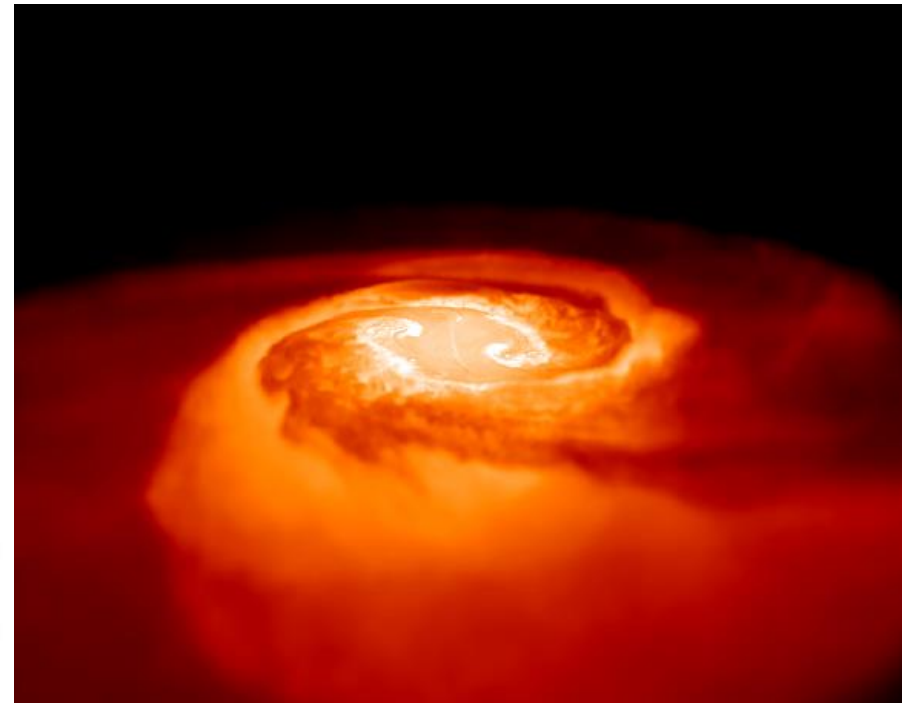
«The r -process alliance» Hansen et al. (2018)
In comparison to Roederer et al. (2014, grey dots)

Simulations of Neutron Star Mergers

Rosswog et al.
A&A 341 (1999)
499



Neutron stars are very neutron-rich, $n/p\text{-ratio} > 20$



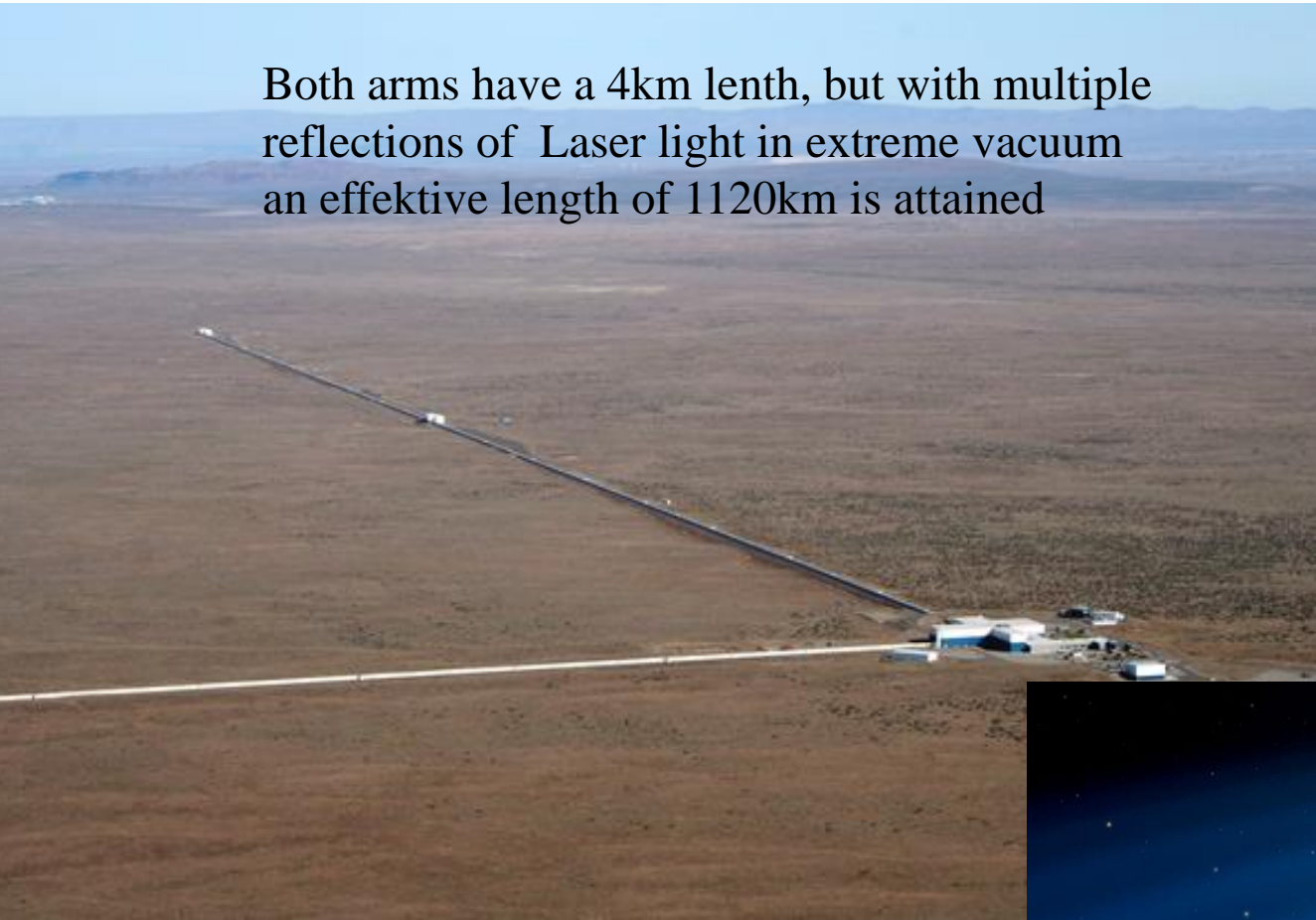
Rosswog et al. 2014

The tidal arms are partially ejected, in the center a black hole is formed

LIGO Hanford Detector for Gravitational Waves

Both arms have a 4km length, but with multiple reflections of Laser light in extreme vacuum an effective length of 1120km is attained

small length differences in the two arms (detectable down to the size of a proton, 10^{-15}m) lead to interferences and show how gravitational waves are passing through the detector



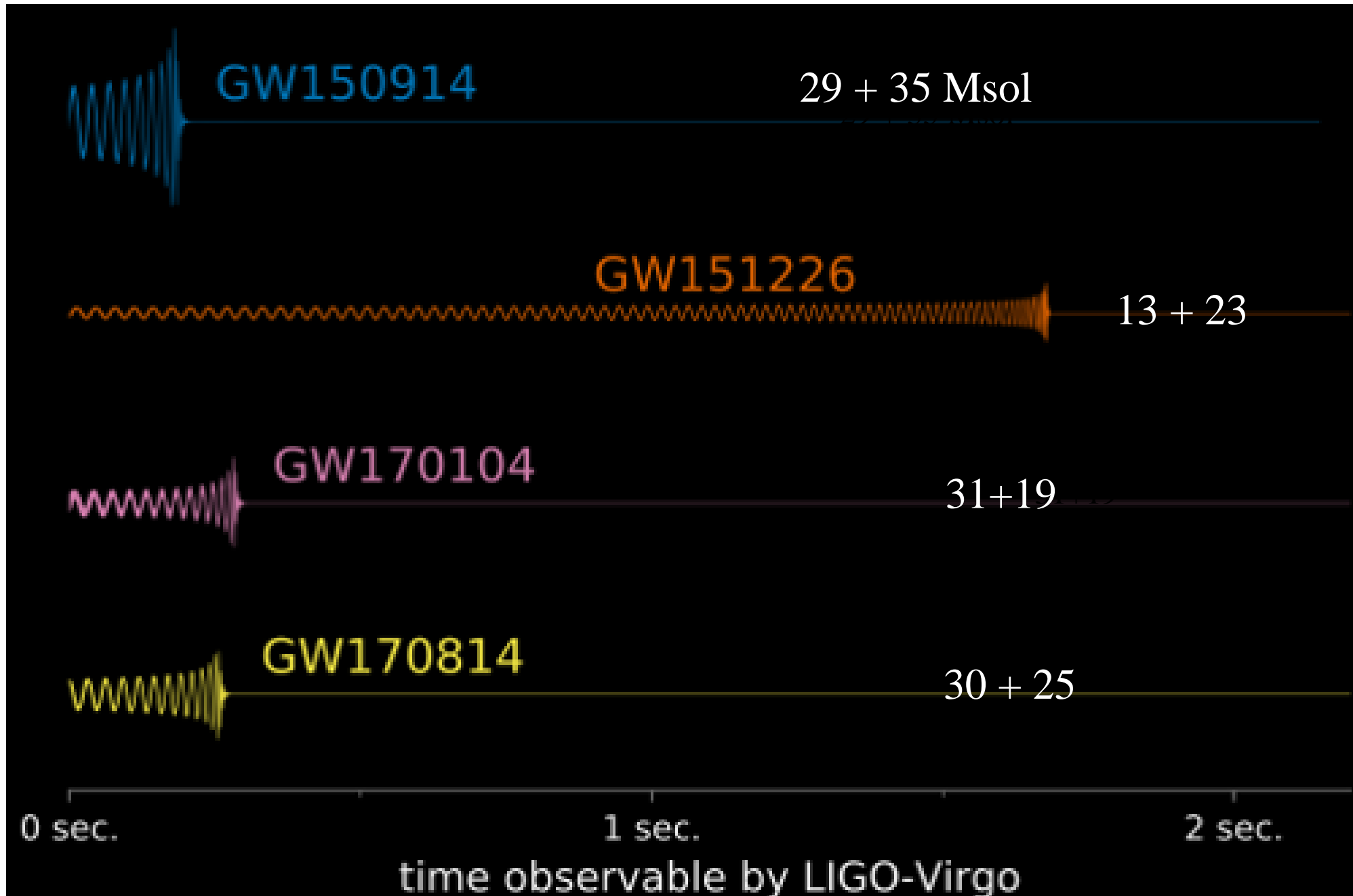
Presently three active detectors (2 from LIGO), in addition Virgo (near Pisa), soon also KAGRA (Japan)

GW170817 (a neutron star merger) was observed for more than 100s!!

$$m_1 \in (1,36 - 1,60)M_{\odot} \quad m_2 \in (1,17 - 1,36)M_{\odot}$$



Observed Black Hole Mergers



short duration

**Gamma Ray Burst
GRB170817A**

observed by Fermi
and Integral satellites
1.7 s after Merger

GW170817

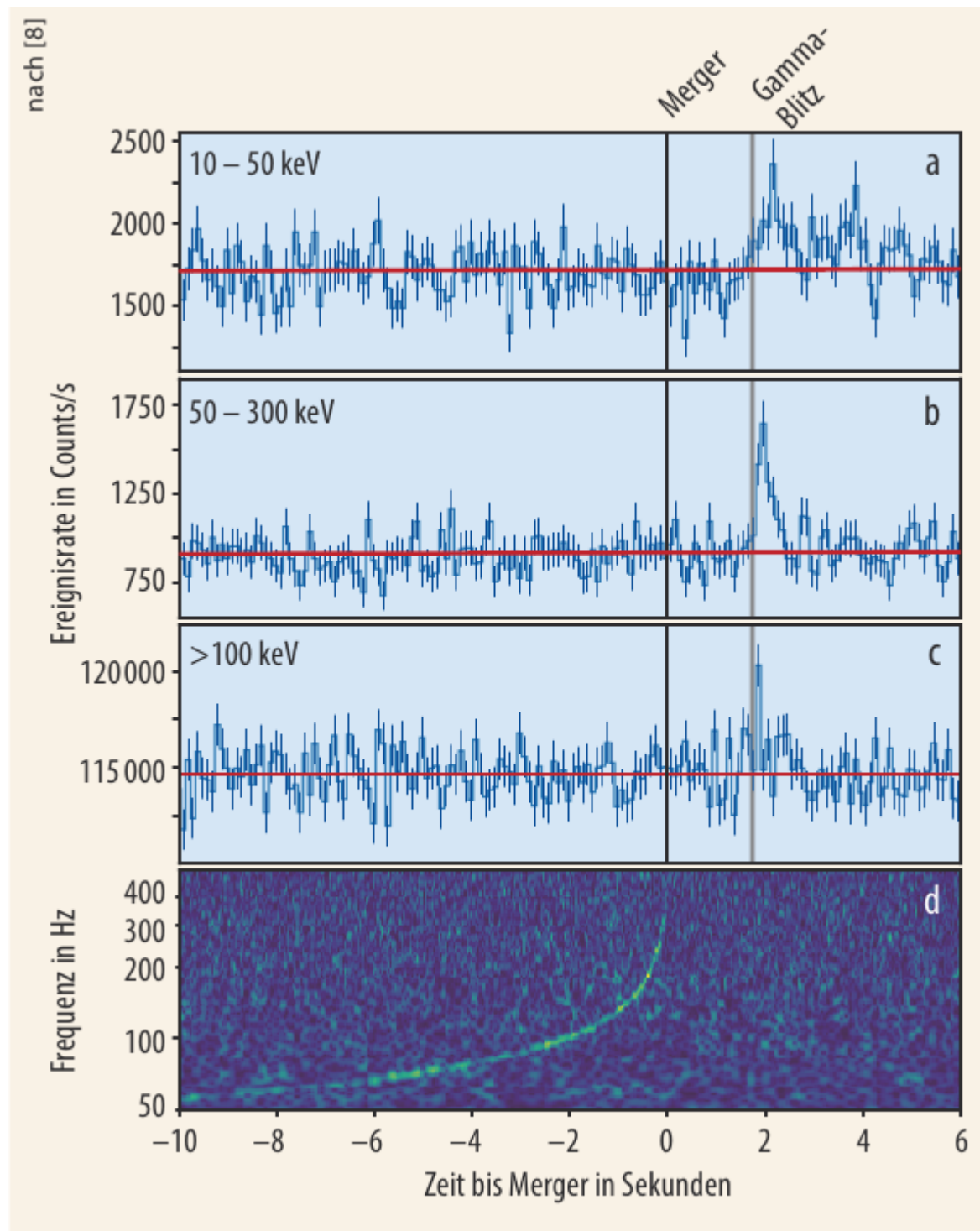
observed for more than 100s!!

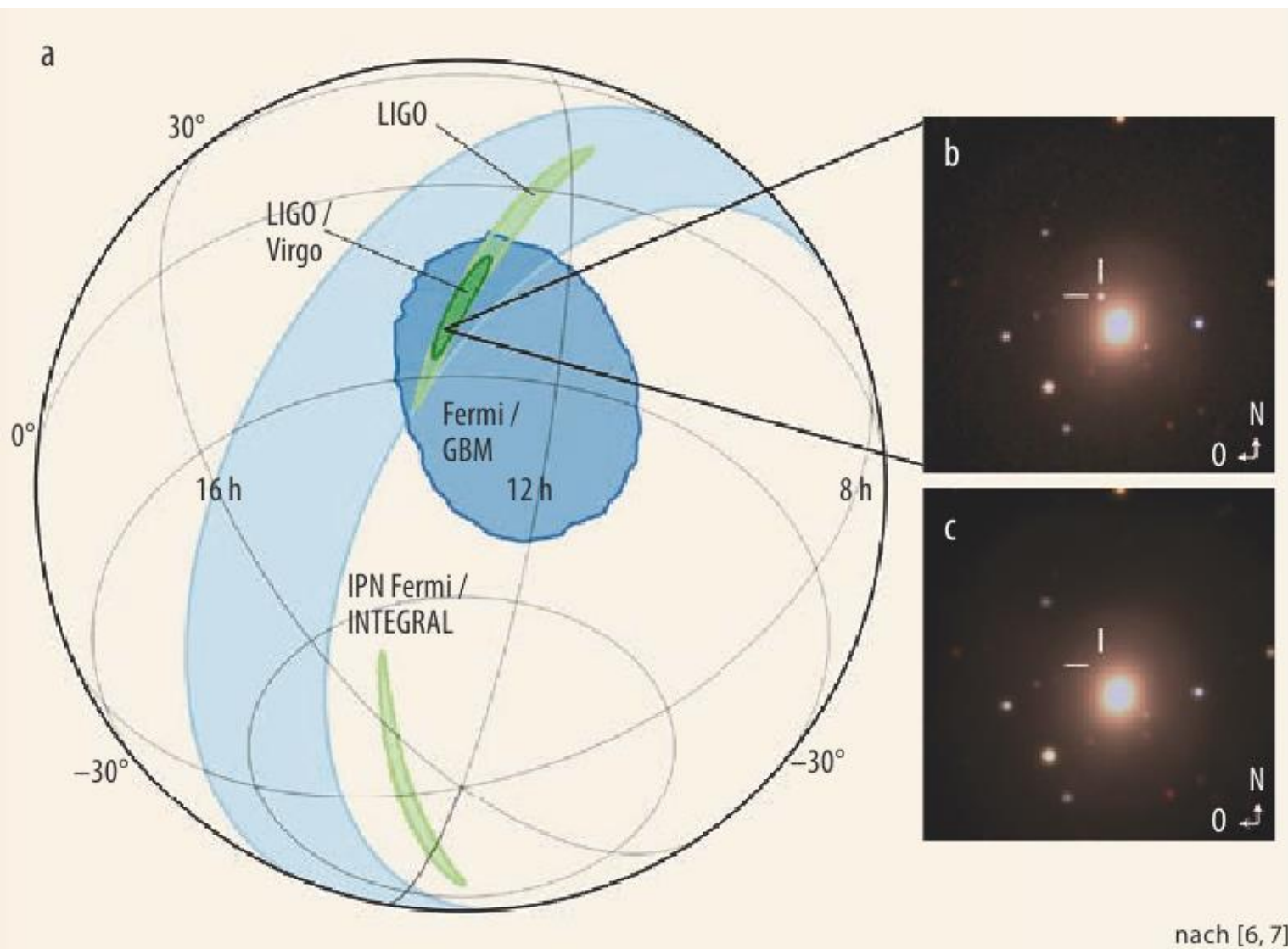
frequency change permits
determination of the *Chirp Mass*
 $1.186\text{--}1.192 M_{\odot}$,

from further info

$$m_1 \in (1.36 - 1.60)M_{\odot} \quad m_2 \in (1.17 - 1.36)M_{\odot}$$

→two neutron stars!!





Multi-Messenger-event:

1. **Gravitational waves**
2. **Gamma Ray Burst (GRB) 1.7s**
3. **optical (blue) and near Infrared (after 11 hrs. or 3 days)**

in galaxy
NGC 4993
with distance
40 Mpc=
130 Mill.
lightyears

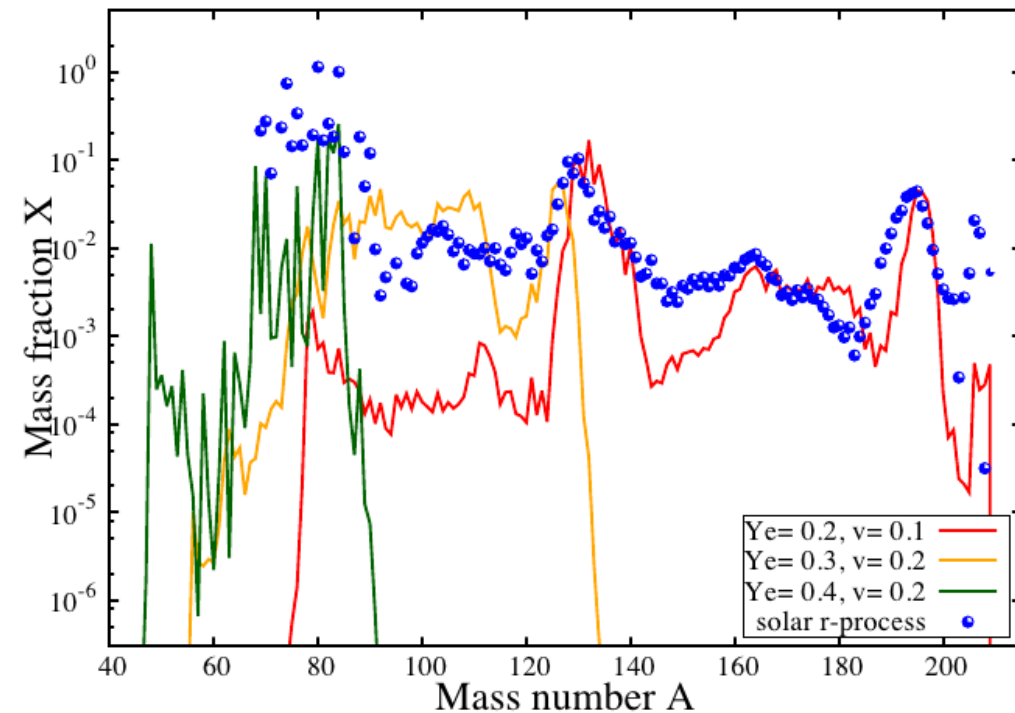
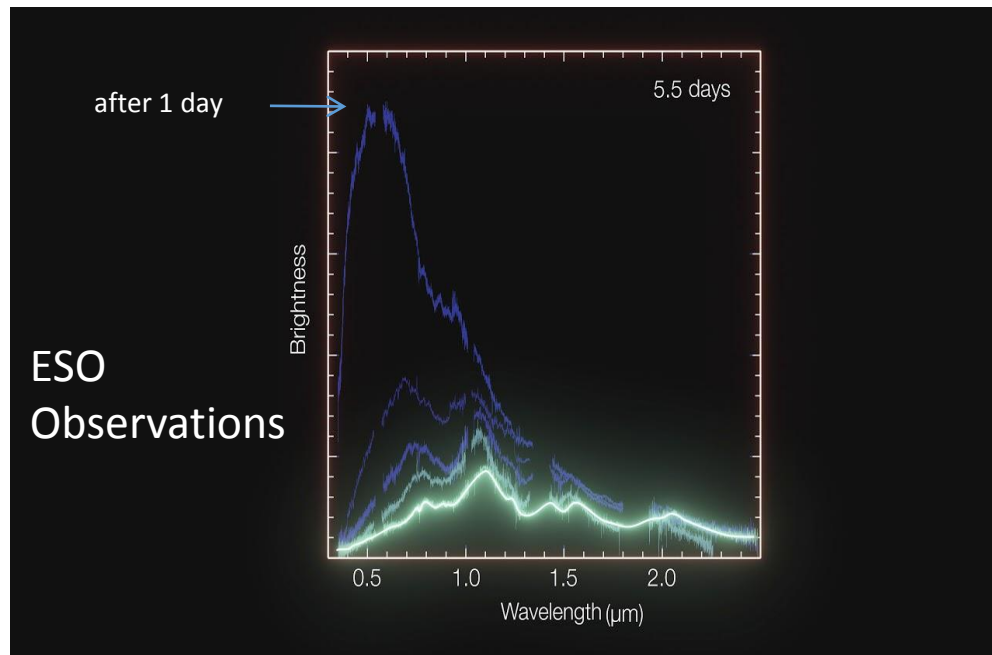
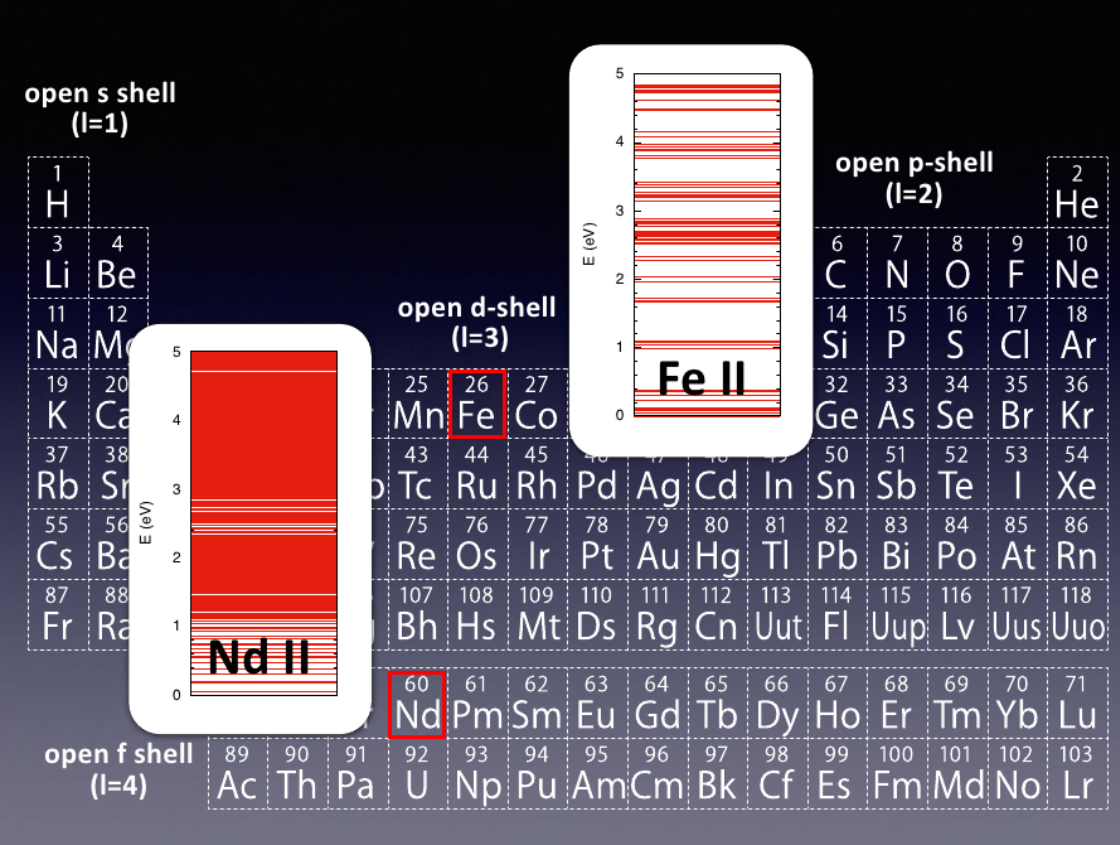
Abb. 2 Als Quelle der Gravitationswellen lokalisierten die LIGO-Detektoren einen Bereich von 190 deg^2 (a, hellgrün), die Kombination mit Virgo schränkt diesen auf 31 deg^2 ein (grün). Die Triangulation der Signale von Fermi und INTEGRAL

(hellblau) und die Daten von Fermi/GBM ergaben konsistente Positionen für den Gamma-Blitz. Im optischen Bereich registrierte DECam etwa einen Tag nach dem Verschmelzen ein Signal (b), das nach mehr als 14 Tagen verschwindet (c).

Different opacities of matter due to density of atomic states

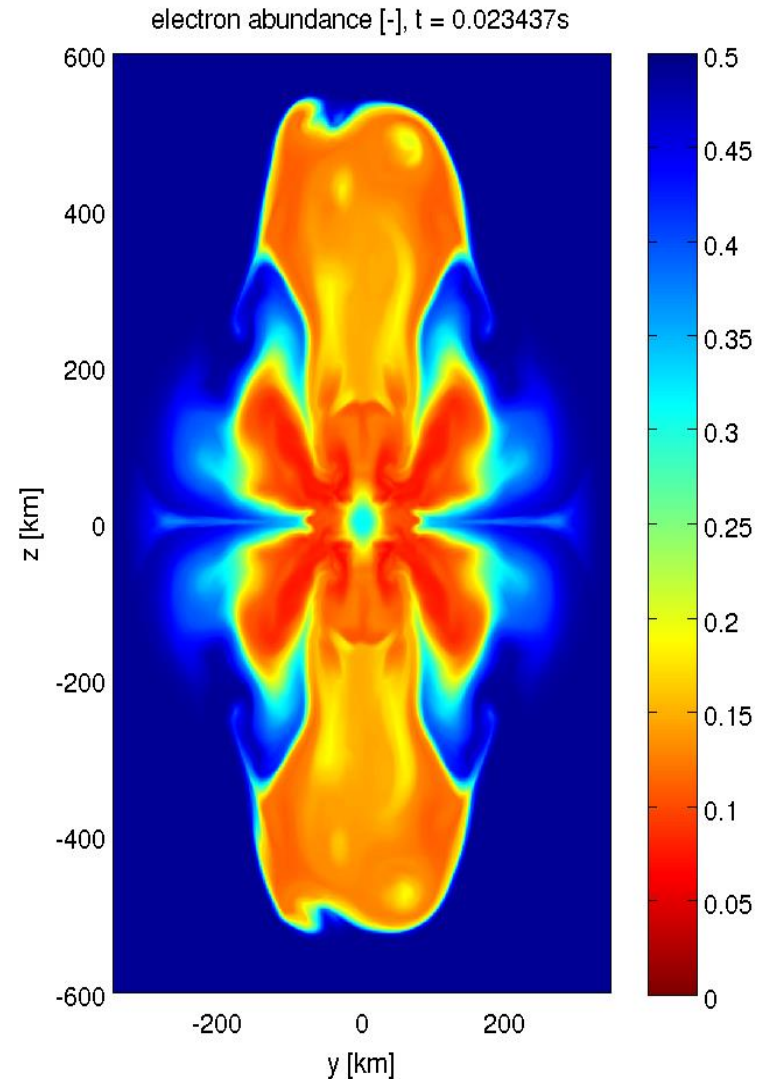
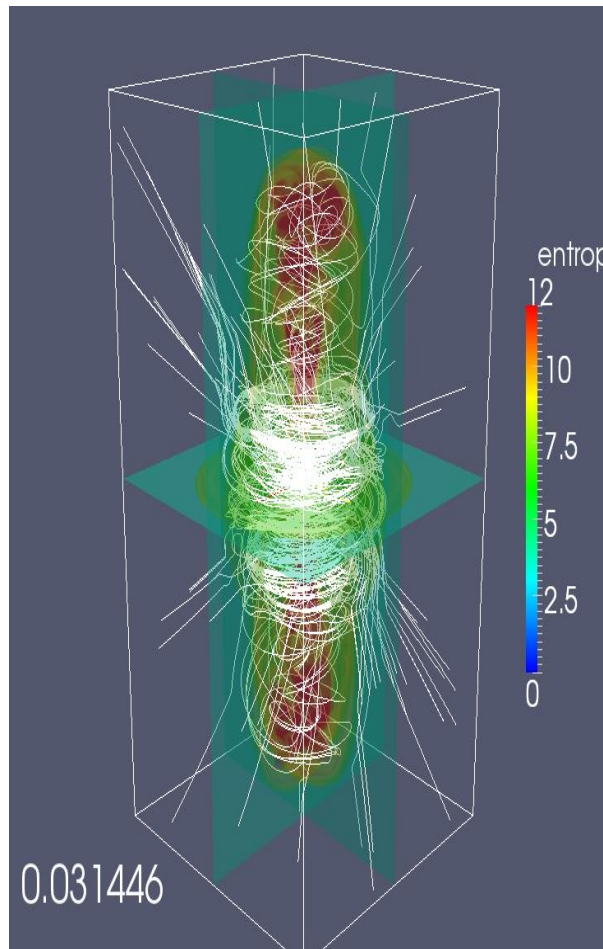
(from M. Tanaka 2017)

Kilonova aspects



A rare class of supernovae with fast rotation and high magnetic fields

*Leading to fast rotating neutron stars with extreme magnetic fields
(magnetars, 10^{15} Gauss)*

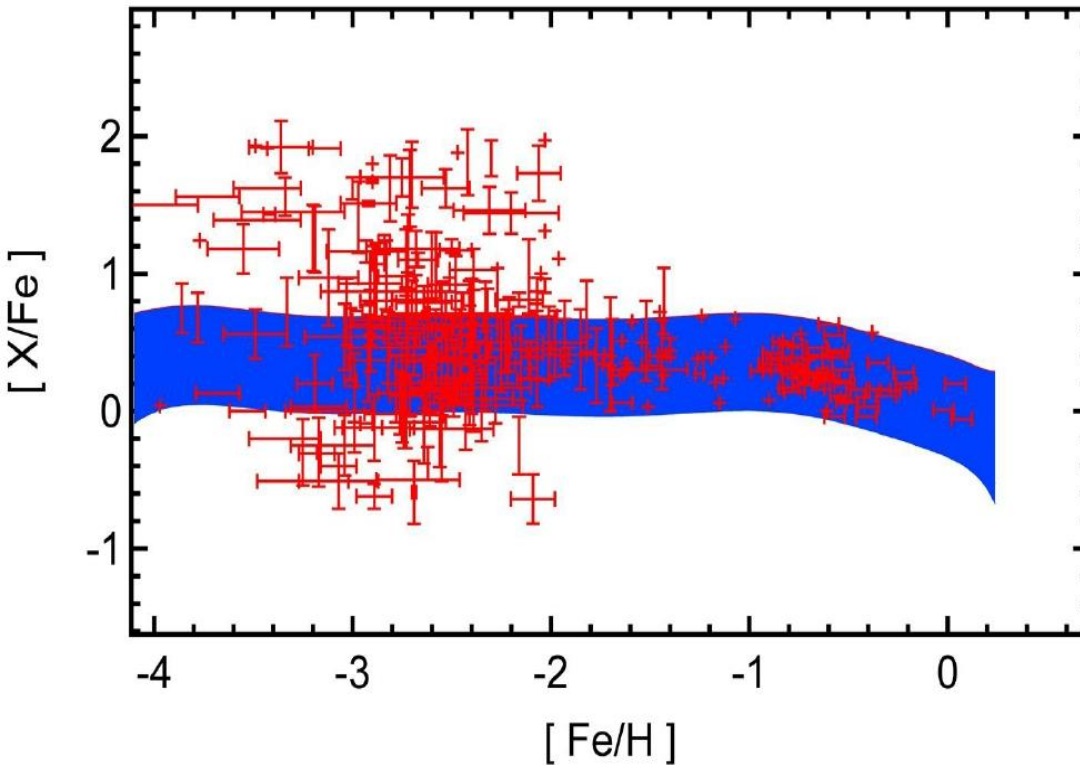


n/p-ratio
of 10

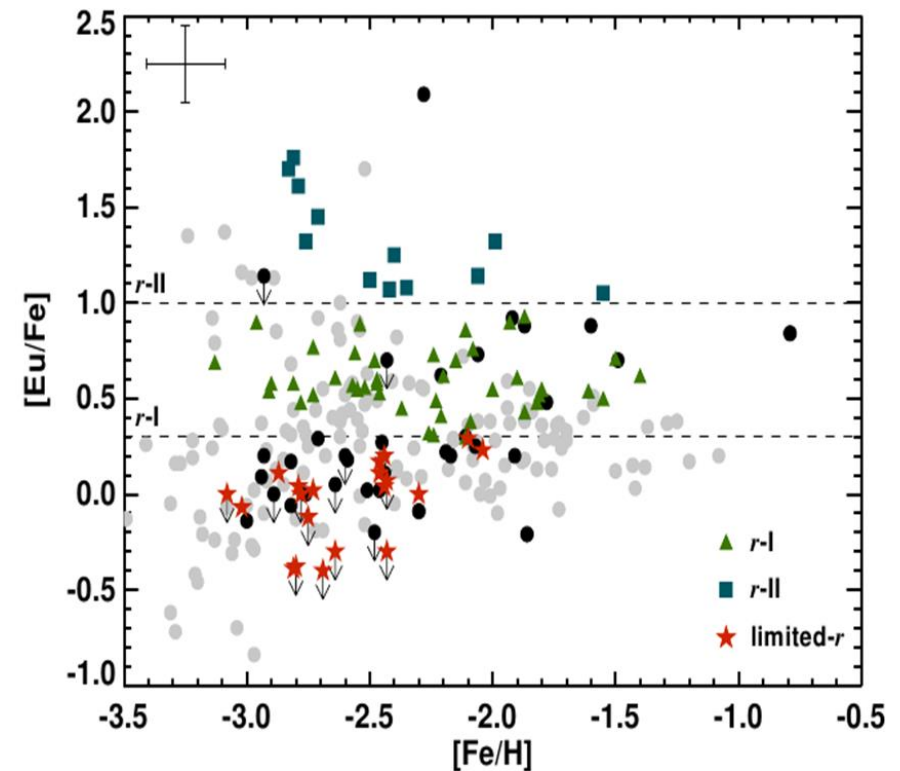
C. Winteler, R. Käppeli, M. Liebendörfer et al. 2012, Eichler et al. 2015

Rare events lead initially to large scatter before
an average is attained in galactic evolution!
Need for inhomogeneous modeling!

Data from SAGA
database



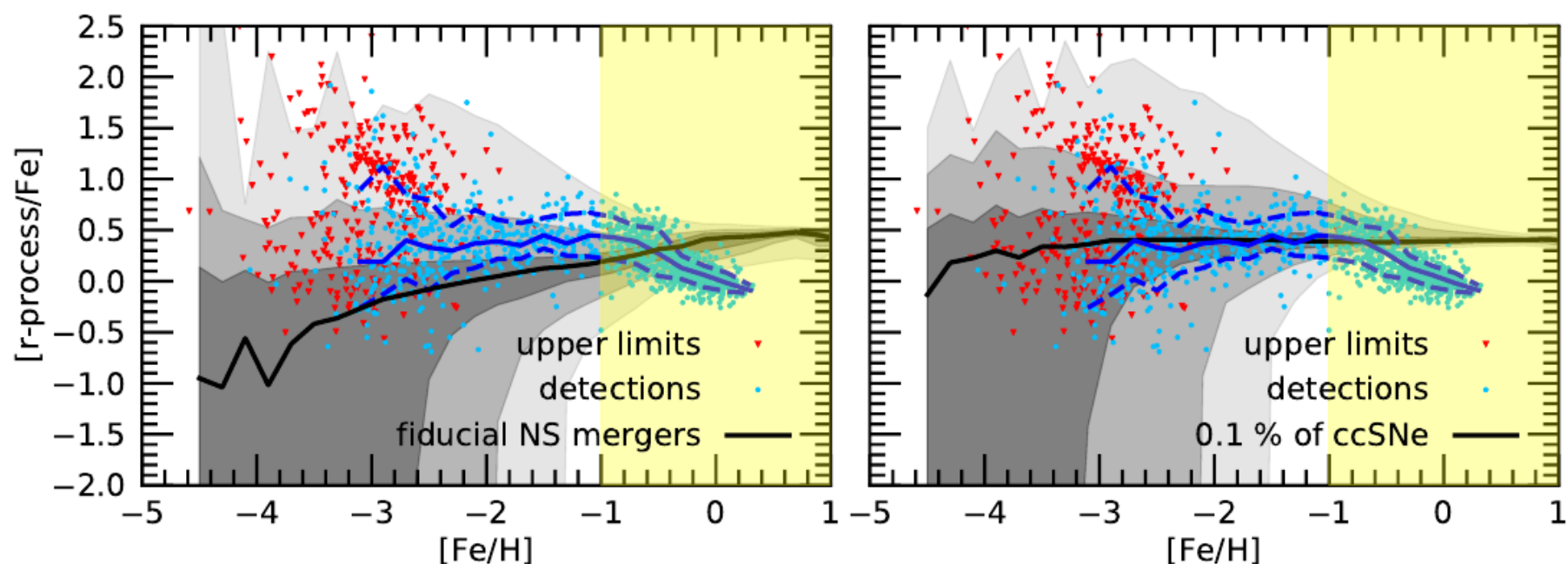
«The r-process alliance» Hansen et al. (2018)
In comparison to Roederer et al. (2014, grey dots)



Blue band: Mg/Fe observations (95%), explained from *frequent* CCSNe,
red crosses: individual Eu/Fe obs.

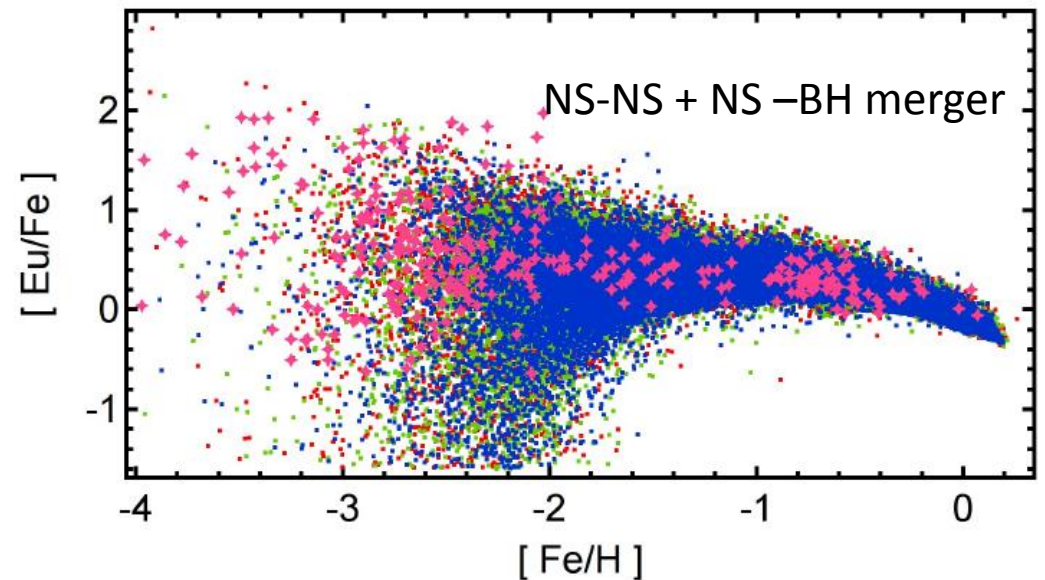
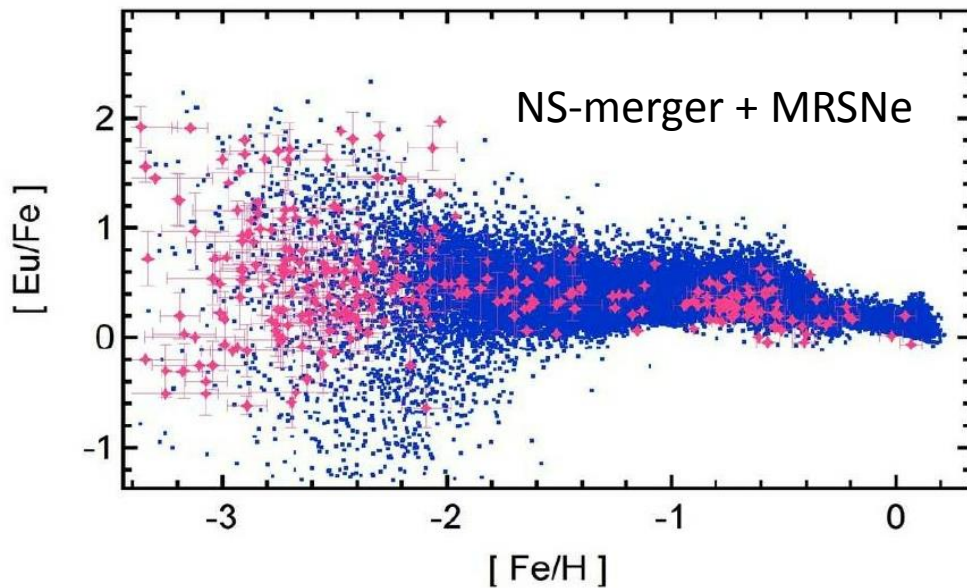
^{60}Fe and ^{244}Pu measurements in deep sea sediments also indicate that the strong r-process is
rare in comparison to CCSNe!

Cosmological simulation by F. van de Voort et al. (2019), including mixing processes, which move $[\text{Eu}/\text{Fe}]$ to lower metallicities. But also in this case NS-mergers alone cannot explain the full spread/scatter at low metallicities, still produce a rising rather than flat median trend. Only the inclusion of rare single massive star events (1 permille of CCSNe) leads to a flat median and a consistent scatter.



Combination of (a) NS mergers and magneto-rotational jets or (b) NS-BH and NS-mergers (occurring earlier/at lower metallicity in galactic evolution, either (a) because of massive star origin or (b) because only one SN explosion of the binary system ejects Fe, less SNe occur due to BH formation, and shorter delay times because of more massive BHs) in (stochastic) inhomogeneous GCE

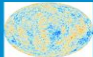
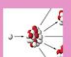




Wehmeyer, Pignatari, Thielemann (2015), Wehmeyer et al. (2019)



variations in minimum mass for BH formations

⇒ Options to solve the low metallicity problem,

The Origin of the Solar System Elements

1 H	big bang fusion 					cosmic ray fission 					2 He						
3 Li	4 Be	merging neutron stars 					exploding massive stars 					5 B	6 C	7 N	8 O	9 F	10 Ne
11 Na	12 Mg	dying low mass stars 					exploding white dwarfs 					13 Al	14 Si	15 P	16 S	17 Cl	18 Ar
19 K	20 Ca	21 Sc	22 Ti	23 V	24 Cr	25 Mn	26 Fe	27 Co	28 Ni	29 Cu	30 Zn	31 Ga	32 Ge	33 As	34 Se	35 Br	36 Kr
37 Rb	38 Sr	39 Y	40 Zr	41 Nb	42 Mo	43 Tc	44 Ru	45 Rh	46 Pd	47 Ag	48 Cd	49 In	50 Sn	51 Sb	52 Te	53 I	54 Xe
55 Cs	56 Ba		72 Hf	73 Ta	74 W	75 Re	76 Os	77 Ir	78 Pt	79 Au	80 Hg	81 Tl	82 Pb	83 Bi	84 Po	85 At	86 Rn
87 Fr	88 Ra																
		57 La	58 Ce	59 Pr	60 Nd	61 Pm	62 Sm	63 Eu	64 Gd	65 Tb	66 Dy	67 Ho	68 Er	69 Tm	70 Yb	71 Lu	
		89 Ac	90 Th	91 Pa	92 U												

links the individual sites and their occurrence frequency to the temporal evolution of the Galaxy.

J. Johnson (2019): in terms of stellar origins (still a bit ambiguous, as there are weak and strong s-processes and r-processes, and possibly even multiple strong r-process sites, and additional processes like the vp-process)